The Dissertation Committee for Paola Andrea Arias Gomez
certifies that this is the approved version of the following dissertation:

CLIMATE VARIABILITY OVER THE AMERICAN MONSOON AND AMAZONIAN REGIONS DURING THE LAST DECADES

Committee:

Rong Fu, Supervisor

Robert E. Dickinson

Kerry H. Cook

Zong-Liang Yang

Kingtse C. Mo

CLIMATE VARIABILITY OVER THE AMERICAN MONSOON AND AMAZONIAN REGIONS DURING THE LAST DECADES

by

Paola Andrea Arias Gomez, Título de Ingeniería Civil; Magister en Ingeniería; M.S. Earth & Atm. Sci.

Dissertation

Presented to the Faculty of the Graduate School of

The University of Texas at Austin

in Partial Fulfillment

of the Requirements

for the Degree of

Doctor of Philosophy

The University of Texas at Austin

August 2011

Dedication

A mi padre, con quien estaré eternamente agradecida por mostrarme un camino de integridad, dedicación y respeto. Porque he llegado hasta aquí gracias a su ejemplo, cariño y constante motivación.

Acknowledgements

After all these years living such an amazing journey, I am deeply thankful with all the persons who have supported me and inspired me.

I would not have been able to reach this point without the motivation and inspiration from my wonderful supervisor, Dr. Rong Fu. After five years working with her, I learned that not only the academic aspects make a good scientist. Her warmth and charisma encouraged me to improve everyday and help me to move over the most difficult times. I feel very lucky to be her student and always will consider her one of my most dear teachers.

Thanks to all my professors in Georgia Tech. They showed me a whole new world. Now, I am eager to share that world in my home country.

Thanks to all the staff in Georgia Tech and Jackson School of Geosciences. They made easier for me to access new opportunities.

I have been very lucky to find excellent scientists to work with. Thanks to Drs. Carlos D. Hoyos, Wenhong Li, Liming Zhou, and Kingtse C. Mo for their insightful contributions to our publications. I feel inspired by their work.

I acknowledge my committee members, Dr. Robert E. Dickinson, Kerry H. Cook, Zong-Liang Yang, and Kingtse C. Mo for their important feedback during my defense process.

Thanks to Universidad de Antioquia in Colombia for giving me the opportunity to return to my country and contribute to education.

I also acknowledge my research teammates in Georgia Tech and UT… It has been a pleasure to share with all of you.

To be far away from your home country and your family is not an easy task, but everything gets better when you have good friends by your side. My dear friends in Georgia Tech: Sara, Vincent, Douglas, Lina, Yuley, Manuel Z., Carlos, Paula, Jaime, Katia, and Jud… You made my world much happier… Porque las maratones de alegría total me mantuvieron firme!!!

I also found good friends in Austin… Anmar and Daniel, you helped me to adapt to a new city… to a new experience… Son un éxito absoluto!!! Thanks to my dear friends in Colombia. They gave me strong support every time I needed it (Luisa, Catalina, Susana, Jorge R., Jorge V., Manuel C., Felipe, and David).

I deeply thank my family… They have been my motivation during all these years and their unconditional support brought me here.

But most of all, to the two most lovely persons! César… Gracias por apoyarme incondicionalmente, por transmitirme calma en los momentos más difíciles, por alegrar mi vida con tu cariño. And finally and most importantly, to my father… The best example I could ever have! Porque tengo el mejor padre del mundo y siempre he sido consciente de ello… Te admiro profundamente por ser la persona más inteligente que he tenido en mi vida. Me siento orgullosa de ser tu hija!!!

CLIMATE VARIABILITY OVER THE AMERICAN MONSOON AND AMAZONIAN REGIONS DURING THE LAST DECADES

Publication No._____

Paola Andrea Arias Gomez, PhD

The University of Texas at Austin, 2011

Supervisor: Rong Fu

This dissertation aims to identify the main changes in monsoon activity observed over the American monsoon and Amazonian regions during the last decades and the possible links between such changes. To address this, several observational and reanalysis datasets were used. The results suggest the occurrence of two regime types of the North American monsoon during 1948-2009: two dry regimes during 1948-1959 and 1990-2009 and one wet regime during 1960-1989. The occurrence of such regimes is modulated by the Atlantic Multidecadal Oscillation. However, the two dry regimes have different causes. In particular, the more recent dry regime is mainly due to both an anomalous westward expansion of the North Atlantic Subtropical High and a northward displacement of the subtropical jet stream over the United States. The former enhances the low-level flow from the Gulf of Mexico to the Great Plains and weakens moisture transport to Mexico and the southwestern US.

In addition to such a weakening of the North American monsoon during the last two decades, this research shows that the American monsoon systems have shortened after 1978 due to a trend toward earlier retreats of the North American monsoon and delayed onsets of the southern Amazon wet season. These changes produce a longer transition season between both monsoon systems. Whether these changes are caused by a common factor or they are the consequence of independent and unrelated causes was not clear previously. The results discussed here indicate that the observed changes in the American monsoons are partially a consequence of the westward expansion of the North Atlantic surface high observed since 1978. Such a westward expansion enhances the activity of easterly waves over the southern Caribbean Sea and northern South America, producing a dominant easterly flow over the region, which in turn prevents the reversal of the cross-equatorial flow necessary to transport moisture to the southern Amazon and the South American monsoon domain and contributes to its delayed onset.

This investigation provides evidence that the shortening and weakening of the American monsoons and the lengthening of the transition season between them are associated with the same large-scale forcing, which may be caused by anthropogenic influence.

Table of Contents

List of Tables ……..…….…..... xii

List of Figures ……..……... xiii

Chapter 1 General introduction ……...……... 1

Chapter 2 Changes in cloudiness over the Amazon rainforests during 1984-2007 ...….... 9

2.1 Introduction ……....…. 9

2.2 Data and methodology ……...…… 13

2.3 Results ……...……. 19

2.3.1 Changes in surface incoming radiation and convective cloudiness over the Amazon ……...……..……. 19

2.3.2 Changes in surface temperature and humidity ……...……. 25

2.3.3 Possible causes of the changes in cloudiness over the Amazon 26

2.3.3.1 Changes in vegetation and land use ……...….. 26

2.3.3.2 Links to decadal changes over the tropical Pacific and Atlantic Oceans ……...…. 27

2.3.3.3 The underlying processes ……...…….. 38

2.4 Implications to the observed growth rate increase over the Amazon forests ……..……...….. 41

2.5 Conclusions ……...… 42

Chapter 3 Changes in the monsoon regime over northwestern Mexico during 1948-2009 ……... 45

3.1 Introduction ……...……. 45

3.2 Data and methodology ……...…. 48

3.3 Results ……...……. 52

3.3.1 Identification of two types of monsoon regime during 1948-2009 …..…. 52
3.3.2 Associated changes in precipitation during the monsoon season.... 54
3.3.3 Associated circulation changes and their links to decadal climate variability modes …….……...…..... 60
3.3.3.1 Variation in lower troposphere circulation …….....…... 60
3.3.3.2 Variation in upper troposphere circulation ……..…... 71
3.3.3.3 Connection to changes of sea surface temperatures ...… 73
3.4 Discussion ……...……..……. 81
3.4.1 Causes of the early NAMS retreat ……...…….….. 81
3.4.2 Relative influence of the decadal variability versus global climate change …….……...…….. 84
3.5 Conclusions ……...……. 85
Chapter 4 A connection between the North American monsoon and the southern Amazon wet season after 1978…...…….……...…..... 88
4.1 Introduction …….…..…...…. 88
4.2 Data and methodology ……...…… 89
4.3 Results ……...…. 93
4.3.1 A longer transition season between the American monsoons …… 93
4.3.2 The role of the North Atlantic surface high expansion on delaying the wet season over the southern Amazon ..…….……...…….. 97
4.3.2.1 Impact on surface circulation …….……...……... 97
4.3.2.2 Impact on easterly waves activity ..…..…….. 103
4.4 Discussion……..……..... 107
4.5 Conclusions ……...……...… 108

Chapter 5 General conclusions and future work ……...……. 111

References ……..…… 117

Vita ……. 141

List of Tables

Table 1: Seasonal trends for surface data from Dai (2006) and VIMT from NCEP-NCAR Reanalysis averaged over northern and southern Amazon (see geographical location in Fig. 1). Values represent the total change in each variable during 1984-2005 (1984-2007 for VIMT). Values in bold are statistically significant at the 5% level according to the Mann-Kendall test with Sen's statistics (Sen 1968) …… 26

Table 2: Number of years with statistically significant at 5% level positive (PP) and negative (NP) phases for the SST variability indices considered here. ENSO contributions are removed. Positive (negative) phases are selected as those years with an index value above (below) 1σ of its climatological value. Statistical significance is tested using a boostrap test (Efron 1979) ……..…… 28

Table 3: Retreat dates over NWMEX during 1948-2009 from CPC-USMex rain rate data. The retreat date is identified using a criterion that considers both an objectively defined rain rate threshold and persistence throughout time following Li and Fu (2004) (see section 3.2). Dates in bold (asterisks) correspond to early (late) retreat events ……..….. 56

List of Figures

Figure 1: Seasonal trend in a)-d) SW down-welling radiation and e)-h) high cloudiness from ISCCP during 1984-2007 over the Tropical Americas. Trends shown are statistically significant at the 5% level according to the Mann-Kendall test with Sen's statistics (Sen 1968). Boxes represent northern and southern Amazon domains, respectively …….. 21

Figure 2: Domain average time series for total and high clouds (black curves) and OLR (blue curves) during SON (DJF) over the northern (southern) Amazon. Domain average OLR is obtained for values lower than 240 W/m2. Red dotted lines indicate the dates of satellite reposition according to ISCCP D2 data set documentation (available at http://isccp.giss.nasa.gov/index.html). Solid lines represent statistically significant trend at the 5% level according to the Mann-Kendall test with Sen's statistics (Sen 1968) …. 23

Figure 3: DJF correlations (color shades) between detrended SST anomalies from NOAA-CDC and detrended domain average high level clouds over a) northern Amazon and b) southern Amazon. Correlations shown are statistically significant at the 5% level based on Monte Carlo test and the spatial patterns shown are also statistically significant at 5% level (Livezey and Chen 1983). Contours represent trends in SST anomalies during 1984-2007. Trends shown are statistically significant at the 5% level according to the Mann-Kendall test with Sen's statistics (Sen 1968). Contours are plotted with interval of 0.1°C per decade. Solid (dashed) contours represent warm (cold) SST anomalies ……. 31

Figure 4: Composite high cloud difference for positive and negative phases of the WPWP (No ENSO) for DJF. Statistical significance for difference is tested using a bootstrap test (Efron 1979) at 5% level. Contours indicate trends in high cloud anomalies statistically significant at the 5% level according to the Mann-Kendall test with Sen's statistics (Sen 1968). Solid (dashed) lines represent increasing (decreasing) clouds. Contours are plotted each 1% per decade …….…….. 32

Figure 5: Same as Fig. 3b but for MAM ……...……..… 33

Figure 6: Composite high cloud difference for positive and negative phases of the AMO (No ENSO) for MAM. Statistical significance for difference is tested using a bootstrap test (Efron 1979) at 5% level. Contours indicate trends in high cloud anomalies statistically significant at the 5% level according to the Mann-Kendall test with Sen's statistics (Sen 1968). Solid (dashed) lines represent increasing (decreasing) trends. Contours are plotted with interval of 1% per decade ……..... 34

Figure 7: Same as Fig. 3 but for SON ……...…….. 36

Figure 8: Composite high cloud difference for positive and negative phases of a) the Atlantic SSTG (No AMO, No ENSO) and b) the WPWP (No ENSO) for SON. Statistical significance for difference is tested using a bootstrap test (Efron 1979) at 5% level. Contours indicate trends in high cloud anomalies statistically significant at the 5% level according to the Mann-Kendall test with Sen's statistics (Sen 1968). Solid (dashed) lines represent increasing (decreasing) trends. Contours are plotted with interval of 2% per decade …….. 37

Figure 9: Trends in streamfunction during a) DJF and b) SON. Differences between -1σ decrease and 1σ increase of high clouds events in the southern Amazon for streamfunction at 0.22 sigma level (~200 hPa) during c) DJF and d) SON. Statistical significance for difference is tested using a bootstrap test (Efron 1979) at 5% level. Trends are statistically significant at the 5% level according to the Mann-Kendall test with Sen's statistics (Sen 1968) ……..……. 40

Figure 10: a) Monsoon region (NWMEX) considered for onset and retreat computations based on Barlow et al. (1998) and Higgins et al. (1999). b) Monsoon onset (black) and retreat (gray) dates over NWMEX during 1948-2009 obtained from CPC-USMex rain rate …… 53

Figure 11: Relationship between total monsoon rainfall and a) onset date and b) retreat date over NWMEX. Correlation coefficient and its significance level for 1948-2009 are indicated in each plot. Dashed lines represent mean rainfall during 1948-1960, 1960-1990, and 1990-2009, respectively……...…… 55

Figure 12: Changes in a) onset and b) retreat dates over the SW US and Mexico between weak and strong monsoons. Composite difference between weak and strong monsoons for c) total monsoon precipitation anomalies and d) daily average monsoon rain rate. Contours indicate the differences that are statistically significant according to a bootstrap test (Efron 1979) …….. 58

Figure 13: Composite difference in JA mean rain rate between a) weak and strong monsoons and b) early and late-retreat monsoons. Contours indicate the differences that are statistically significant according to a bootstrap test (Efron 1979) ..…….. 59

Figure 14: 850 hPa streamlines composite for a) strong monsoons three pentads before the monsoon retreat. Difference in 850 hPa streamlines between weak and strong retreat events during b) 1948-1959 and c) 1990-2009. Color scale indicates wind speed in m/s ……... 63

Figure 15: Same as Fig. 14 but for early and late-retreat monsoons ……...……... 64

Figure 16: a) SLP composite difference between weak and strong monsoons five pentads before the monsoon retreat during a) 1948-1959 and b) 1990-2009. c) and d) Same but three pentads before the monsoon retreat. Contours indicate differences that are statistically significant according to a bootstrap test (contours) (Efron 1979) …… 65

Figure 17: Same as Fig. 16 but for early and late-retreat monsoons ……...……... 66

Figure 18: Position of 1560 meter of geopotential height (gpm) contour line at 850 hPa for weak (gray dotted line), strong (black dotted line), early (gray line) and late- retreat (black line) NAMS events three pentads before the monsoon retreat during a) 1990-2009, b) 1960-1989, and c) 1948-1959 …….. 68

Figure 19: a) Location of the NASH western boundary averaged during the last five pentads of the monsoon season (black) and the monsoon retreat over NWMEX (gray). b) Location of the NASH western boundary averaged during the entire monsoon season (black) and monsoon total rainfall over NWMEX (gray). Asterisks (diamonds) in a) represent monsoon events with early (late) retreat …….. 69

Figure 20: a) Correlations between zonal wind anomalies averaged over the monsoon region and geopotential height anomalies at 850 hPa, five pentads before the monsoon retreat. b) Same as a) but for meridional wind at 850 hPa averaged over the central US. Correlations are statistically significant at the 5% level based on Monte Carlo test (Livezey and Chen 1993). Linear trends were removed before computing correlations. Boxes indicate the regions corresponding to wind anomalies average …… 70

Figure 21: 200 hPa streamlines composite for strong monsoons a) and weak monsoons during b) 1948-1959 and c) 1990-2009, three pentads before the monsoon retreat. Color scale indicates wind speed in m/s …… 72

Figure 22: Same as Fig. 21 but for early and late-retreat monsoons ……...…….. 73

Figure 23: Changes in SLP (shades) and wind at 850 hPa (arrows) between the positive and the negative phase of a) WPWP and b) AMO, two pentads before the NAMS retreat during 1948-1959. c) Same but for difference between westward and eastward location of the summer NASH western boundary and d) but for difference between early and late NAMS retreat events. Vector scale is shown in the right-bottom corner of each panel .. 77

Figure 24: Same as Fig. 23 but for 1990-2009 …….……...…….... 78

Figure 25: Same as Fig. 24 but for zonal wind at 200 hPa (shades) and geopotential height at 200 hPa (contours) during 1990-2009 …….. 80

Figure 26: NAMS retreat date obtained using CPC US-Mex data and southern Amazon wet season onset date obtained using a) Silva data and b) SA21 data. Linear trends are tested using a Mann-Kendall test with Sen's statistics (Sen 1968) and their confidence level is indicated in each panel …… 96

Figure 27: Length of the transition season from the NAMS to the SAMS obtained using a) Silva data and b) SA21 data. Linear trends are tested using a Mann-Kendall test with Sen's statistics (Sen 1968) and their confidence level is indicated in each panel. Asterisks (diamonds) correspond to NAMS events with an early (late) retreat …….. 97

Figure 28: OLR (shades), 850 hPa horizontal winds (arrows), and 1560-gpm line (contour) composited throughout the transition season from the NAMS to the SAMS. Composites correspond to a) 16 pentads before the southern Amazon wet season onset (~NAMS retreat pentad), b) 8 pentads before the southern Amazon wet season onset, and c) the southern Amazon wet season onset pentad. Southern Amazon wet season onset dates were obtained using Silva data. Boxes indicate the South American V-Index domain …… 100

Figure 29: South American V-Index evolution from the NAMS to the SAMS season for early NAMS retreat events (black solid line) and late NAMS retreat events (gray dashed line) …… 101

Figure 30: Regression patterns of 850 hPa horizontal winds (arrows) and OLR (shades) associated with a) -30 longitude degrees (westward expansion) and b) +30 longitude degrees (eastward retreat) fluctuations of the NASH western ridge during SON. c) Pattern difference a)-b) zoomed over northern South America. Boxes indicate the South American V-Index domain …… 103

Figure 31: Same as Fig. 30 but for 700 hPa relative vorticity anomalies …… 105

Figure 32: Isentropic winds (arrows) and low-pass filtered potential vorticity (shades) at 310K composited for events with a) a NASH westward expansion and b) a NASH eastward retreat during SON. Contours for 0 and 0.2 PVU correspond to the red and black lines, respectively. Boxes indicate the South American V-Index domain …….... 107

Chapter 1

General introduction

Summer precipitation over both North and South America contributes with more than half of their total annual precipitation (Figueroa and Nobre 1990; Higgins et al. 1997). Such rainfall amounts are produced by the monsoon systems that take place over both continents. The regions affected by the North American monsoon system (NAMS) are among the zones with most rapidly growing population of the United States (US) and Mexico whereas the South American monsoon system (SAMS) affects large and highly populated regions of Brazil, Argentina, and Paraguay. The circulation patterns established by these monsoon systems control the summer weather over these regions and have important implications in both economy and society.

The American monsoon systems share many of the characteristics exhibited by the Asian monsoon (Vera et al. 2006a). Some of these features include (i) the strong land-sea thermal contrast, (ii) the thermally direct circulation with continental rising motion and oceanic subsiding motion, (iii) the local land-atmosphere interactions due to the presence of elevated topography, (iv) the surface low pressure (due to the strong land heating) and the upper-troposphere anticyclonic circulation, (v) the strong moisture transport from the adjacent oceans to the continent, and (vi) the associated seasonal rainfall changes over the continent (increases in summer and decreases in winter). Furthermore, Ramage (1971) proposed a criterion that demands that a monsoon may be

characterized by a large-scale wind regime that reverses between winter and summer. Although the Americas experience a strong seasonal cycle in rainfall, the dominant wind direction is mainly unchanged between winter and summer (Slingo 2002). However, Zhou and Lau (1998) demonstrated that the main features of such a reversal of the seasonal circulation over South America are observed when the annual mean winds are removed.

The seasonal cycle of precipitation over the subtropical Americas exhibits strong regularity. Furthermore, both the NAMS and the SAMS can be considered as the extremes of such a cycle (Vera et al. 2006a). The NAMS rainfall starts by early to mid June over southwestern Mexico and advances to northwestern Mexico and the southwestern (SW) US by July (e.g., Douglas et al. 1993; Higgins et al. 1997; Barlow et al. 1998). During this evolution, large amounts of moisture are transported from the Gulf of California (at surface) and the Gulf of Mexico (at mid-levels in the atmosphere) to the monsoon region (Higgins et al. 1997; Adams and Comrie 1997). Once the NAMS is fully developed, precipitation amounts are larger over the Mexican domain (influenced by abundant tropical moisture and thunderstorms) and lighter over the SW US (influenced by midlatitude effects and gulf surges) (Higgins et al. 1999; Stensrud et al. 1995). The NAMS retreats by late September-October in association with diminished precipitation over the SW US and western Mexico. Simultaneously to this retreat, the convection migrates from Central America into South America, initiating the wet season over the equatorial Amazon by September. The onset of the wet season starts in the equatorial

western Amazon and spreads quickly to the east and the southeast. By October, monsoon activity starts over the southern Amazon and the Brazilian highlands whereas it reaches southeastern Brazil by November (e.g., Vera et al. 2006a; Marengo et al. 2010, and references cited therein). The mature phase of the SAMS occurs from late November to late February, when large amounts of precipitation fall across the Amazon basin (Wang and Fu 2002). During this phase, the monsoon core is located over central Brazil. The convection produced by the southern Amazon wet season and the South Atlantic Convergence Zone (SACZ) is an important feature of the SAMS mature phase (Lenters and Cook 1995). The monsoon upper-level circulation is characterized by the establishment of a strong anticyclone known as the "Bolivian High", which is a response to the strong convective heating over the Amazon and central Brazil. Throughout this evolution, important moisture amounts are transported by a northerly low-level cross-equatorial flow (Wang and Fu 2002) and the South American low-level jet, which transports moisture between the Amazon and the La Plata basins (Berbery and Barros 2002). During March to May, the regions of large precipitation over subtropical South America reduce in size and migrate slowly toward the equator, indicating the retreat of the SAMS.

Different studies have focused on the variability of the American monsoons at different timescales. This variability appears to be partially modulated by both local changes of sea surface temperatures (SSTs) and anomalies induced by the remote influence of different ocean-atmosphere variability modes (Vera et al. 2006a and

references therein). The NAMS is affected at interannual and interdecadal time scales by the Pacific Decadal Oscillation (PDO), the El Niño Southern Oscillation (ENSO), the Atlantic Multidecadal Oscillation (AMO), and the Arctic Oscillation (AO) (e.g., Higgins and Shi 2000; Enfield et al. 2001; Castro et al. 2001, 2007; Schubert et al. 2004; McCabe et al. 2004; Seager et al. 2005; Hu and Feng 2008, 2010; Kushnir et al. 2010; Mo 2010). On the other hand, the SAMS is mainly influenced by the Atlantic SST anomalies (Mechoso et al. 1990; Giannini et al. 2001) although the PDO and ENSO also contribute to rainfall variability over the region (Moura and Shukla 1981; Pisciottano et al. 1994; Grimm et al. 1998; Marengo et al. 2004). The SST changes associated with these ocean-atmosphere variability modes influence the land-sea thermal contrast necessary for monsoon circulation and/or induce circulation anomalies that modify the moisture transport to both monsoon regions.

Monsoon precipitation over the Americas is also affected by intraseasonal activity related to the Madden-Julian oscillation (MJO; Madden and Julian 1994). Such an influence on the NAMS could be induced by changes in tropical cyclones activity associated with the MJO (Higgins and Shi 2001) or modulation of tropical easterly wave and gulf surge activity (Higgins et al. 2004). On the other hand, the MJO modulates the persistence of intense SACZ events (Carvalho et al. 2004), which in turn affect the SAMS.

Large scale circulations associated with teleconnection patterns such as the Pacific-North American (PNA) and the Pacific-South American (PSA) patterns also modulate monsoon activity over both continents. The PNA pattern is associated with changes in the upper-troposphere NAMS anticyclone (Higgins et al. 1998) whereas the PSA pattern causes anticyclonic (cyclonic) anomalies that enhance (reduce) precipitation over southeastern South America (Grimm et al. 2000). Although both patterns are partially influenced by ENSO, other independent factors also contribute to their variability (Higgins et al. 2000b; Silvestri and Vera 2003).

In addition, land surface conditions such as evaporation and recycling (Anderson et al. 2004; Li and Fu 2004; Zhu et al. 2007), synoptic-scale transient systems (Gonzalez et al. 2007; Douglas and Englehart 2007), and cold air incursions (Li and Fu 2004; Raia and Cavalcanti 2008) also modulate monsoon rainfall over the Americas.

Recent publications have reviewed the main characteristics of the American monsoons, the recent advances in understanding their variability, and the most important challenges to improve the modeling, prediction, and predictability of these monsoon systems (Vera et al. 2006a; Marengo et al. 2010). Moreover, a unified view of the American monsoon systems has begun to emerge in association with the development of the World Climate Research Programme/Climate Variability and Predictability/ Variability of the American Monsoon Systems (WCRP/CLIVAR/VAMOS) program (Vera et al. 2006a). However, whether these monsoon systems have changed during the

recent decades and whether there exists an interaction between both systems is still not clear. Therefore, the investigation presented in this dissertation aims to identify the main changes in monsoon activity observed over the American monsoon regions during the last decades and the possible links between such changes.

This dissertation is divided in three main chapters. Each chapter corresponds to an independent manuscript, already published or in revision, where different data sets and approaches were used to answer the scientific questions raised. Chapter 2 focuses on the study of cloud changes over the Amazon forests, which lead to changes of the diabatic heating, important for the SAMS onset. Although rainfall variability and its recent changes over the SAMS domain and the Amazon basin has been investigated in the past, changes in cloudiness over these regions, which are deeply related to those in precipitation, have not been studied in detail. Since convection over the Amazon basin plays an important role during the SAMS, the main objective of Chapter 2 is to investigate whether cloudiness and surface solar radiation have changed over this region from 1984 to 2007, and if so, how these changes are linked to tropical decadal climate variability. The material presented in this chapter is already published in *Climate Dynamics* (Arias et al. 2010).

Chapter 3 investigates the changes in the NAMS regime during 1948-2009 with particular emphasis on its retreat phase. Although the NAMS onset and its variability have been widely documented, the variability of its retreat has not received as much

attention. For this reason, the main objective of Chapter 3 is to identify the possible changes in the decay phase of the NAMS during the last decades, their implications to the monsoon strength, and their possible causes. The material discussed in this chapter is under review by *Journal of Climate* (Arias et al. 2011).

Finally, Chapter 4 combines the results obtained in Chapter 3 with those documented by Fu et al. (2011). In particular, Fu et al. (2011) showed evidence of a lengthening of the dry season over the southern Amazon since 1978 in association with a delayed onset of the wet season whereas Chapter 3 identifies a shorter and weaker NAMS due to an earlier retreat of the monsoon. Thus, the ultimate goal of this chapter is to determine whether there is a common factor that induces such changes in the American monsoon systems or they are the consequence of independent and unrelated causes. This chapter corresponds to a third publication to be submitted to *Journal of Climate* in the next weeks (Arias and Fu 2011). In addition, the author of this dissertation also contributed to the research presented by Fu et al. (2011), especially to the analysis of the wet season onset and the dry season length over the southern Amazon and its links to thermodynamic stability.

Each one of the chapters described above is organized using the same structure. Thus, they are presented in five sections: (i) introduction, (ii) data and methodology description, (iii) results and their analyses, (iv) discussion, (v) and concluding remarks.

Finally, a fifth chapter summarizes the global conclusions and findings obtained from this dissertation.

Chapter 2

Changes in cloudiness over the Amazon rainforests during 1984-2007

2.1. Introduction

Tropical forests contain as much as 40% of the carbon stored as terrestrial biomass and account for 30 to 50% of terrestrial productivity (Phillips et al. 1998). Approximately 55% of the contingent rainforest is located in the Amazon basin. This river basin also provides ~18% of global fresh water discharge. Through its control on evapotranspiration and runoff, the Amazon rainforest plays an important role in regulating the water cycle in this basin. The Amazon hosts the wettest tropical rainforest with a mean annual rainfall of 1500 to 3000 mm. These forests exhibit flushes of new leaf growth with increased photosynthesis in the dry season that closely coincide with seasonal peaks in solar irradiance (Myneni et al. 2007; Wright and van Schaik 1994), indicating that photosynthesis in these rainforests is radiation limited (Shuttelworth 1989), instead of water limited. The balance of the Amazon forest is primarily determined by land use and climate change and has important consequences to the global carbon and water cycle.

Recent studies have reported a widespread increase of the growth and mortality rates of mature rainforest (Phillips et al. 1998; Nemani et al. 2003; Lewis et al. 2004a). Such a growth rate increase is more robust over the forests that are least disturbed by

human activities (e.g. the western Amazon), suggesting that a direct impact of land use is unlikely to be the cause. Several other causes have been hypothesized including CO_2 fertilization, climate change, increasing aerosol induced diffuse light, and nutrient recycling (Laurance et al. 2004; Nemani et al. 2003; Gu et al. 2003; Artaxo et al. 2002, Lewis et al. 2004b). Among them, CO_2 fertilization has received the most attention (Lewis et al. 2004a,b; Laurance et al. 2004). However, Nemani et al. (2003) and Ichii et al. (2005) suggested that the increased rate of forest growth is too large to be explained by CO_2 fertilization alone and proposed changes in solar radiation, most likely due to changes in cloudiness, as a possible contributor. However, whether cloudiness has significantly changed over the tropical forests, and if so, what is the cause of such a change has not been clear.

Decadal changes of cloudiness over the global tropics have been previously detected (Wieliki et al. 2002; Chen et al. 2002). Over South America, Warren et al. (2007) found a declining trend in cloudiness by analyzing an in-situ product. Other studies indirectly associated with cloudiness suggest mixed conclusions. The analysis of long-term rain gauges in the Amazon basin suggest that decadal change of rainfall is insignificant over the southern Amazon (5°-15°S) and marginally significant in the northern Amazon (5°S-5°N; Marengo 2004). Although the decadal runoff changes are significant, such changes have been attributed either to evapotranspiration changes (Gedney et al. 2006) or to land use (Coe et al. 2009). The association of these previous studies with decadal changes of cloudiness is not clear.

What processes could potentially cause decadal variability of the cloudiness over the Amazon? Many previous studies have explored the empirical links between rainfall changes in South America and several well-known sources of decadal variability in the tropics. For example, Marengo (2004) identified a correlation between wetter conditions over the entire forest during 1946-1975 associated with the cold phase of the Pacific Decadal Oscillation (PDO; Mantua et al. 1997) and drier conditions over the western Amazon during 1976-1998 associated with the warm phase of the PDO. Kayano and Andreoli (2007) found that El Niño-Southern Oscillation (ENSO) effects in rainfall over South America are enhanced (weakened) when ENSO and the PDO are in the same (opposite) phases. Using a set of model simulations, Knight et al. (2006) show that the positive Atlantic Multidecadal Oscillation (AMO; Kerr 2000) phase is associated with a northward displacement of precipitation over the tropical Atlantic Ocean, along with a northward cross-equatorial wind anomaly. These changes imply a shift in the mean Intertropical Convergence Zone (ITCZ) to the north of its climatological March-April-May (MAM) position, and hence a reduction in northeastern Brazil rainfall.

The positive phase of the Indian Ocean Dipole (IOD; Saji et al. 1999) also has been found to be correlated with an anomalous divergence and negative rainfall anomaly over central Brazil (Chan et al. 2008). Saji and Yamagata (2003) showed that positive IOD events are associated with warm land surface anomalies and reduced rainfall over

Brazil. How the changes of these tropical decadal modes influence cloudiness over the Amazon has not been investigated thoroughly.

In addition to tropical influences, the Amazon rainfall is also modulated by extratropical variability. Wave trains extending along the south Pacific link convective pulses to the South Pacific Convergence Zone (SPCZ) and South Atlantic Convergence Zone (SACZ) regions (Kalnay et al. 1986; Grimm and Silva Dias 1995; Nogues-Paegle and Mo 1997; Lenters and Cook 1995). Positive rainfall anomalies in the SACZ region are, in turn, associated with negative rainfall anomalies in the Amazon on both intraseasonal and interannual scales (e.g., Nogues-Paegle and Mo 1997; Liebmann et al. 2004). In addition, Fu et al. (2001) reported that a wave train anomaly in the south Pacific and South American sector could produce upper level cyclonic conditions that potentially suppress precipitation over the eastern Amazon.

Although rainfall variability over the Amazon basin has been investigated in the past, changes in cloudiness over these forests have not been studied in detail. This work investigates whether cloudiness and surface solar radiation have changed over this region from 1984 to 2007, and if so, how these changes are linked to tropical decadal climate variability. To answer this question, the trends in cloudiness and solar incoming radiation over the Amazon basin and their links to decadal variability over the adjacent oceans are shown. In addition, the underlying mechanisms that have contributed to these observed links are discussed. This chapter is organized as follows. Data and methodology are

described in section 2.2. Results are presented in section 2.3. The implications of these results to the growth of the Amazon rainforests are discussed in section 2.4. Finally, conclusions are presented in section 2.5.

2.2. Data and methodology

The International Satellite Cloud Climatology Project (ISCCP) cloudiness and solar incoming radiation, and the National Oceanic and Atmospheric Administration (NOAA) interpolated Outgoing Longwave Radiation (OLR) datasets were analyzed in order to determine the changes of cloudiness and the resultant change of downward surface solar radiation over the Amazon during the period 1984-2007. Other variables such as surface temperature, relative and specific humidity, vertically integrated moisture transport (VIMT), sea surface temperature anomalies (SSTA), as well as other well-established indices of sea surface temperature (SST) variability were also studied to uncover the physical processes associated with regional changes of cloudiness over the Amazon basin. The trends of these variables were estimated using the non-parametric Mann-Kendall test (Sen 1968). Correlation and composite analyses were used to link cloud cover variability in South America with tropical climate variability. Due to differences in rainfall seasonality between the northern and southern Amazon regions (Wang and Fu 2002; Marengo 2005), the Amazon basin was divided in two parts: the

northern (70°W-50°W, 5°N-5°S) and the southern Amazon (70°W-50°W, 5°S-15°S) (Fig. 1).

Monthly data from the ISCCP database for shortwave (SW) down-welling radiation (FD datasets) and clouds (D2 datasets) with a 2.5-degree resolution during the period 1984-2007 (Rossow et al. 1996; Rossow and Schiffer 1999; Zhang et al. 2004), available at ISCCP website (http://isccp.giss.nasa.gov/index.html) was used. ISCCP-FD is a product of the Goddard Institute for Space Study (GISS) radiative transfer model calculation using inputs from the ISCCP cloud product (D1), the Television Infrared Observation Satellite (TIROS) Operational Vertical Sounder (TOVS) data, and the Total Ozone Mapping Spectrometer data, along with other ancillary data for specifying the radiative properties of the atmospheric and surface (Zhang et al. 1995; Zhang et al. 2004). Thus, the changes of surface downward solar radiation are mainly a result of the cloudiness change in the ISCCP data.

Recent studies have highlighted the sensitivity of the ISCCP cloudiness to changes in satellite viewing angle caused by satellite reposition (Campbell 2004; Norris 2005; Evan et al. 2007). Norris (2005) found that an increase of the number of geostationary satellites over time has produced a tendency towards lower viewing angles at many locations, generating an apparent decline in the ISCCP planetary albedo and cloud cover. However, not all the types of clouds are equally affected by changes in satellite viewing angle. The low-level clouds top temperature is closer to the background

clear sky temperature and thus is more sensitive to small temperature changes due to the shift of satellite viewing angle than that of the middle and high-level clouds.

OLR data was obtained from polar-orbiting satellites. Its biases due to orbital drift or changes in satellite are uncorrelated to the geostationary satellite repositions. Thus, monthly NOAA interpolated OLR on a 2.5˚ resolution (Liebmann and Smith 1996) was used to verify the changes detected by the ISCCP data.

Surface temperature, relative humidity, and specific humidity records corresponding to *in situ* data interpolated in a 5 x 4-degree grid for the period 1976-2005 were used. These records were provided and described by Dai (2006).

Monthly streamfunction at 0.22 sigma level (~200 hPa) and the VIMT calculated using the NCEP-NCAR Reanalysis (Kalnay et al. 1996) were also used. For calculations of the VIMT, daily 2.5-degree grid data for zonal and meridional wind and specific humidity at different pressure levels from the National Center for Environmental Project-National Center for Atmospheric Research (NCEP-NCAR) Reanalysis (Kalnay et al. 1996) were used. Since atmospheric moisture is an order of magnitude lower above the mid troposphere compared to that in the lower troposphere, the vertical integration was done between 1000 hPa and 600 hPa levels over the northern Amazon and southern Amazon, respectively. VIMT was calculated by integrating the moisture flux over the box defined by the limits of the domain in consideration, as follows (Li and Fu 2004)

$$\mathrm{VIMT} = \frac{\left[(\overline{\mathrm{uq}_2} - \overline{\mathrm{uq}_1}) + (\overline{\mathrm{vq}_2} - \overline{\mathrm{vq}_1})\right]}{\rho A}$$

$$\overline{\mathrm{uq}_i} = \left[\frac{1}{g}\int_{Lat1}^{Lat2}\int_{p2}^{p1} \mathrm{uq}\,\mathrm{dp}\,\mathrm{dy}\right]_{Loni} \qquad (1)$$

$$\overline{\mathrm{vq}_i} = \left[\frac{1}{g}\int_{Lon1}^{Lon2}\int_{p2}^{p1} \mathrm{vq}\,\mathrm{dp}\,\mathrm{dx}\right]_{Lati}$$

where g is acceleration of gravity (m/s^2), u is zonal wind (m/s), v is meridional wind (m/s), q is specific humidity (kg/kg), p_1 is pressure in the surface layer ($1000\ hPa$), p_2 is pressure in the upper layer ($600\ hPa$), *Lon1* is longitude for the left side of the box, *Lon2* is longitude for the right side, *Lat1* is latitude for the southern side, *Lat2* is latitude for the northern side, ρ is density of water ($1000\ kg/m^3$), and A is the area of the box (m^2). Integrations were averaged on a monthly basis. Units for VIMT are given in *mm/day* and positive values represent convergence.

SST data was obtained from the extended reconstructed monthly mean SST from the NOAA Climate Diagnostic Center (CDC) (Reynolds 1988). The spatial resolution of the data is 2˚x2˚. For the period of analysis considered here, the SST was derived from blended satellite and in situ measurements.

To identify how the cloudiness changes are linked to tropical climate variability, indices for the PDO, the expansion of the western Pacific warm pool (WPWP), the IOD,

the AMO, and the tropical Atlantic SST gradient (SSTG) were considered. The AMO index is available from http://www.cdc.noaa.gov/data/timeseries/AMO/ (Enfield et al. 2001). The PDO index was obtained from http://jisao.washington.edu/pdo/PDO.latest (Mantua 1997). The intensity of the IOD is represented by the Dipole Mode Index (DMI) and is available at http://www.jamstec.go.jp/frsgc/research/d1/iod/dmi_nature.index. The WPWP index was defined as the area over the equatorial Pacific between 20°S-20°N and 140°E-150°W, where SSTs are higher than 28°C. This index is considered to be an overarching index of western Pacific variability. The tropical Atlantic SSTG was defined as the area mean SST difference between the north (5°N-25°N, 60°W-30°W) and south (5°S-25°S, 30°W-0°E) Atlantic (Giannini et al. 2004). Finally, the indices to characterize ENSO variability (Niño3, Niño4, and Niño3.4) were obtained from http://www.cdc.noaa.gov/data/climateindices/List/.

Correlation coefficients were computed to identify the links between the cloud changes over the Amazon and the circulation changes over the adjacent oceans. Trends were removed before computing correlations since the existence of a trend can induce spurious correlations that are not related to the interannual variability but only to the decreasing/increasing trends of the time series. The statistical significance of the correlations was determined by the Monte Carlo Test for spatial pattern (Livezey and Chen 1983). A total of 1000 iterations were performed and a threshold for statistical significance equal to 95% (p=0.05) was used.

Composites for positive (> 1 standard deviation, σ) and negative phases (< -1σ) of (i) the PDO index, (ii) the AMO index, (iii) the WPWP index, (iv) the tropical Atlantic SSTG, and (v) the Indian Ocean DMI were computed. Given the limited occurrence of these events relative to the total temporal samples, composite analysis would more clearly highlight the cloud changes over the Amazon associated with the aforementioned indices than that provided by the correlation analysis. These composites were obtained with and without the ENSO influence on each index. The statistical significance of the difference between the composites for the positive and the negative phases was tested using a bootstrap test (Efron 1979). A total of 1000 iterations with a threshold for statistical significance equal to 95% (p=0.05) were performed using the bias corrected and accelerated percentile method for the confidence interval estimation.

Correlation analysis was used to identify the SSTAs patterns, thus the decadal SST variability modes that are linked to the cloud changes over the Amazon. The composite cloud changes associated with strong anomalies of such decadal modes were thus analyzed.

2.3. Results

2.3.1 Changes in surface incoming radiation and convective cloudiness over the Amazon

Figs 1a)-1d) show the seasonal trends of the ISCCP SW down-welling radiation (contours) during 1984-2007 over the tropical Americas. Boxes show the geographical location for the northern and southern Amazon regions. The linear trends shown in these figures are statistically significant at the 5% level according to the Mann-Kendall test (Sen 1968). The strongest trends occur in September-October-November (SON) over the entire Amazon. A general increase of solar SW radiation over the southern Amazon domain also occurs during the December-January-February (DJF) and MAM seasons. Decreasing total cloud cover over the Amazon is observed (not shown), in agreement with Warren et al. (2007), who also found a declining trend in cloudiness from their analysis of an in-situ product during the period 1971-1996 (see their Fig.5).

The ISCCP data show a significant decrease of high clouds during DJF and MAM over the southern Amazon and during SON over the entire Amazon in Fig. 1e)-h). Areas of decreasing high cloudiness over the Amazon generally coincide with increasing SW down-welling radiation, except over the northwestern Amazon during MAM, when the reduction of high clouds occurred mainly over the southern domain (Fig. 1). By contrast, low and middle clouds do not show any significant change (not shown). Fig. 2 shows the

domain average time series for total and high clouds over the northern Amazon during SON and the southern Amazon during DJF, and the distribution of the ISCCP satellite reposition dates during the period considered here (1984-2007). The high cloud changes mostly occur well within the field of view of the geostationary satellites, where the change of satellite viewing angle has less impact on cloud detection than that near the edge of the satellite field of view. Thus, the satellite changes do not appear to cause a systematic decrease of total and high clouds over the region. By contrast, low-level clouds over the oceans do have a significant decrease (not shown) along the edge of the satellite field of view that matches the geostationary ‘‘footprints’’ due to satellite viewing angle change (Evan et al. 2007).

To verify if these changes in ISCCP high clouds are consistent with changes in OLR, monthly NOAA interpolated OLR was used. Since OLR includes changes from all type of clouds, water vapor, and surface temperatures, only values lower than 240 W/m^2 were considered in order to be consistent with the ISCCP high clouds. An OLR value of 240 W/m^2 is an appropriate threshold for detecting deep convection (Murakami 1980; Lau and Chan 1983). Fig. 2 shows the domain averaged OLR over both the northern and the southern Amazon for the seasons with the largest changes in high clouds. In general, the reduction of high clouds is consistent with a statistically significant increase of OLR for both DJF and SON on decadal timescale. The spatial pattern of the OLR changes (not shown) agrees with that for the high clouds (Fig. 1). The general consistency between these two fields measured by different satellite-born instruments suggests that the change in ISCCP high clouds is unlikely an artifact of satellite measurement biases.

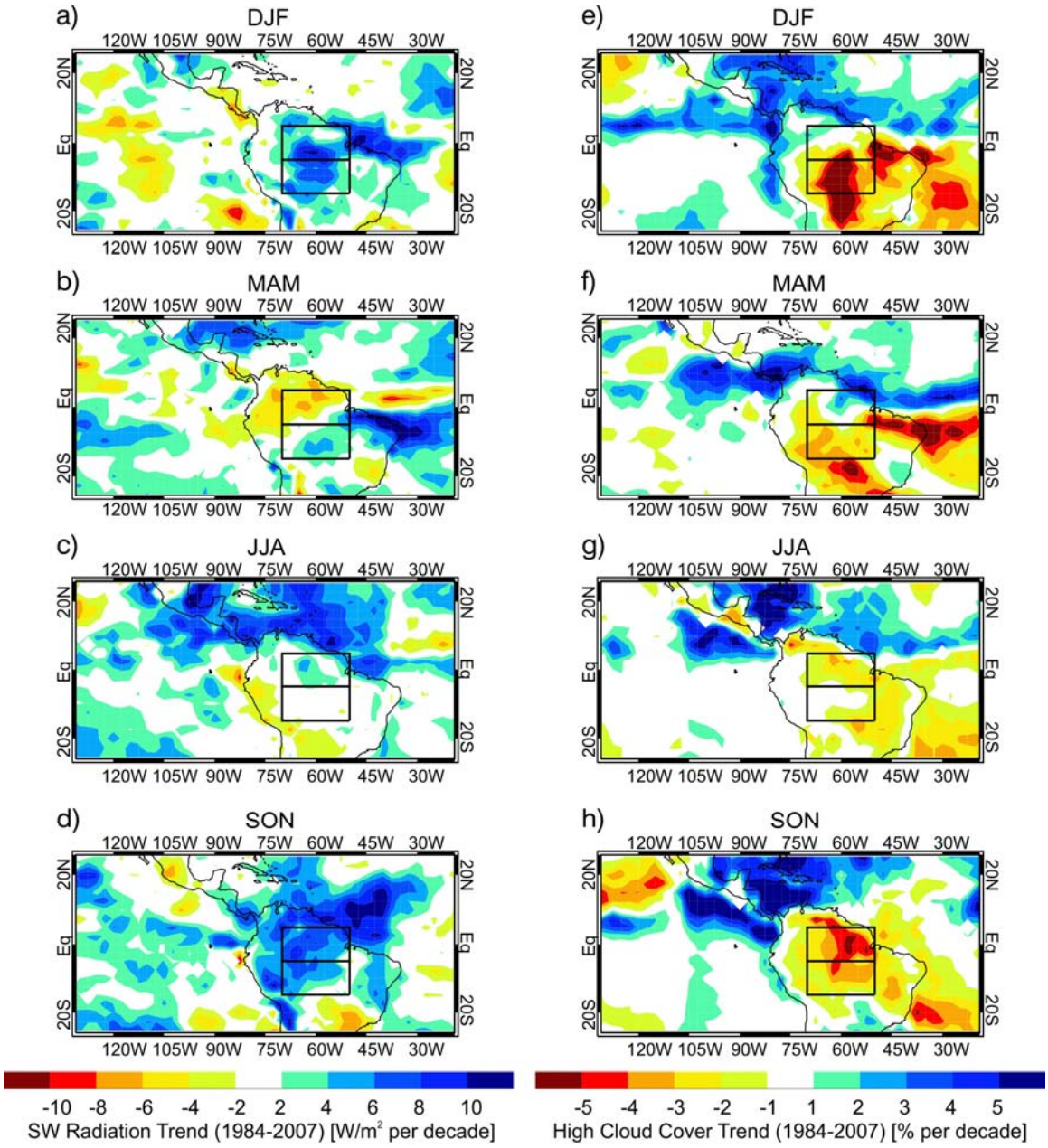

Fig. 1 Seasonal trend in a)-d) SW down-welling radiation and e)-h) high cloudiness from ISCCP during 1984-2007 over the Tropical Americas. Trends shown are statistically significant at the 5% level according to the Mann-Kendall test with Sen's statistics (Sen 1968). Boxes represent northern and southern Amazon domains, respectively.

The interannual variations of the SON OLR over the northern Amazon agree with those of the high clouds, except during 1997. The DJF OLR averaged over the southern Amazon is out of phase with the high clouds during some years. This discrepancy is presumably caused by insufficient diurnal sample of the OLR. During the wet season in the southern Amazon (DJF), convection is contributed by two different types of clouds associated with different large-scale atmospheric circulation (Rickenbach et al. 2002). These two convective cloud types have different diurnal cycles (Rickenbach 2004). Interannual variations of the large-scale circulation can alter the diurnal cycle of convection over the southern Amazon. The OLR daily value is derived from two measurements at a twelve-hour interval whereas the ISCCP daily value is computed from eight measurements at three-hour intervals. Thus, the monthly average of the daily OLR would be different from that corresponding to the daily ISCCP high cloud amount, even for a moderate change in diurnal cycle. Another possible cause for this discrepancy relies on the fact that the NOAA OLR measurements (broad band channel) are sensitive to atmospheric temperatures, water vapor, and the presence of clouds, while the ISCCP infrared channel is within the atmospheric window spectra, mainly sensitive to clouds. Thus, changes in atmospheric temperatures and water vapor could induce differences between OLR and high clouds measurements.

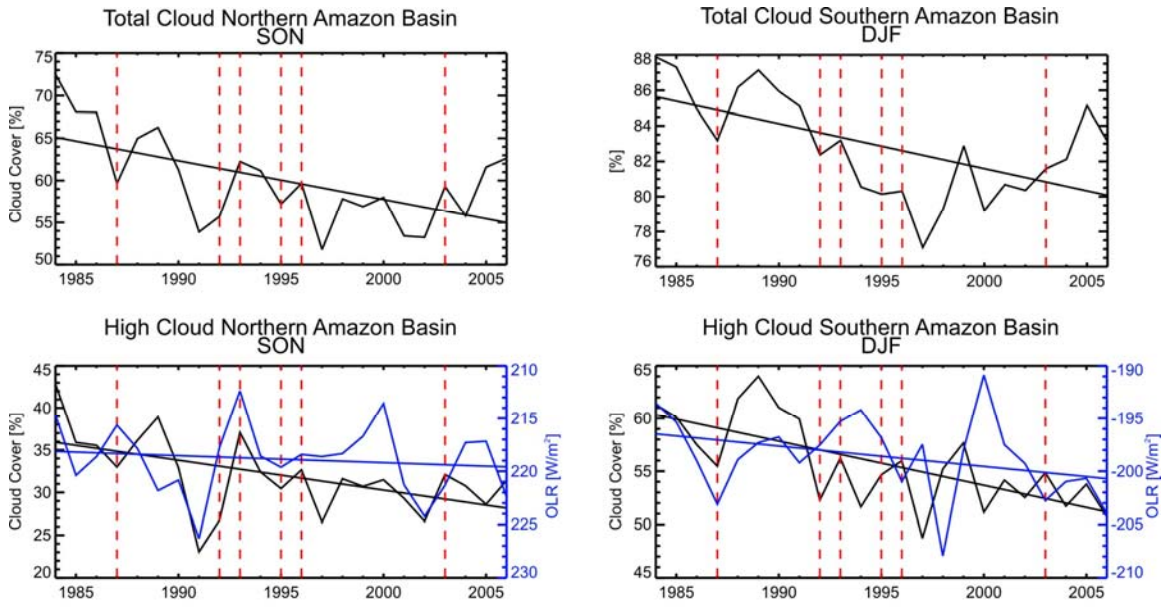

Fig. 2 Domain average time series for total and high clouds (black curves) and OLR (blue curves) during SON (DJF) over the northern (southern) Amazon. Domain average OLR is obtained for values lower than 240 W/m^2. Red dotted lines indicate the dates of satellite reposition according to ISCCP D2 data set documentation (available at http://isccp.giss.nasa.gov/index.html). Solid lines represent statistically significant trend at the 5% level according to the Mann-Kendall test with Sen's statistics (Sen 1968).

Several previous studies suggested that the DJF rainfall (either measured by station reported value or OLR estimated) has probably increased over the Amazon basin during the recent decades (Chu et al. 1994; Chen et al. 2001). These seemingly different results from the ones discussed here may be due to the use of different geographic domains and periods of analysis. For example, Chu et al. (1994) show a general decrease of DJF OLR during the period 1974-1990 over the region 0˚–5°N and 78°W–70°W, which is outside the domains considered in this study. The ISCCP high clouds and the NOAA OLR averaged over this region during DJF (not shown) indicate decreasing OLR

and increasing high clouds, consistent with the increasing rainfall reported by Chu et al. (1994).

On the other hand, Chen et al. (2001) reported an increase of precipitation over the Amazon from 1958-1977 to 1978-1998 for a geographic domain that is significantly larger than the one used in this study (15°S–15°N, 70°W–50°W). Since the high cloud changes during DJF are negative over the southern domain and insignificant with slightly positive trend over the northern domain (Fig. 1e), the cloud change averaged over the region considered by Chen et al. (2001) becomes insignificant for the period 1984-2007. The OLR and high clouds variations were compared with Chen et al.'s (2001) results for the period of 1984-1996, when the ISCCP data overlaps with their second analysis period. Results show negative OLR changes over the southern Amazon before the mid-90's, consistent with the increasing rainfall reported by Chen et al. (2001). These increasing OLR and decreasing high clouds mainly occurred after the mid-90s over the Amazon, especially over the southern domain.

Furthermore, taking in consideration the relatively short analysis period in this study, the sensitivity of the trends of the high clouds and OLR to different time periods within 1984-2007 was tested (not shown). Results indicate that the spatial pattern reported in Fig. 1 remains generally the same.

2.3.2 Changes in surface temperature and humidity

Table 1 shows the seasonal trends during 1984-2005 for temperature, specific humidity, and relative humidity from the surface station data described by Dai (2006). Relative humidity decreases for June-July-August (JJA) and SON over both the northern and the southern Amazon. This decrease is more highly correlated with warmer surface temperatures than with declining specific humidity (see Table 1). A significant increase of surface temperature is also observed by Malhi and Wright (2004). The warmer surface temperatures over the Amazon are not purely due to the increases in solar SW radiation. Previous observations have shown that the change of daytime temperature is primarily controlled by changes of surface solar radiation and wetness in the Amazon whereas the change of nighttime temperature is primarily influenced by water vapor and other greenhouse gases.

The decreasing relative humidity over the Amazon basin is consistent with the observed decreasing cloudiness over the region. The radiosonde data from the University of Wyoming show reductions of the atmospheric buoyancy over the southern Amazon (not shown), consistent with atmospheric instability reductions over the region.

Table 1 Seasonal trends for surface data from Dai (2006) and VIMT from NCEP-NCAR Reanalysis averaged over northern and southern Amazon (see geographical location in Fig. 1). Values represent the total change in each variable during 1984-2005 (1984-2007 for VIMT). Values in bold are statistically significant at the 5% level according to the Mann-Kendall test with Sen's statistics (Sen 1968).

	DJF	**MAM**	**JJA**	**SON**
		Northern Amazon		
q (g/kg)	0.24	0.00	-0.15	-0.11
RH (%)	-1.19	1.22	**-4.05**	**-4.92**
T (°C)	**0.68**	0.00	**0.52**	**1.01**
VIMT (mm/day)	0.85	**1.89**	**-1.60**	**-1.83**
		Southern Amazon		
q (g/kg)	**0.82**	**0.52**	-0.39	-0.09
RH (%)	**1.70**	**2.55**	-0.14	-2.06
T (°C)	**0.53**	0.46	**0.66**	0.45
VIMT (mm/day)	**1.24**	-0.42	**-0.97**	-0.42

2.3.3 Possible causes of the changes in cloudiness over the Amazon

2.3.3.1 Changes in vegetation and land use

Whether changes in vegetation and land use affect cloudiness over the Amazon forests is explored by comparing the pattern of decreasing cloudiness (Fig. 1) and that of deforestation available in literature. Results from World Wildlife Fund (WWF) published by BBC News (http://news.bbc.co.uk/2/hi/americas/7360258.stm) indicate that the deforested regions are localized over the southern edge of the Amazon during 1970-1997, but a northward migration is observed during 1998-2006. These findings suggest that the southern and southeastern Amazon domains are more affected by recent deforestation while the northern Amazon remains less affected by such land use. Studies by Drigo and

Marcoux (1999) also show that the southern Amazon experienced more deforestation than the northern region during the period 1980-1990 (http://www.fao.org /sd/wpdirect/WPan0030.htm). The reductions of cloudiness shown in Fig. 1 occurred over the entire Amazon, at a much larger spatial scale compared to that of the deforestation. Thus, changes in vegetation and land use cannot be the primary contributors to the observed large-scale changes in cloudiness over the Amazon forests.

2.3.3.2 Links to decadal changes over the tropical Pacific and Atlantic Oceans

Most of the high clouds detected by the ISCCP satellites are optically thick cirrus clouds produced by deep tropospheric convection (Rossow et al. 1996). Thus, this investigation focuses on understanding the causes of the decreasing convection and rainfall over the Amazon basin. Many previous studies have shown a clear correlation between the convection and moisture transport changes and the interannual SSTAs in the Pacific or the Atlantic oceans. Changes in the mid-lower troposphere VIMT, which are determined independently from cloud observations, were examined to verify the cloud changes.

Table 1 shows a statistically significant decrease of VIMT over the northern Amazon during JJA and SON and over the southern Amazon during JJA, which is consistent with the decrease of high cloudiness independently detected by the ISCCP during the dry and transition seasons (Fig. 1). To determine whether these changes are

linked to external SST forcing, composite changes of high clouds during the positive and the negative phases (> 1σ and < -1σ, respectively; see section 2.2) of different ocean-atmosphere variability modes were calculated. The number of events in each phase corresponding to the different variability indices considered here is shown in Table 2. The statistical significance of the difference between composites was tested using the bootstrap test (Efron 1979).

Table 2 Number of years with statistically significant at 5% level positive (PP) and negative (NP) phases for the SST variability indices considered here. ENSO contributions are removed. Positive (negative) phases are selected as those years with an index value above (below) 1σ of its climatological value. Statistical significance is tested using a boostrap test (Efron 1979).

	DJF		**MAM**		**SON**	
	NP	PP	NP	PP	NP	PP
AMO	5	6	5	3	5	5
PDO	3	4	5	5	5	5
WPWP	4	4	4	4	3	4
DMI	5	2	4	5	3	4
Atlantic SSTG	4	1	3	4	4	5
Atlantic SSTG (No AMO)	3	3	2	2	3	2

Since ENSO-related changes could be dominant at decadal scales during the period considered here, these contributions were removed from all the SST variability indices. This was done by subtracting the temporal variations that are correlated with the ENSO index as determined by the linear regression from the original time series for any specific SST index (e.g., AMO, PDO, etc). The composites were obtained based on the residual time series of these indices. Results suggest that after the ENSO influence is

removed, changes in cloudiness due to the PDO and the DMI become insignificant for all the seasons, indicating that the effects of both the PDO and the IOD on the Amazon cloudiness cannot be separated from that of ENSO.

Although the AMO signal is correlated with the tropical Atlantic SSTG, previous studies suggest that it may be physically independent from the SST changes in the southern tropical Atlantic (Chang et al. 2006). To clarify the physical processes, especially that of the AMO, behind the influence of the tropical Atlantic SSTG, its correlation with the Amazon cloudiness with and without the AMO influence was analyzed.

The development of convection over the southern Amazon and its further migration to the northern Amazon are part of a characteristic cycle over the Amazon rainforest that produces seasonal differences between both regions: (i) DJF corresponds to the peak in rainfall over the southern Amazon, although there are still heavy precipitation events over this region during MAM, (ii) rainfall over the northern Amazon has its peak during MAM, and (iii) SON corresponds to the transition between dry and wet conditions over the southern Amazon. The analysis presented here is organized based on these seasonal patterns and the discussion will focus on the DJF, MAM, and SON seasons, when significant decrease of cloudiness has been detected.

a) DJF

Fig. 3 shows the linear trends of the DJF tropical SSTAs and the correlation between detrended SSTAs and detrended domain average high cloud for a) the northern and b) the southern Amazon. There is a general warming over the equatorial oceans, except over the south tropical Atlantic, where cooling is observed. Correlation between SSTAs and high clouds for both domains shows a strong link to the central and eastern Pacific SSTs, suggesting that the change of high cloudiness in the Amazon is especially sensitive to SST changes in these oceanic regions during austral summer. This link is consistent with the well documented relationship between rainfall changes over the northern Amazon and the Pacific SSTAs (Marengo 1992). In addition, Fig. 3a also suggests that warmer temperatures over the Indian Ocean are linked to decreasing high clouds over the northern Amazon. The correlation between the changes in high clouds over the southern Amazon and the equatorial central and eastern Pacific SSTAs is stronger than that estimated based on rain gauge data shown in previous studies (e.g., Marengo 1992).

Both the WPWP and the IOD can be affected by ENSO. To determine to what extent they are correlated with the cloudiness change over the Amazon independently of ENSO, ENSO-related SSTA changes were removed from both the WPWP and the IOD indices. The result shows that only the WPWP area is still significantly correlated to the cloud changes over the northern Amazon (-0.51), i.e., the western Pacific warm pool expansion is correlated with a decrease of high cloudiness over that region.

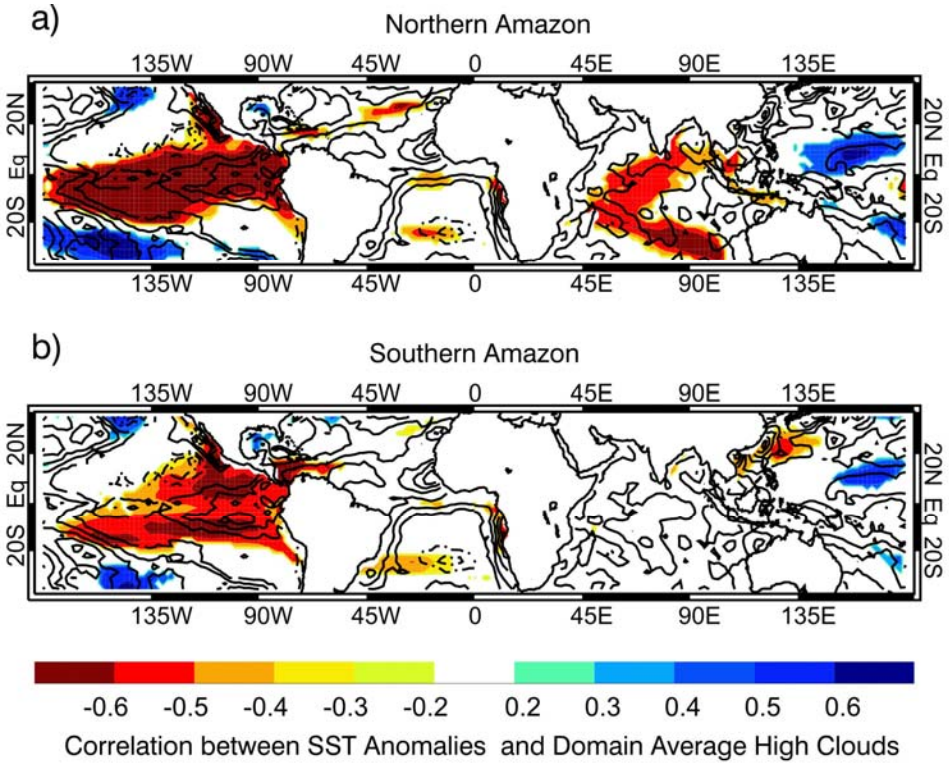

Fig. 3 DJF correlations (color shades) between detrended SST anomalies from NOAA-CDC and detrended domain average high level clouds over a) northern Amazon and b) southern Amazon. Correlations shown are statistically significant at the 5% level based on Monte Carlo test and the spatial patterns shown are also statistically significant at 5% level (Livezey and Chen 1983). Contours represent trends in SST anomalies during 1984-2007. Trends shown are statistically significant at the 5% level according to the Mann-Kendall test with Sen's statistics (Sen 1968). Contours are plotted with interval of 0.1°C per decade. Solid (dashed) contours represent warm (cold) SST anomalies.

Composite analyses for this season indicate that high clouds over the Amazon decrease during the western Pacific warm pool expansion events (not shown). To determine whether these changes are an artifact of the ENSO contribution to the increasing WPWP area, the changes of the WPWP index that are correlated with the ENSO index were removed. Since the warm pool expansion mainly occur over the central Pacific, the ENSO influence on the WPWP index was removed based on its

regression with the Niño4 index (i.e., SSTs averaged over the western Pacific domain bounded by 160°E-150°W and 5°S- 5°N). Significant changes in high clouds between the positive and the negative phases of the WPWP are still retained even after the removal of the ENSO influence (Fig. 4).

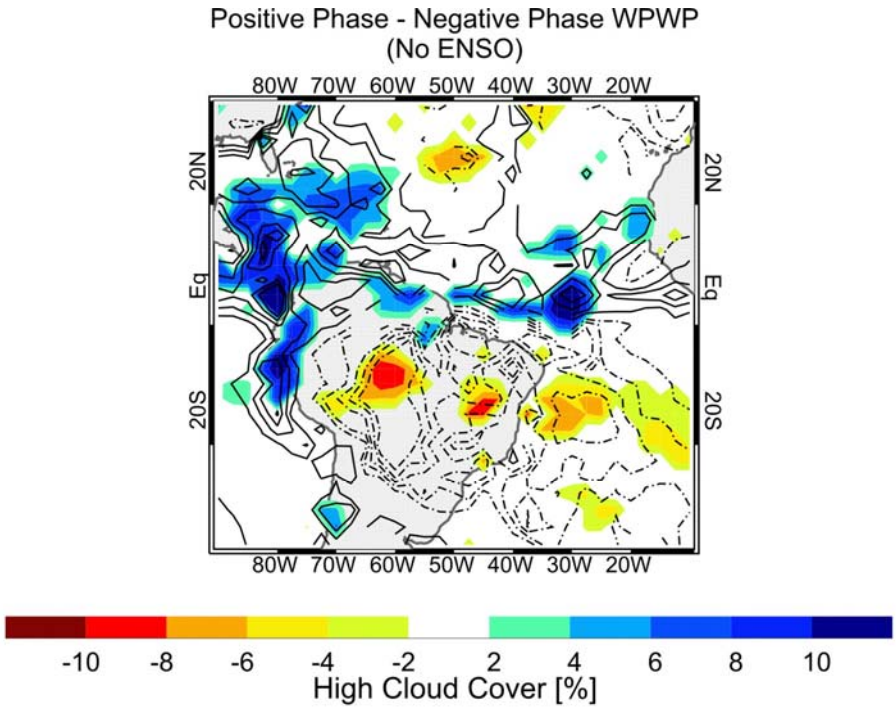

Fig. 4 Composite high cloud difference for positive and negative phases of the WPWP (No ENSO) for DJF. Statistical significance for difference is tested using a bootstrap test (Efron 1979) at 5% level. Contours indicate trends in high cloud anomalies statistically significant at the 5% level according to the Mann-Kendall test with Sen's statistics (Sen 1968). Solid (dashed) lines represent increasing (decreasing) clouds. Contours are plotted each 1% per decade.

b) MAM

Fig. 5 shows a positive SST gradient (warming on the north side and cooling on the south side of the equator) in the tropical Atlantic and a strong warming in the eastern Pacific during MAM. The decrease of high clouds over the southern Amazon is

correlated with these SST increases. The high cloud changes over the northern Amazon are weak (Fig. 1f), thus no significant correlations with SSTAs are detected (not shown).

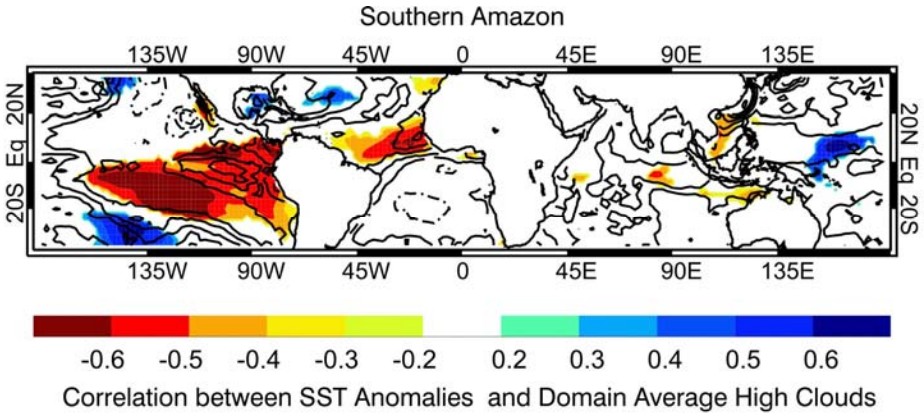

Fig. 5 Same as Fig. 3b but for MAM.

The Atlantic SSTG is dominated by the Atlantic meridional dipole mode (Nobre and Shukla 1996). This mode has the strongest variability during MAM and is controlled by the AMO and the southern Atlantic Ocean SSTAs. The composite changes of high clouds using the AMO index (Fig. 6) suggest a significant decrease of high cloudiness in the Amazon during the positive AMO phases. The dipole pattern of the high cloud change over the tropical Atlantic resembles the northward shift of the Atlantic ITCZ associated with the positive phase of the Atlantic meridional dipole mode (e.g., Nobre and Shukla 1996; Chiang et al. 2000). The spatial pattern of this cloudiness change also resembles that for the trend of high cloud change. The composites shown in Fig. 6 are statistically significant according to the bootstrap test (Efron 1979).

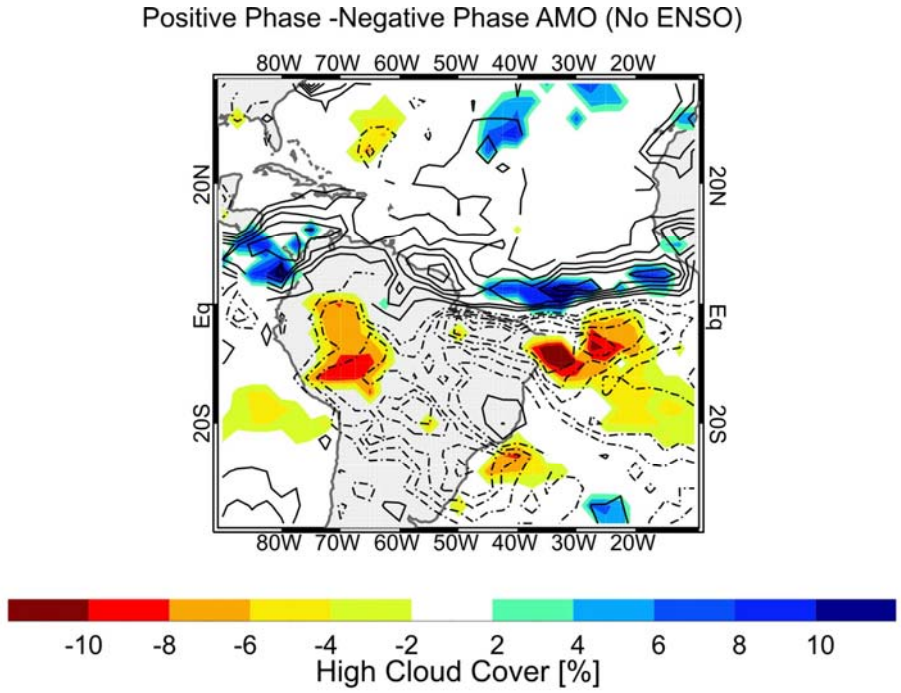

Fig. 6 Composite high cloud difference for positive and negative phases of the AMO (No ENSO) for MAM. Statistical significance for difference is tested using a bootstrap test (Efron 1979) at 5% level. Contours indicate trends in high cloud anomalies statistically significant at the 5% level according to the Mann-Kendall test with Sen's statistics (Sen 1968). Solid (dashed) lines represent increasing (decreasing) trends. Contours are plotted with interval of 1% per decade.

The composites using the Atlantic SSTG (not shown) also indicate reductions of high cloudiness over the southern Amazon when this gradient increases. However, after the removal of the AMO influence, the correlation between the high cloud changes over the Amazon and the Atlantic SSTG becomes insignificant. Thus, the decrease of high clouds in the southern Amazon during MAM is only consistent with the circulation changes associated with the positive phase of the AMO. Significant correlations between

high cloud change in the southern Amazon and the AMO (not shown) also support this result.

As shown in Fig. 5, high clouds over southern Amazon are negatively correlated with SSTAs over the eastern Pacific during MAM. This pattern is observed even after the eastern Pacific ENSO influence, as represented by the Niño3 index, is removed (not shown). Thus, the link between the eastern Pacific warming and the reduced high cloudiness over the southern Amazon appears to be statistically independent of ENSO.

c) SON

During this season, the decrease of high clouds in the northern Amazon is correlated with warmer SSTs in the central Pacific and cooler SSTs in the southern tropical Atlantic (Fig. 7). The decrease of high clouds in the southern Amazon, which is weaker than that in the northern Amazon, is correlated with cooler SSTs in the southern tropical Atlantic (Fig. 7b).

The composite difference of high clouds between the positive and the negative Atlantic SSTG phases is statistically significant, even when the AMO contributions are removed (Fig. 8a). Because the AMO is primarily associated with SSTAs in the northern tropical Atlantic, the above result confirms the correlation between high clouds and SSTAs over the southern tropical Atlantic shown in Fig. 7. Fig. 8a shows that high clouds decrease basin wide, especially in the western, central northern, and southern Amazon, when a strong positive Atlantic SSTG occurs in association with cooler SSTs in the

southern tropical Atlantic. The areas and pattern of decreasing clouds match the trend of decreasing high clouds in the western and central Amazon, suggesting that a change toward cooler SSTs in the southern tropical Atlantic probably contributes to the decrease of high clouds in this region.

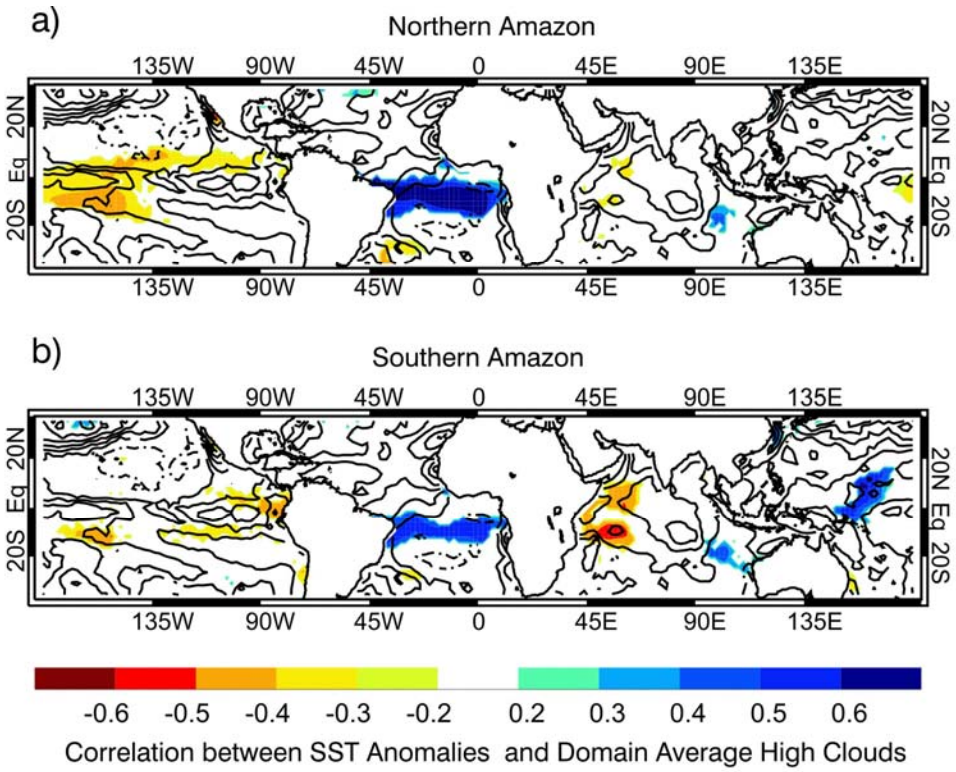

Fig. 7 Same as Fig. 3 but for SON.

Reductions of high clouds over the northeastern Amazon and the Nordeste region are also observed when the western Pacific warm pool expands during SON (see Fig. 8b). This is consistent with the correlation between the high cloud changes in the northern Amazon and the SSTAs in the tropical central Pacific shown in Fig. 7a. Fig. 8b suggests that the expansion of the western Pacific warm pool probably contributes to the

decreasing high clouds over western tropical South America. Results obtained from the correlation analysis are consistent with those of the composite analysis shown in Fig. 8 (the correlation coefficients over the region vary from -0.5 to -0.6 for the Atlantic SSTG and from -0.3 to -0.4 for the WPWP; not shown).

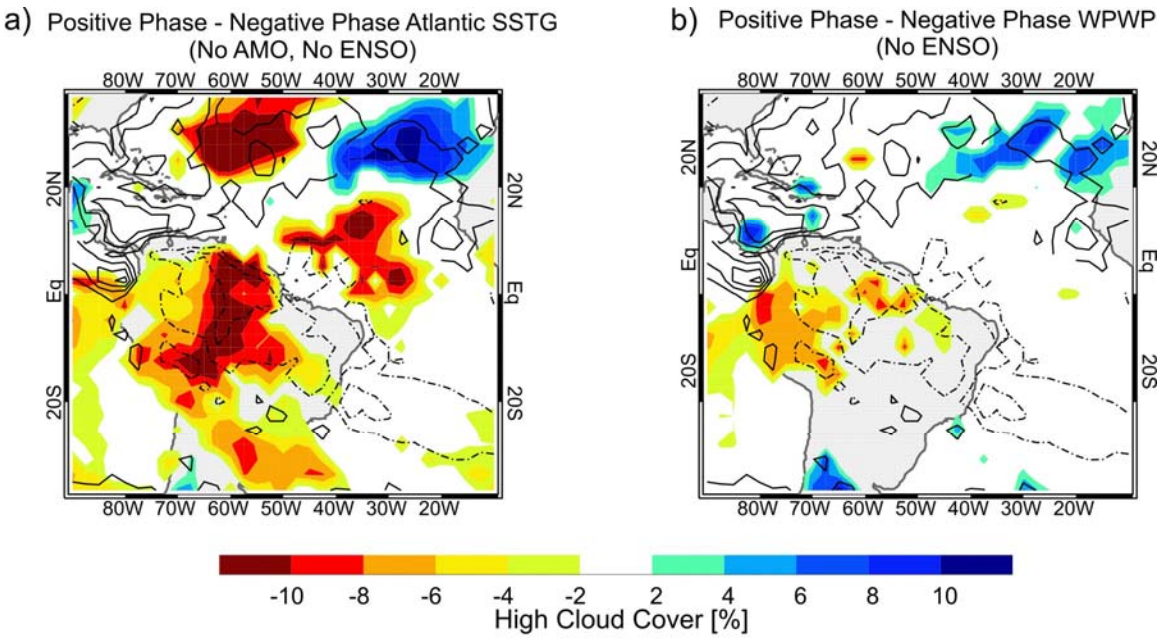

Fig. 8 Composite high cloud difference for positive and negative phases of a) the Atlantic SSTG (No AMO, No ENSO) and b) the WPWP (No ENSO) for SON. Statistical significance for difference is tested using a bootstrap test (Efron 1979) at 5% level. Contours indicate trends in high cloud anomalies statistically significant at the 5% level according to the Mann-Kendall test with Sen's statistics (Sen 1968). Solid (dashed) lines represent increasing (decreasing) trends. Contours are plotted with interval of 2% per decade.

2.3.3.3 The underlying dynamic processes

What processes are responsible for the observed relationship between the changes of cloudiness and the aforementioned ocean-atmosphere variability modes? Previous studies suggest two possible mechanisms: (i) an anomalous change of the direct thermal circulation either zonally or meridionally (e.g., Moura and Shukla 1981; Chiang and Sobel 2002; Neelin et al. 2003) and (ii) a change of the planetary wave trains from the tropical central Pacific to South America (e.g., Kalnay et al. 1986; Fu et al. 2001; Liebmann et al. 2004). The former would show clearly in seasonal mean correlations between changes in moisture transport and high clouds, whereas the latter would be dominated by transient disturbances instead of by seasonal mean anomalies.

The analysis discussed here and the correlations between VIMT and SSTAs (not shown) suggest that the changes of moisture transport over the northern Amazon are well correlated to SSTs changes; however, this relationship is very weak for the southern domain. This suggests that a decrease of moisture transport has likely contributed directly to the decrease of cloudiness in the northern Amazon (as previously suggested by Wang 2002 and Yoon and Zeng 2010), but not necessarily in the southern Amazon. Other dynamic mechanisms need to be explored.

Planetary wave trains link anomalies of convection in the SPCZ to that of the SACZ (Kalnay et al. 1986; Grimm and Silva Dias 1995; Nogues-Paegle and Mo 1997;

Lenters and Cook 1995; Fu et al. 2001). The latter is anti-correlated with rainfall variability in the Amazon (Liebmann et al. 2004). These anomalous wave trains could alter the equatorward incursion of the extratropical synoptic disturbances reaching South America, thus they would influence cloudiness. To test this hypothesis, composites for differential streamfunction at 0.22 sigma level (~200 hPa) between years with southern Amazon average high clouds above and below 1σ its climatology were estimated. The difference was tested using a bootstrap test (Efron 1979). The number of years with southern Amazon average high clouds above/below 1σ is six/four during DJF and three/five during SON from 1984 to 2007.

Figs. 9a and 9b show the trends in the 0.22 sigma level streamfunction during the period 1984-2007 for DJF and SON, respectively. Results indicate a stronger cyclone-anticyclone-cyclone tripole structure over the South Pacific-South America region, especially during SON, typically observed in the PSA wave trains (Fu et al. 2001). The relationship between upper tropospheric streamfunction and decreasing high clouds over the southern Amazon are shown in Figs. 9c and 9d. Blue (red) colors indicate statistically significant strengthening of the cyclonic (anticyclonic) circulation when high clouds are reduced over the southern Amazon. Composites for DJF and SON (Figs. 9c and 9d) show that the structure associated with the PSA wave trains is enhanced during those years when high cloudiness over the southern Amazon is reduced.

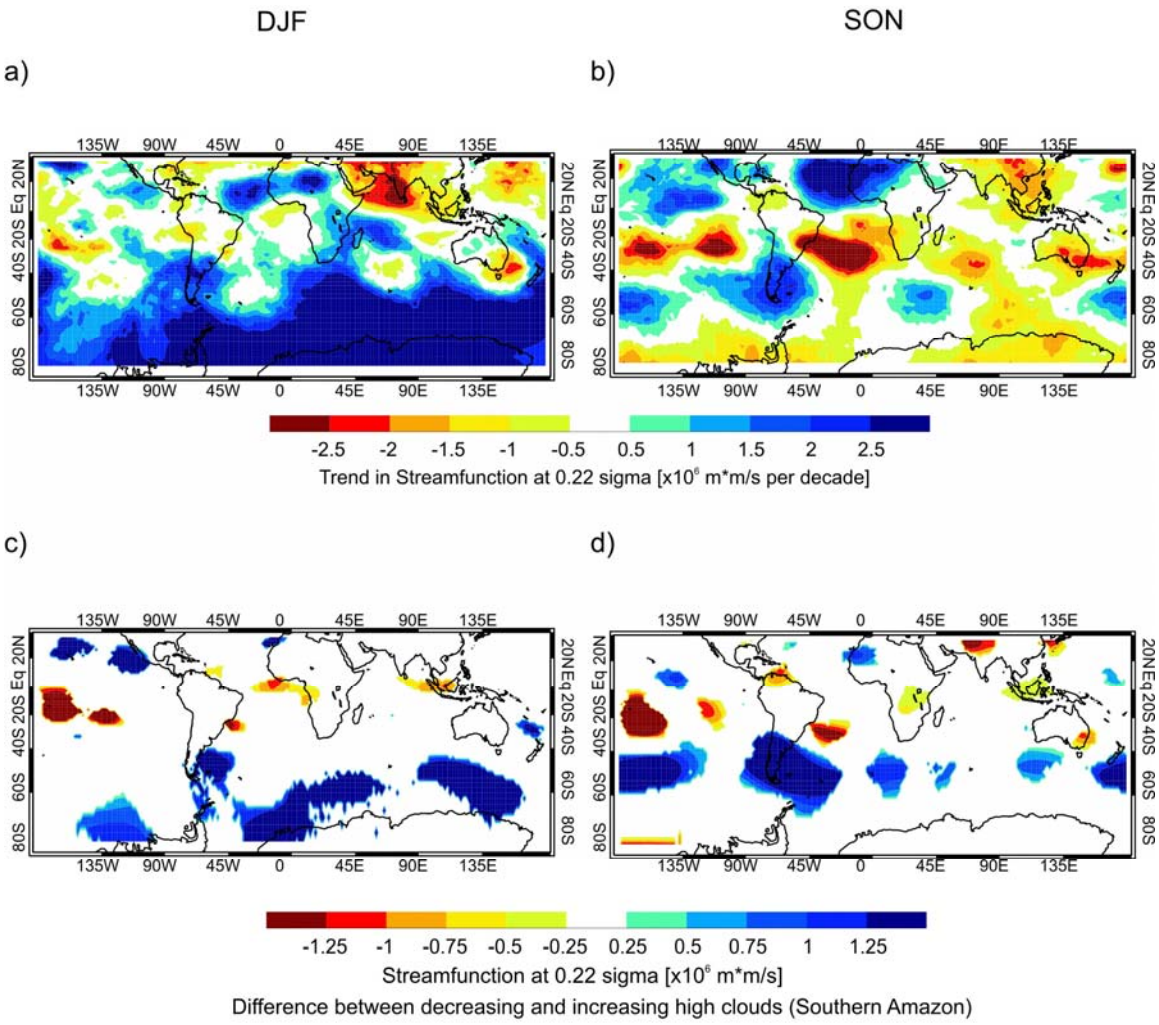

Fig. 9 Trends in streamfunction during a) DJF and b) SON. Differences between -1σ decrease and 1σ increase of high clouds events in the southern Amazon for streamfunction at 0.22 sigma level (~200 hPa) during c) DJF and d) SON. Statistical significance for difference is tested using a bootstrap test (Efron 1979) at 5% level. Trends are statistically significant at the 5% level according to the Mann-Kendall test with Sen's statistics (Sen 1968).

The association between these wave trains and the Pacific Ocean variability has been previously established on seasonal and interannual timescales (Kalnay et al. 1986; Fu et al. 2001; Liebmann et al. 2009). In particular, when the SSTs in the central–eastern

equatorial Pacific Ocean are warm, the anomalous wave train from the tropical central Pacific to the extrotropical southeastern Pacific to South America tends to enhance the SACZ. The latter tends to suppress convection over the southwestern Amazon (Nogues-Paegle and Mo 1997). This result suggests that the reduction of high clouds over the southern Amazon rainforest on multi-decadal decadal scale is likely linked to stronger wave trains in the south Pacific and South American sector, which in turn are associated with SST changes over the Pacific.

2.4. Implications to the observed growth rate increase over the Amazon forests

A statistically significant increase of biomass and net primary productivity (NPP) over the Amazon forest has been previously documented (Phillips et al. 1998; Nemani et al. 2003; Lewis et al. 2004a; Laurance et al. 2004). Phillips et al. (1998) found a widespread increase of the neotropical forests biomass over the recent decades. They suggested possible mechanisms that may explain this change, including (i) a response to continental-scale cyclical climate change (e.g., ENSO), (ii) a response to widespread disturbance, either natural (e.g., volcano aerosols) or anthropogenic (e.g., increasing atmospheric CO_2), (iii) an enhanced forest productivity due to a secular change in climate or an increased nutrient availability (due to increased N and P deposition from Saharan dust and biomass burning), and (iv) the CO_2 fertilization.

The increasing atmospheric CO_2 concentration has received the most attention among the aforementioned potential causes (Lewis et al. 2004a,b; Laurance et al. 2004). However, Nemani et al. (2003) reported that the increasing NPP, at least during 1982 - 1999, is too large to be explained by CO_2 fertilization alone. They further suggested that an increase in solar radiation over these radiation-limited forests is the most likely explanation for the increasing tropical NPP. The results presented here show a multi-decadal scale decrease of cloudiness and an increase of downward solar SW surface radiation over the Amazon. Thus, these results imply that an increase of surface solar radiation and a reduced cloudiness, forced by decadal scale variation of the SSTs changes in the tropical Pacific and Atlantic oceans, would contribute to the increasing Amazon forest growth rate, as proposed by Nemani et al. (2003). Since the AMO has begun to change toward a negative phase in recent years, whether or not the forest growth rate in the coming decade would change will provide an opportunity to clarify the relative roles between the CO_2 fertilization and the surface solar radiation change.

2.5. Conclusions

The analysis of the ISCCP cloud and SW radiation data performed in this study suggests increasing SW down-welling radiation and decreasing total clouds cover over the Amazon forests during 1984-2007. The total cloudiness change, which is mainly the result from decreasing high clouds, is not caused by changes in satellite viewing angle of

the ISCCP geostationary satellites or by deforestation and land use. By contrast, this change is consistent with large-scale circulation changes determined independently from the cloud observations. The cloud changes are consistent with rising temperatures over this forest, as shown by the surface meteorological station data, decreasing vertically integrated moisture transport between the 1000 hPa and 600 hPa levels, as shown by the NCEP-NCAR reanalysis, and the drying of the middle-lower troposphere over the Amazon, based on the upper-air meteorological data.

Although the high clouds decrease during all the seasons except the dry season (JJA), their spatial patterns and their links to the decadal ocean-atmosphere variability vary seasonally. During DJF and MAM, high clouds decrease in the southern Amazon. Such a change is primarily linked to the expansion of the tropical Pacific warm pool during DJF and to the AMO and the eastern Pacific SSTAs during MAM. During SON, the decrease of cloudiness occurs in both the northern and the southern Amazon. The cloud change over the western Amazon is linked to cooler SSTs in the southern tropical Atlantic whereas the change of clouds in the northeastern Amazon and the Nordeste region are mainly linked to the expansion of the western Pacific warm pool.

What could cause the decrease of high clouds over the Amazon basin? The high cloud reductions over the northern Amazon are consistent with an enhanced subsidence, which compensates enhanced rising motion in the northern equatorial Atlantic and the Nordeste region (e.g., Moura and Shukla 1981; Chiang and Sobel 2002; Neelin et al.

2003). This suggests that changes in the direct thermal circulation, which could reduce moisture transport and stabilize the upper troposphere, are probably responsible for the decreasing high clouds in that region. By contrast, the changes in moisture transport and low-level anomalous wind in the southern Amazon are not well correlated to the SSTAs. Further analyses suggest that anomalous Pacific-South American planetary wave trains may reduce high clouds over the southern Amazon. It has been shown by previous studies that these wave trains are linked to SST variability over the Pacific Ocean. Whether the observed changes are part of natural climate variability or due to anthropogenic influences needs to be investigated.

The decrease of cloudiness over the Amazon and the resultant increase of solar SW radiation since 1984 support the hypothesis that increasing surface solar radiation contribute to the increasing forest growth rate over the Amazon, as proposed by Nemani et al. (2003).

The analysis period considered in this study is too short to fully assess the impact of multi-decadal SST variability on cloudiness change over the Amazon. Thus, whether the cloud changes and their underlying causes found in this study adequately represent the multi-decadal variations or trends has to be tested when data with longer record periods becomes available in future.

Chapter 3

Changes in the monsoon regime over northwestern Mexico during 1948-2009

3.1. Introduction

Summer monsoon precipitation over the southwestern (SW) US and Mexico, also known as the North American Monsoon System (NAMS) or the Mexican Monsoon (Douglas et al. 1993; Stensrud et al. 1995), has important impacts on water resource consumption and availability in that region, which is among the most rapidly growing zones of the US and Mexico.

The monsoon rain starts in early to mid June over southwestern Mexico (SWMEX) and advances to northwestern Mexico (NWMEX) and the SW US by early July (Barlow et al. 1998; Higgins et al. 1997). During its sudden onset, weather in the monsoon region changes from a relatively hot and dry regime to a cool and rainy regime (Higgins et al. 1999). This onset of the summer rainfall over western Mexico and the SW US coincides climatologically with decreased rainfall over the Great Plains and increased precipitation over the eastern coast of the US (Douglas et al. 1993; Douglas and Englehart 1996; Higgins et al. 1997; Mo et al. 1997; Barlow et al. 1998). The underlying processes that cause such a correlation are still not clear. Higgins et al. (1997) and Adams and Comrie (1997) indicate that two main sources of moisture feed the monsoon: the

northern Gulf of California provides most of the moisture below 850 hPa while the Gulf of Mexico provides moisture at and above 850 hPa. Thus, changes in these moisture sources can influence both the length and the strength of the monsoon.

Adjacent oceans, especially the Pacific, play an important role in the NAMS interannual variability. In general, strong (weak) monsoon onsets are linked to a positive (negative) thermal gradient from the Pacific to the SW US (Higgins and Shi 2001; Zhu et al. 2007; Turrent and Cavazos 2009). Interannual variability of the summer monsoon over this region is modulated by decadal fluctuations in the north Pacific sea surface temperature (SST) associated with the Pacific Decadal Oscillation (PDO) (Higgins and Shi 2000; Castro et al. 2001). Time-evolving tele-connections associated with Pacific SSTs either delay or accelerate monsoon evolution (Castro et al. 2007). The El Niño-Southern Oscillation (ENSO) also affects the monsoon strength: wet (dry) monsoons in SWMEX tend to occur during La Niña (El Niño) due to the impact of eastern Pacific SST anomalies (SSTA) on the land–sea thermal contrast (Higgins et al. 1999) whereas above-average July precipitation in northeast Mexico (west-central Arizona) occurs with El Niño (La Niña) (Harrington et al. 1992).

Hu and Feng (2008) documented the influence of Atlantic SSTs on the NAMS variability: distinctive circulation anomalies in central and western North America occur during both phases of the Atlantic Multidecadal Oscillation (AMO). The AMO warm phase boosts strong moisture transport from the regions near the Gulf of Mexico into the central US, causing more rainfall over that region and decreasing monsoon precipitation

to the west. Consequently, the AMO warm phase produces drier monsoons than the cold phase. In a later study, Hu and Feng (2010) investigated the modulation of the North American summer climate by the Arctic Oscillation (AO). Their findings suggest that the AO positive phase induces a northward displacement of the subtropical jet stream, which in turn leads to anomalous downward motion and moisture divergence over the central US, reducing precipitation in that region.

After the monsoon onset, rainfall may be strongly modulated by land surface conditions, such as evaporation and recycling (Anderson et al. 2004; Zhu et al. 2007), and by synoptic-scale transient systems (Douglas and Englehart 2007; Vera et al. 2006). The NAMS onset and its variability have been widely documented; however, the variability of its retreat has not received as much attention. This study aims to identify whether there was a change in the timing and strength of the NAMS during the period 1948-2009, and if so, what could have caused such a change. Precipitation and reanalysis data were used to identify changes in the monsoon strength and in the onset/retreat dates. The influences of lower and upper troposphere circulation and SSTs were analyzed using reanalysis data and extended reconstructed mean SSTs. This chapter is organized in five sections. Section 3.2 describes the data and the methodology. Section 3.3 identifies changes in monsoon regime and their possible causes. Section 3.4 presents a short discussion about the link between the observed changes and global warming. Finally, section 3.5 concludes with the main findings from this study.

3.2. Data and methodology

Changes in the timing and the strength of the NAMS during the period 1948-2009 were analyzed using both daily observational and reanalysis data over the northwestern Mexico region selected on the basis of the studies by Barlow et al. (1998) and Higgins et al. (1999) (see Fig. 10a). The daily rain rate was averaged over each region and converted to mean pentad values (i.e., 5-day averages) before obtaining the onset/retreat dates.

Different definitions have been previously suggested to determine the North American monsoon onset/retreat. For example, Douglas et al. (1993) and Stensrud et al. (1995) have characterized the onset of the Mexican monsoon by analyzing heavy rainfall over southern Mexico. Douglas et al. (1993) and Barlow et al. (1998) studied the precipitation change during the Mexican monsoon onset using the June-to-July change. These approaches allow the main features of the onset phase to be characterized but do not identify the specific onset date. Higgins et al. (1997) used a precipitation index (i.e., the area average daily precipitation over Arizona and western Mexico) to define the monsoon onset using a threshold-crossing procedure (with thresholds of 10.5 mm/day for rainfall and 3 days for duration). Although Higgins et al. (1997) carefully selected the grid points to be included in the area average precipitation, their procedure considers a duration criterion of only three days; thus the persistence of rainfall changes necessary for the monsoon onset may not be captured by this methodology. Zeng and Lu (2004) proposed a unified method to estimate the monsoon onset and retreat dates based on precipitable water data. Even though their results appear to be reasonable over the NAMS

region, precipitable water data is available mainly from reanalysis instead of rain gauge measurements. Thus, the aforementioned definitions of the monsoon onset/retreat dates may have issues related to the objectivity of the rain threshold considered, the persistence in time of the rainfall changes, and/or the reliability of the required data.

Li and Fu (2004) proposed a procedure that considers both an objectively defined rain rate threshold and the persistence in time to define the wet season onset. Their results over South America showed consistency with previous studies. Therefore, the definition of the NAMS onset and retreat dates applied in this study follows Li and Fu's methodology. The onset (retreat) date was defined as the pentad before which the rain rate was less (more) than the climatological annual mean rain rate during 6 out of 8 preceding pentads and after which the rain rate was greater (lower) than the climatological annual mean rain rate during 6 out of 8 subsequent pentads. When these thresholds did not allow identifying the monsoon onset (or retreat) date for a specific year, the duration threshold was relaxed from 6 to 5 consecutive pentads. One advantage of this methodology is that long-term rain gauge data can be used instead of reanalysis products.

The 1-degree grid daily precipitation over the US and Mexico during 1948-2009 from the National Oceanic and Atmospheric Administration (NOAA) Climate Prediction Center (CPC) was used. This dataset is described by Higgins et al. (1999, 2000a) and is available at ftp://ftp.cpc.ncep.noaa.gov/precip/wd52ws/us-mex/. This gridded data is

collected from about 2500 gauges with hourly records over the US and about 161 stations with daily records over Mexico (Higgins et al. 1999).

To identify the causes of the observed changes in the monsoon strength and timing, daily 2.5-degree grid data for surface temperature, SLP, geopotential height, and zonal and meridional wind at different pressure levels were used. These datasets were obtained from the National Center for Environmental Project-National Center for Atmospheric Research (NCEP-NCAR) Reanalysis (Kalnay et al. 1996) from 1948 to the present.

The extended reconstructed monthly mean SST from the NOAA Climate Diagnostic Center (CDC) (Reynolds 1988) described in section 2.2 was used.

To determine whether the changes of the monsoon regime are linked to tropical climate variability, the indices for PDO, ENSO, AO, and AMO were used. The PDO index (Mantua 1997) was obtained from http://jisao.washington.edu/pdo/PDO.latest. ENSO was represented by Niño3, Niño4, and Niño3.4 indices, available at http://www.cdc.noaa.gov/data/climateindices/list/. The AO index (Thompson and Wallace 1998) is available at the NOAA CPC site (http://www.cdc.noaa.gov/data/climateindices/list/). The AMO index (Enfield et al. 2001) is available at http://www.cdc.noaa.gov/data/timeseries/AMO/. The effects of the expansion of the western Pacific warm pool on the NAMS regime were also investigated using the WPWP

index defined in section 2.2. Positive (negative) phases of the afore-mentioned indices correspond to the dates with an index value greater (less) than 1 standard deviation (σ) plus (minus) its climatological mean.

Correlation coefficients between different variables were computed. The statistical significance of the correlations was determined by the Monte Carlo Test for spatial pattern (Livezey and Chen 1983) described in section 2.2.

To identify changes in atmospheric fields during early and late retreats, the composites for both cases were obtained and their difference was computed. Early (late) retreat monsoons were identified as those when the retreat date occurred during the period August 25-September 20 (September 30-November 4). The statistical significance of the difference was tested using the bootstrap test (Efron 1979) described in section 2.2.

Changes in the monsoon regime were also examined by considering weak and strong monsoons. Weak (strong) monsoons were identified as those when the monsoon total rainfall was below (above) 0.5σ from its climatological mean.

3.3. Results

3.3.1 Identification of two types of monsoon regime during 1948-2009

Precipitation during the summer NAMS has a characteristic pattern: a precipitation maximum occurs over SWMEX although a significant area of intense precipitation is centered over NWMEX; the lowest values are observed over the SW US (Douglas et al. 1993; Barlow et al. 1998). The monsoon onset occurs first over SWMEX and rapidly progresses northward until reaches the SW US (Douglas et al. 1993; Higgins et al. 1999), where rainfall is more directly influenced by mid-latitude weather systems (Higgins et al. 1999). Due to these differences, Higgins et al. (1999) considered three different regions over western Mexico and the SW US for their study of the NAMS interannual variability (see their Fig.2). In contrast, Barlow et al. (1998) only considered the region over western Mexico where precipitation is more intense (see their Fig.1a).

A recent study by Grantz et al. (2007) revealed a significant delay in the beginning, peak, and closing stages of the monsoon over the SW US during the period 1948-2004. This shift in the monsoon over the SW US is found to be linked to warmer tropical Pacific SSTs and cooler northern Pacific SSTs in the antecedent winter–spring season, which leads to wetter-than-normal conditions over the SW US and, consequently, delays the seasonal heating of the North American continent necessary to establish the monsoonal land–sea thermal contrast. Since Grantz et al. already identified and explained

changes in the SW US monsoon season after 1948, this study focuses on the monsoon changes in the Mexican domain of the NAMS. Furthermore, an exploratory analysis (not shown) suggests that changes in the monsoon are stronger over NWMEX than over SWMEX; hence, this work will focus on the northwestern Mexican domain of the NAMS. This region was selected based on Higgins et al. (1999) and Barlow et al. (1998), as shown in Fig. 10a.

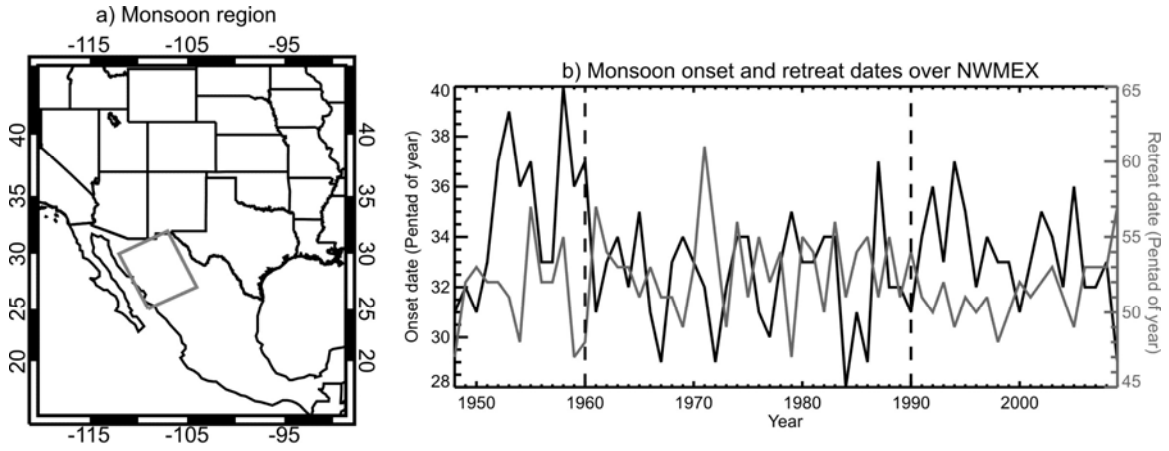

Fig. 10 a) Monsoon region (NWMEX) considered for onset and retreat computations based on Barlow et al. (1998) and Higgins et al. (1999). b) Monsoon onset (black) and retreat (gray) dates over NWMEX during 1948-2009 obtained from CPC-USMex rain rate.

The monsoon onset and retreat dates were defined using a criterion that considers both an objectively defined rain rate threshold and the persistence throughout time, following Li and Fu (2004) (see section 3.2). CPC daily precipitation data for the US and Mexico (hereafter, CPC-USMex) was used. To match the period available for NCEP/NCAR reanalysis data, CPC-USMex rainfall data from 1948 to 2009 was used. The daily rain rate was averaged over the selected region and converted to mean pentad

values (i.e., 5-days average) before the monsoon onset and retreat dates were identified. Onset/retreat dates were obtained for each year.

Fig. 10b shows the time series for the onset and retreat dates over NWMEX. The onset and retreat dates show multi-decadal variations: more late-onset and early-retreat monsoons occurred during the periods 1948-1959 and 1990-2009 whereas more early-onset and late-retreat monsoons occurred during 1960-1989. On interannual scale, early-onset events are associated with late-retreat events while late-onset events are associated with early-retreat events. The monsoon retreat dates over NMMEX during 1948-2009 are shown in Table 3. Following Gutzler (2004), early (late) retreat events were identified as those when the retreat date occurred before September 20 (after September 30). Early (late) retreat events are shown in bold (asterisks) in Table 3. A higher frequency in early-retreat monsoons over NWMEX is observed during the periods 1948-1959 and 1990-2009. Late-retreat monsoons are mainly observed during 1960-1989, when retreat dates have higher variability. Although there are two periods of frequent early-retreat monsoons, the latter period (1990-2009) shows more persistence toward early retreats.

3.3.2. Associated changes in precipitation during the monsoon season

To identify the changes in the monsoon precipitation associated with variations in the monsoon timing, a comparison between the monsoon total rainfall over NWMEX and the monsoon onset and retreat dates is shown in Figs. 11a and 11b, respectively. Annual

monsoon total rainfall was obtained as the total rainfall accumulated between the onset and retreat dates in a year. Results indicate periods of dry monsoon seasons over NWMEX during 1948-1959 and 1990-2009, consistently with the observed late-onset and early-retreat monsoons. Wetter monsoon seasons occur during 1960-1989 in association with early-onset and late-retreat monsoons. Correlations between monsoon total rainfall and onset (retreat) dates support this association.

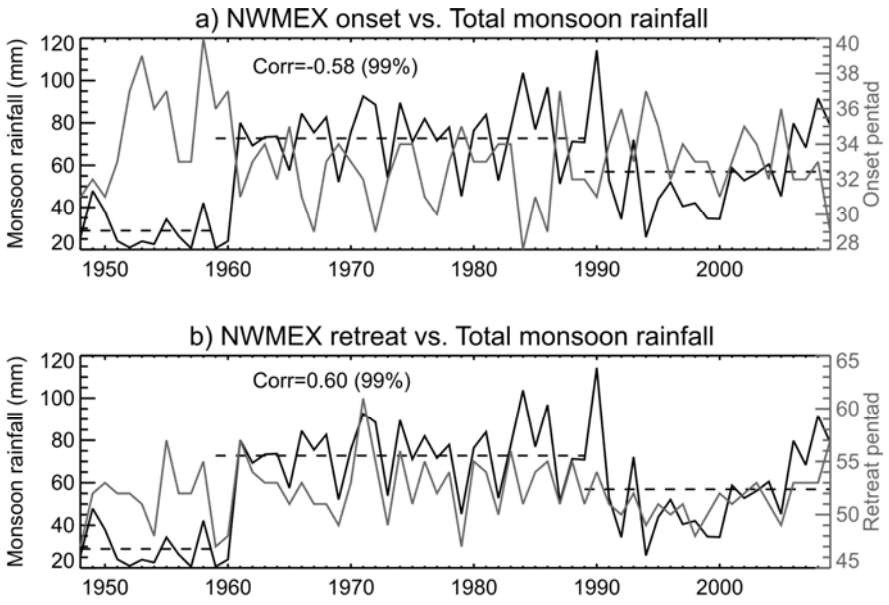

Fig. 11 Relationship between total monsoon rainfall and a) onset date and b) retreat date over NWMEX. Correlation coefficient and its significance level for 1948-2009 are indicated in each plot. Dashed lines represent mean rainfall during 1948-1960, 1960-1990, and 1990-2009, respectively.

Table 3 Retreat dates over NWMEX during 1948-2009 from CPC-USMex rain rate data. The retreat date is identified using a criterion that considers both an objectively defined rain rate threshold and persistence throughout time following Li and Fu (2004) (see section 3.2). Dates in bold (asterisks) correspond to early (late) retreat events.

1948-1959		1960-1989		1990-2009	
Year	**Retreat date**	**Year**	**Retreat date**	**Year**	**Retreat date**
1948	**26-Aug**	**1960**	**31-Aug**	1990*	30-Sep*
1949	**20-Sep**	1961*	15-Oct*	**1991**	**15-Sep**
1950	25-Sep	1962*	30-Sep*	**1992**	**10-Sep**
1951	**20-Sep**	1963	25-Sep	**1993**	**20-Sep**
1952	**20-Sep**	1964	25-Sep	**1994**	**5-Sep**
1953	**15-Sep**	**1965**	**15-Sep**	**1995**	**15-Sep**
1954	**31-Aug**	1966	25-Sep	**1996**	**10-Sep**
1955*	15-Oct*	**1967**	**15-Sep**	**1997**	**15-Sep**
1956	**20-Sep**	**1968**	**15-Sep**	**1998**	**31-Aug**
1957	**20-Sep**	**1969**	**5-Sep**	**1999**	**10-Sep**
1958*	5-Oct*	1970	25-Sep	**2000**	**20-Sep**
1959	**26-Aug**	1971*	4-Nov*	**2001**	**15-Sep**
		1972*	5-Oct*	**2002**	**20-Sep**
		1973	**5-Sep**	2003	25-Sep
		1974*	10-Oct*	**2004**	**15-Sep**
		1975	**15-Sep**	**2005**	**5-Sep**
		1976*	5-Oct*	2006	25-Sep
		1977	**20-Sep**	2007	25-Sep
		1978*	30-Sep*	2008	25-Sep
		1979	**26-Aug**	2009*	15-Oct*
		1980*	5-Oct*		
		1981*	30-Sep*		
		1982	**10-Sep**		
		1983*	10-Oct*		
		1984	**15-Sep**		
		1985*	30-Sep*		
		1986*	5-Oct*		
		1987	**15-Sep**		
		1988*	5-Oct*		
		1989	**15-Sep**		

To understand the effects of changes in the monsoon strength over NWMEX on the onset and retreat dates over the entire monsoon region, the difference in onset/retreat dates between weak and strong monsoons was computed. This difference was obtained from 21 weak and 25 strong-monsoon events. Weak (strong) monsoons were identified as those when the monsoon total rainfall over NWMEX was below (above) 0.5σ from its climatological values. Results suggest that a weakening of the summer monsoon over NWMEX is associated with a later monsoon onset (Fig. 12a) and an earlier retreat (Fig. 12b). In addition, changes in the monsoon retreat associated with variations in the monsoon strength occur over the entire NAMS domain whereas changes in the monsoon onset are more constrained to NWMEX.

To examine the association between changes in the spatial pattern of the anomalous monsoon precipitation and the variations in the monsoon strength, monsoon total precipitation anomalies and daily mean monsoon rain rate were composited for weak and strong monsoons and their difference was tested using the bootstrap test (Efron 1979). Anomalies were computed based on the 1948-2009 climatology. Figs. 12c and 12d show the change in monsoonal total precipitation anomalies and daily average monsoon rain rate, respectively, between weak and strong monsoons. Weaker monsoons are associated with reduced precipitation over the monsoon region and increased rainfall over the central US, not only during the entire monsoon season but also in their average daily rain rate. This out-of-phase relationship between rainfall over the central US and the monsoon region has been extensively documented (e.g. Douglas et al. 1993; Douglas and Englehart 1996; Mo et al. 1997; Higgins et al. 1997; Barlow et al. 1998). Furthermore,

this analysis indicates that the weaker monsoons have a later onset and an early retreat than the stronger ones. Weaker monsoons also show a lower daily rainfall rate (Fig. 12c).

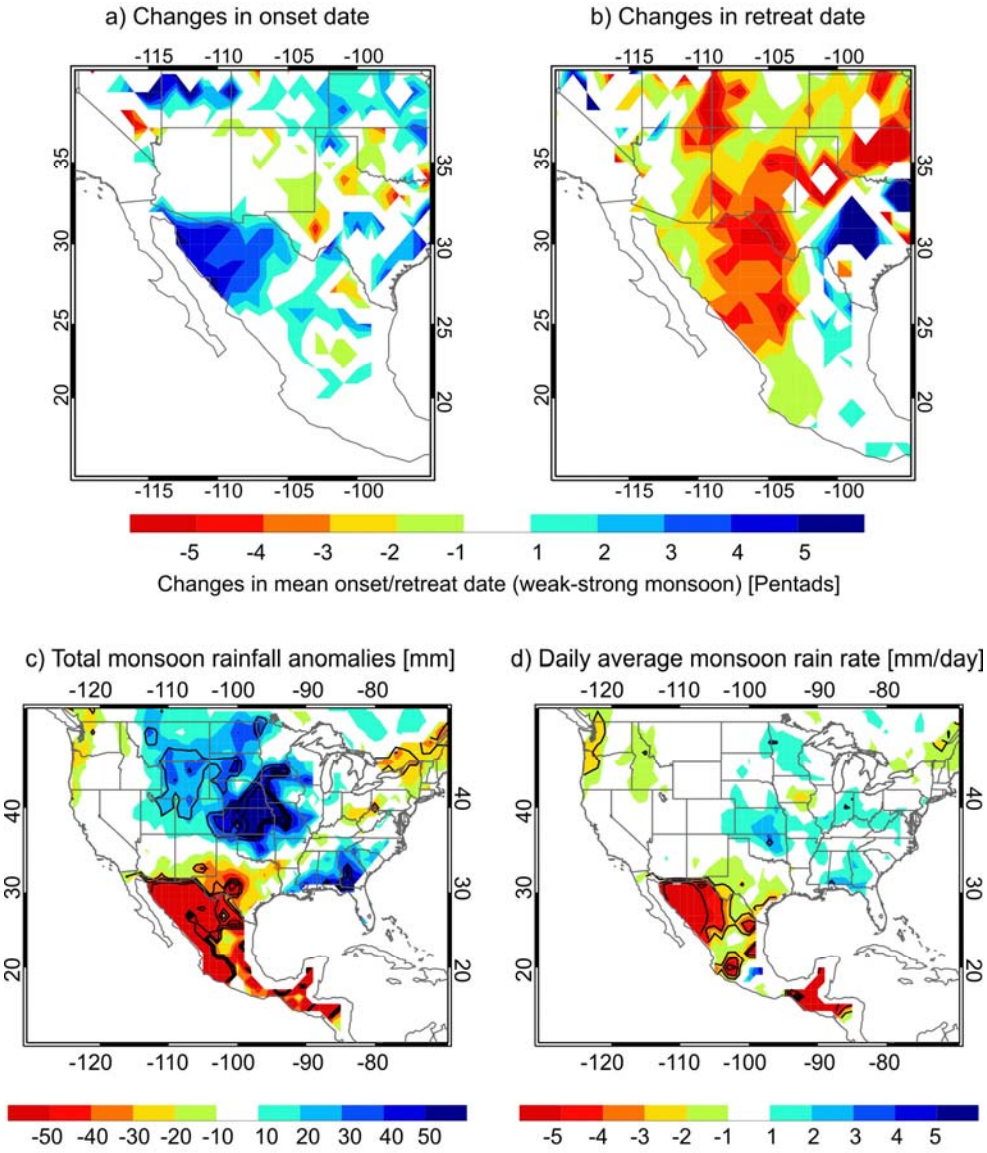

Fig. 12 Changes in a) onset and b) retreat dates over the SW US and Mexico between weak and strong monsoons. Composite difference between weak and strong monsoons for c) total monsoon precipitation anomalies and d) daily average monsoon rain rate. Contours indicate the differences that are statistically significant according to a bootstrap test (Efron 1979).

Fig. 13 shows the difference in July-August (JA) total precipitation between weak and strong monsoons, and early and late-retreat monsoons. The composite difference between early and late retreats was obtained from 36 (17) early (late) retreat events, as indicated in Table 3. JA total rainfall amounts are considered since this season corresponds to the peak of the NAMS (e.g. Barlow et al. 1998). Changes in the monsoon-peak total rainfall associated with a weaker monsoon (Fig. 13a) resemble those observed when the NAMS retreats earlier (Fig. 13b), suggesting that changes in the monsoon strength are associated with changes in the monsoon timing.

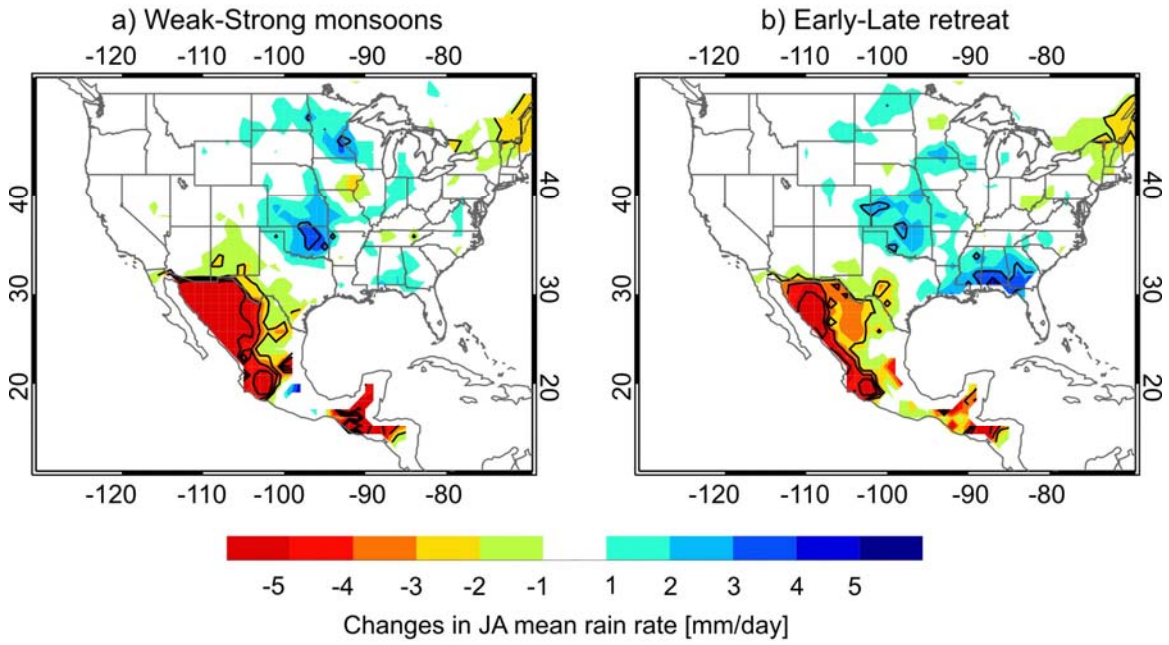

Fig. 13 Composite difference in JA mean rain rate between a) weak and strong monsoons and b) early and late-retreat monsoons. Contours indicate the differences that are statistically significant according to a bootstrap test (Efron 1979).

These results indicate an increased frequency of weak monsoons over North America associated with late onsets and early retreats during 1948-1959 and 1990-2009,

and more frequent strong monsoons associated with early onsets and late retreats during 1960-1989. Such a shift in the NAMS regime has been previously identified by Hu and Feng (2008), who showed that this multi-decadal variability in the monsoon strength is associated with the AMO. However, their study focused on the multi-decadal variability of the monsoon strength but not on the associated changes in the monsoon onset or retreat. This study focuses on the difference between the two dry NAMS periods, the link between the changes in the monsoon retreat and strength, and the underlying causes of these changes.

3.3.3 Associated circulation changes and their links to decadal climate variability modes

3.3.3.1 Variations in lower troposphere circulation

To identify variations in the lower troposphere circulation associated with changes in the monsoon strength and timing, 850 hPa streamlines were composited during each pentad of the monsoon season considering both the monsoon strength and the retreat date. Since weak monsoons are more persistent during the more recent dry regime period (1990-2009) than during the earlier dry period (1948-1959), the changes in surface circulation during these two weak-monsoon periods and those during the period 1960-1989, when the most of the strong monsoons occurred (20 out of a total of 25 events), were compared.

Fig. 14a shows the mean surface circulation occurred three pentads before the retreat of the strong monsoons. Figs. 14b and 14c show the changes in surface circulation between weak monsoons and strong monsoons, for weak monsoons during 1948-1959 and 1990-2009, respectively. Strong monsoons are characterized by a clearly defined cyclonic center over the west coast of Mexico, a characteristic feature of the NAMS. The western edge of the anticyclonic center associated with the North Atlantic Subtropical High (NASH) is located over the southeastern (SE) US. This circulation configuration leads to a southeasterly moisture transport from the Gulf of Mexico to the NWMEX monsoon region (Fig. 14a). By contrast, during the weak monsoons, the western edge of the NASH is shifted southward (Figs. 14b and 14c). A strong anomalous cyclonic center over the SE US leads to anomalous northerly lower level winds over the NAMS region, weakening the moisture transport from the Gulf of Mexico. This anomalous cyclonic center over the SE US becomes stronger and more extensive in the period 1990-2009 (Fig. 14c) than in the period 1948-1959 (Fig. 14b). In addition, an anomalous anticyclonic center appears over the Gulf of Mexico during the period of 1990-2009. In addition, the center of the NASH is displaced northeastward and becomes stronger during weak monsoons, especially in the more recent dry period (Fig. 14c), than during strong monsoons. The mechanism behind the direct effect of this expansion on the NAMS is further explored and discussed in sections 3.3.3.3 and 3.4.

Variations in lower tropospheric circulation associated with changes in the monsoon retreat are shown in Fig. 15. Using a similar approach, late-retreat monsoons

were considered for the period 1960-1989 while early-retreat monsoons were considered separately for 1948-1959 and 1990-2009. The circulation change associated with late-retreat monsoons show a similar pattern as that of the strong monsoons (Figs. 15a and 14a, respectively). The difference in patterns between early and late NAMS retreats (Figs. 15b and 15c) resembles that between weak and strong NAMS events (Figs. 14b and 14c), but shows more clearly defined anomalous anticyclonic centers over the Gulf of Mexico, especially during 1990-2009. The comparison between Figs. 14 and 15 suggests that both the weak monsoons and early retreats are linked to an eastward shift of the cyclonic circulation over the US. In addition, the early NAMS retreats are also linked to an enhanced anticyclonic circulation over the Gulf of Mexico.

Figs. 16 and 17 show the corresponding difference in SLP between (i) weak and strong monsoons and (ii) early and late retreats of the monsoon, respectively. Weak and early-retreat monsoons during both dry periods are accompanied by an intensification of the NASH center during the decay phase. However, a westward expansion of the NASH is only observed during the more recent dry period (Figs. 16b, 16d, 17b, and 17b), consistent with the shift in the position of the low-level anticyclone over the Atlantic Ocean (Figs. 14c and 15c).

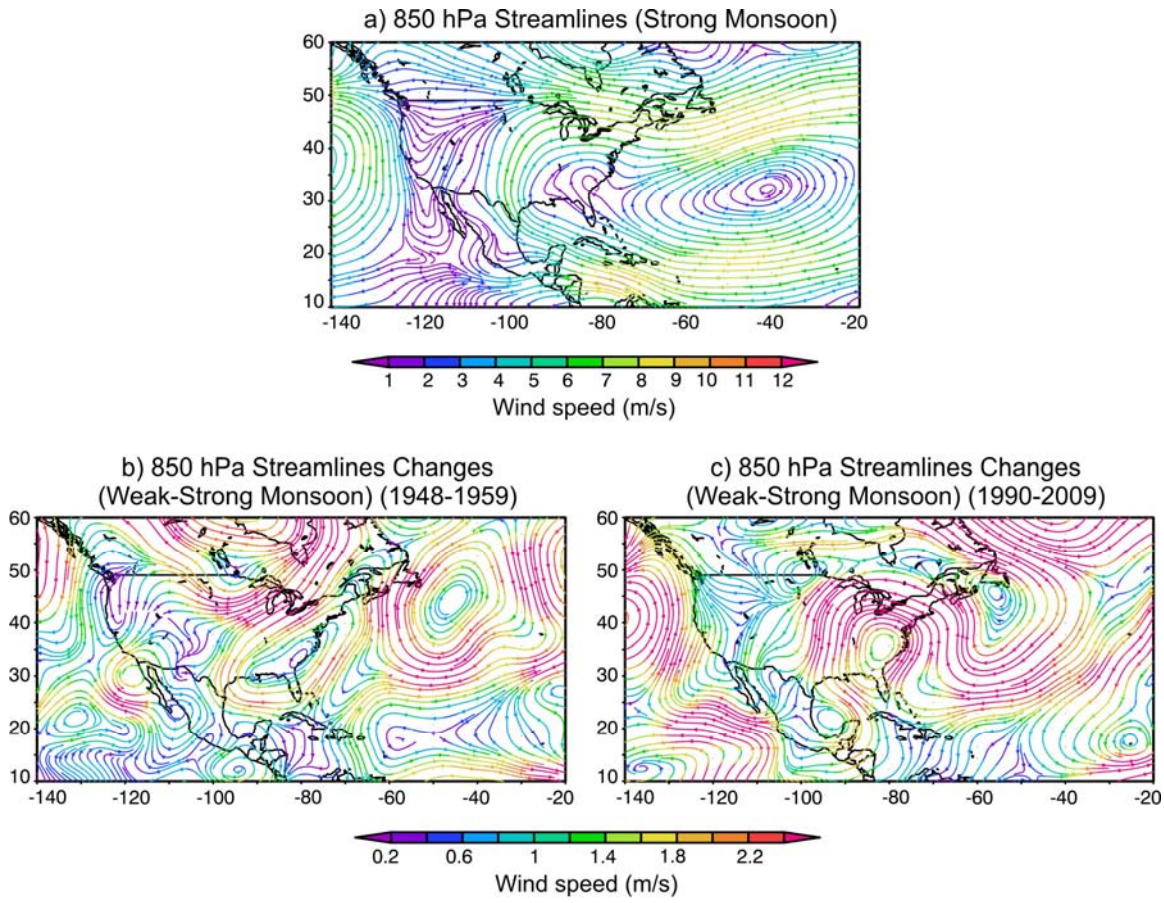

Fig. 14 850 hPa streamlines composite for a) strong monsoons three pentads before the monsoon retreat. Difference in 850 hPa streamlines between weak and strong retreat events during b) 1948-1959 and c) 1990-2009. Color scale indicates wind speed in m/s.

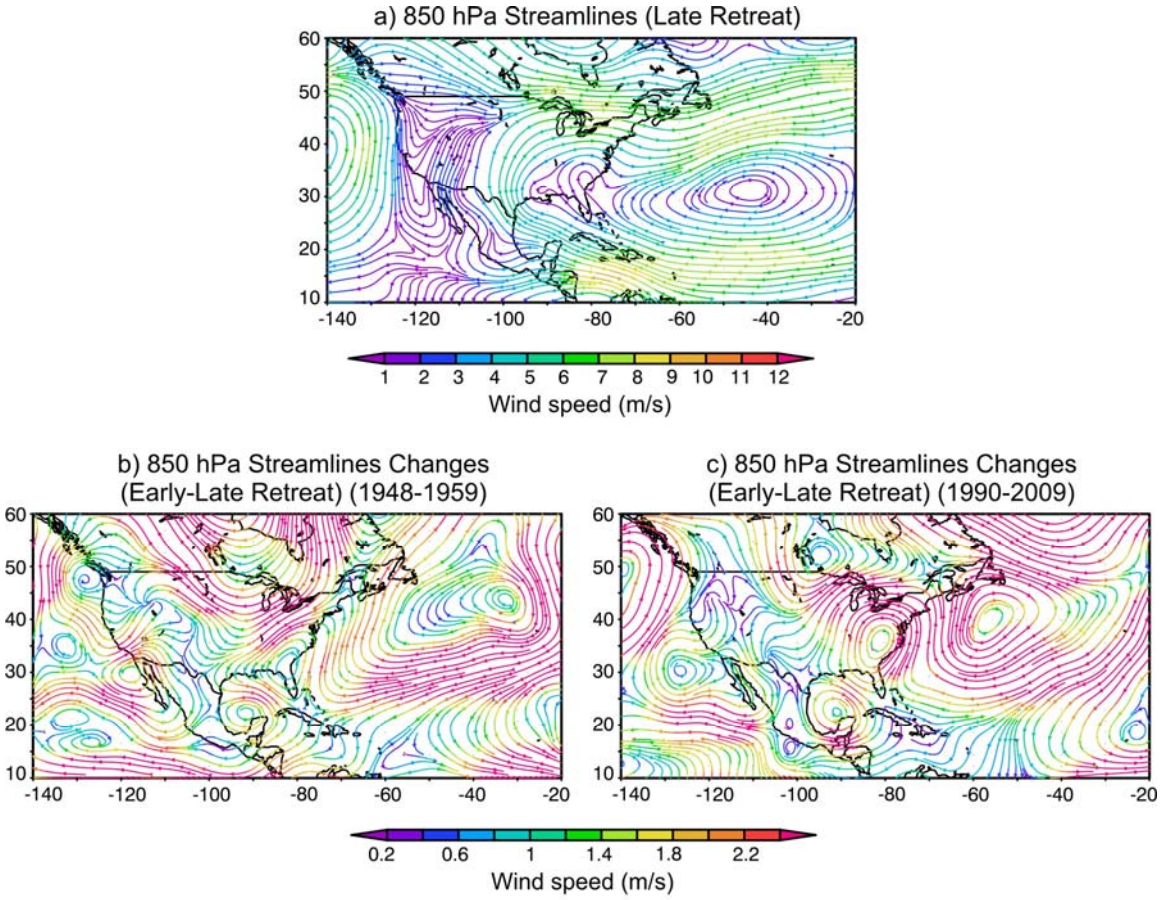

Fig. 15 Same as Fig. 14 but for early and late-retreat monsoons.

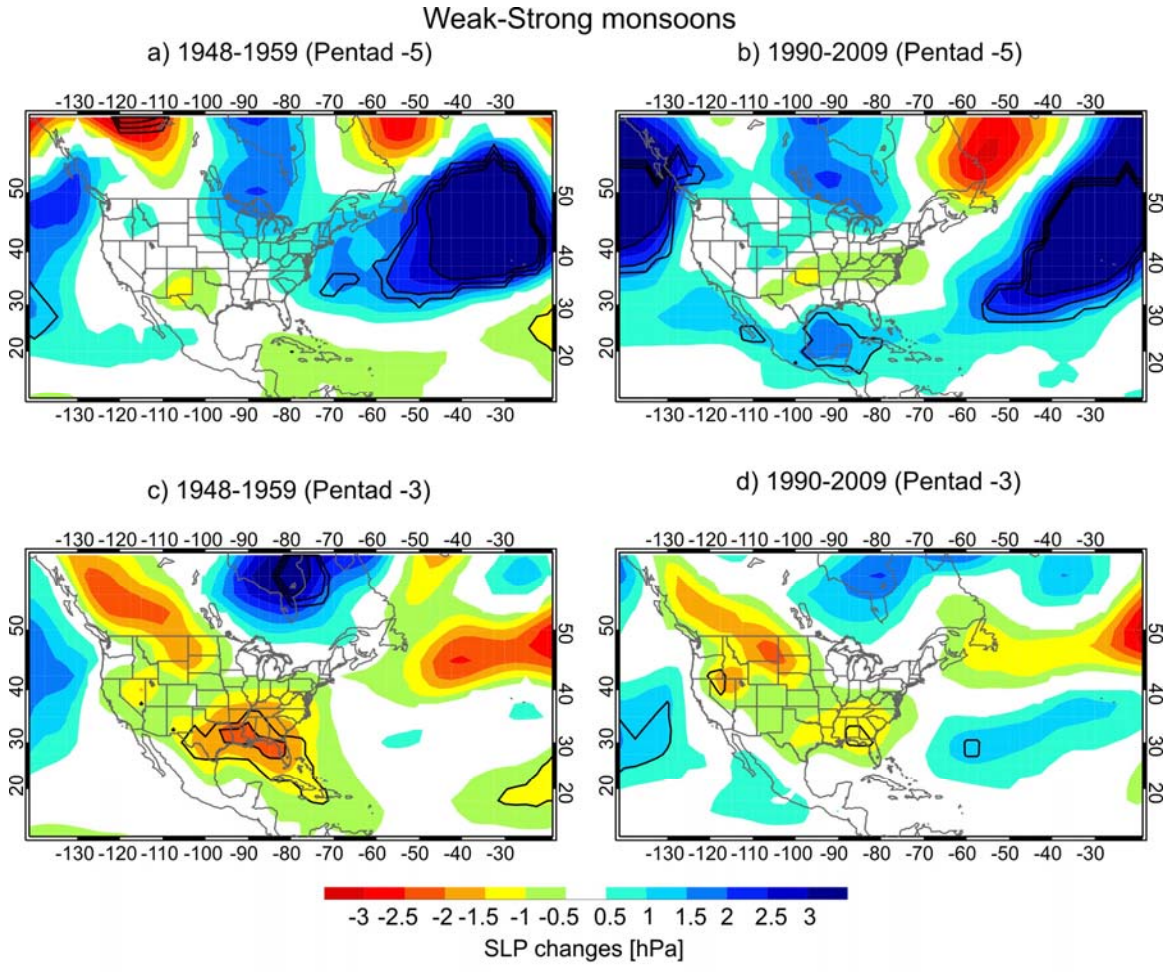

Fig. 16 a) SLP composite difference between weak and strong monsoons five pentads before the monsoon retreat during a) 1948-1959 and b) 1990-2009. c) and d) Same but three pentads before the monsoon retreat. Contours indicate differences that are statistically significant according to a bootstrap test (contours) (Efron 1979).

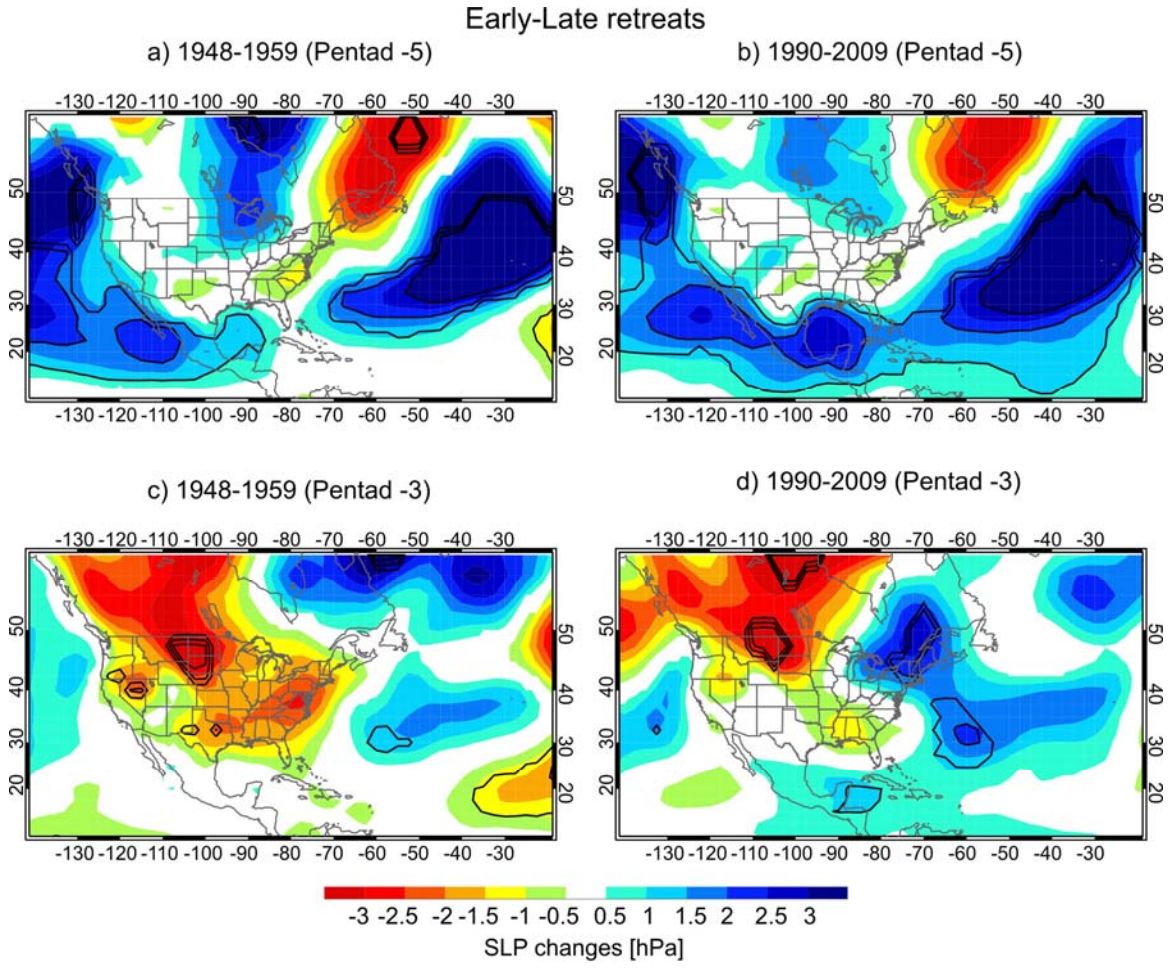

Fig. 17 Same as Fig. 16 but for early and late-retreat monsoons.

A recent study by Li et al. (2011) suggests a westward expansion of the western edge of the NASH and an intensification of its center associated with increased summer rainfall anomalies over the SE US after 1978 (c.f., Katz et al. 2003). To identify whether changes in the western edge of the NASH would influence the strength and retreat phase of the monsoon over NWMEX, Li et al.'s approach was followed using the mean position of 1560m of geopotential height (gpm) line to characterize the western ridge of the NASH during weak and strong monsoons and during early and late NAMS retreats. Fig.

18 shows the position of the western boundary of the NASH three pentads before the monsoon retreat for the weak, the strong, the early-retreat, and the late-retreat monsoons. To determine if changes in the location of the NASH vary with time, the position of its western boundary was obtained during the three observed monsoon regimes (1948-1959, 1960-1989, and 1990-2009). During the two more recent periods (Figs. 18a and 18b), the mean western edge of the NASH shifts from 75°W during strong and late-retreat NAMS events to approximately 95°W during weak and early-retreat events. This westward shift of the western edge of the NASH is observed during the entire monsoon season (not shown). During the earlier dry monsoon regime (Fig. 18c), the western boundary of the NASH is also located further west during weak and early-retreat monsoons than during late retreats; however, it does not reach the SE US, staying over the Atlantic Ocean during the entire monsoon season. Apparently, a westward shift of the NASH over North America is observed only during the more recent decades.

Fig. 19a shows the relationship between the monsoon retreat and the location of the NASH western ridge during the decay stage of the monsoon. Early (late) retreats correspond to a westward (eastward) shift of the NASH, especially after 1960. The western edge of the NASH mostly oscillates between 75˚–90˚W during the period 1948-1989, but becomes more stationary, fixed within 85˚–90˚W after 1990. The early retreats of the NAMS are well correlated with the westward expansion of the NASH on both interannual and decadal scales. Thus, the trend toward early NAMS retreat after 1990 is closely related to the westward expansion of the NASH. On the other hand, the most

delayed monsoon onsets do not correspond to the most westward location of the NASH (not shown) suggesting that the influence of this westward expansion is stronger during the retreat phase of the monsoon.

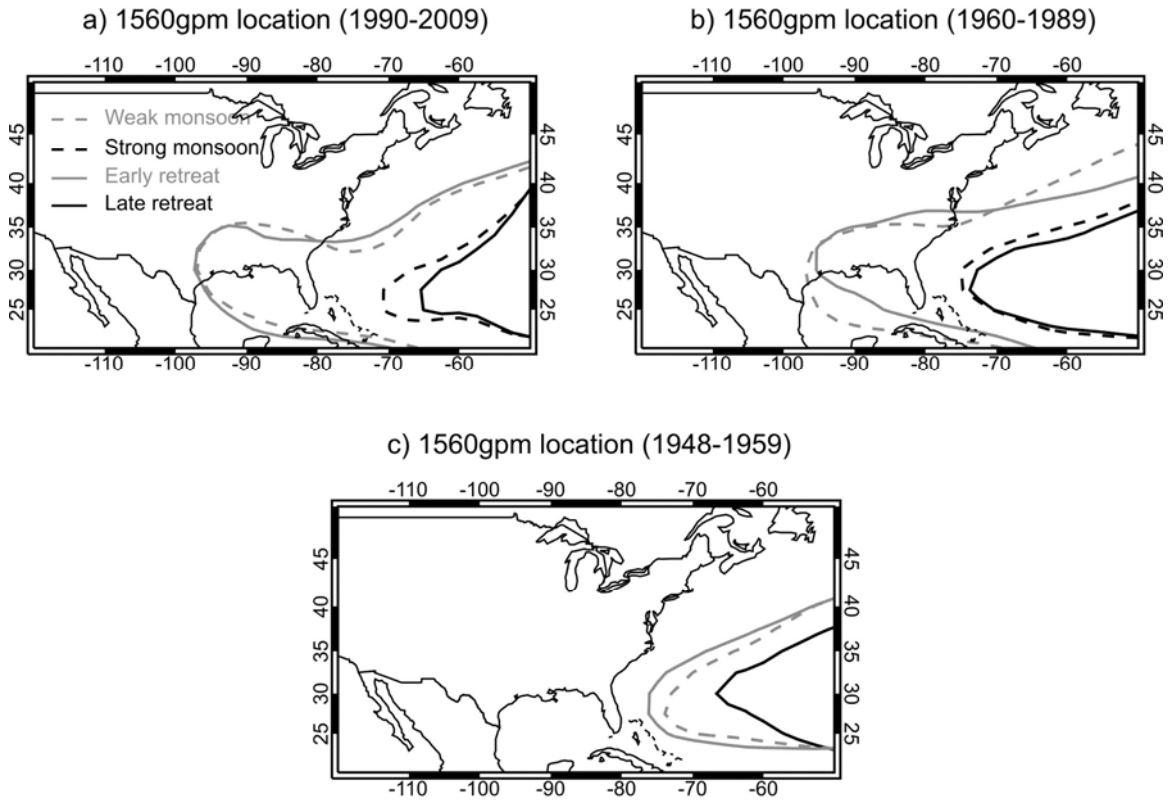

Fig. 18 Position of 1560 meter of geopotential height (gpm) contour line at 850 hPa for weak (gray dotted line), strong (black dotted line), early (gray line) and late- retreat (black line) NAMS events three pentads before the monsoon retreat during a) 1990-2009, b) 1960-1989, and c) 1948-1959.

Fig. 19b suggests that the NASH western boundary location averaged over the monsoon season is as variable during 1948-1959 as that during 1960-1989. However, the monsoon total rainfall is lower and less variable during 1948-1959, indicating that the NASH western boundary location has a stronger influence on monsoon after 1960.

Furthermore, the connection between the monsoon rainfall and the NASH westward shift during the entire monsoon season is not as clear as that for the retreat stage. Evidently, the location of the western boundary of the NASH in recent decades has a stronger influence during the decay phase of the NAMS than during the development and mature phases.

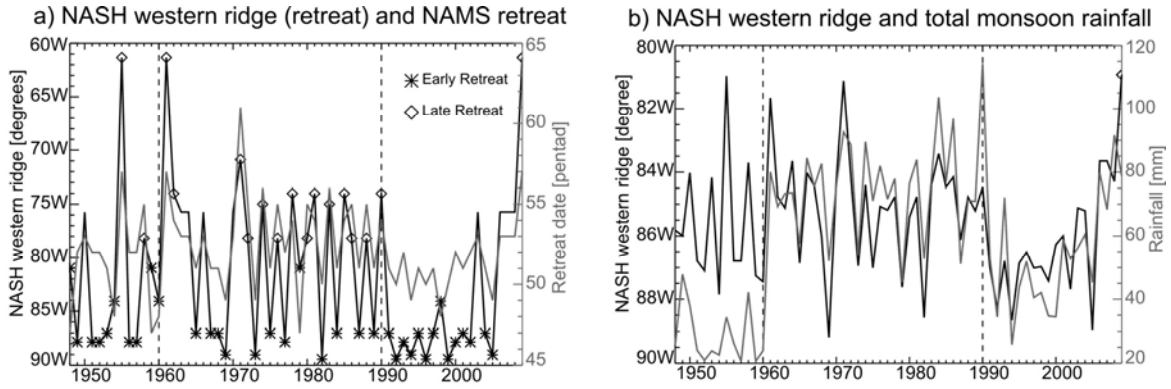

Fig. 19 a) Location of the NASH western boundary averaged during the last five pentads of the monsoon season (black) and the monsoon retreat over NWMEX (gray). b) Location of the NASH western boundary averaged during the entire monsoon season (black) and monsoon total rainfall over NWMEX (gray). Asterisks (diamonds) in a) represent monsoon events with early (late) retreat.

How can the westward expansion of the NASH cause an earlier NAMS retreat? Fig. 20 shows the correlation between changes of the near surface monsoon low-pressure center, the NASH, and the low-level moisture transport to the NAMS region during the period of analysis. Fig. 20a shows that an easterly wind anomaly at 850 hPa in the NWMEX domain, which transports moisture from the Gulf of Mexico to the NAMS region, is correlated with negative geopotential height anomalies at 850 hPa over NWMEX during the NAMS retreat phase. This correlation pattern confirms that the

easterly moisture transport from the Gulf of Mexico is connected to the monsoon circulation, as suggested by previous studies (e.g., Higgins et al. 1997; Adams and Comrie, 1997). In contrast, a southerly wind anomaly over the southern Great Plains is correlated with a positive geopotential height anomaly at 850 hPa over the SE US and the eastern portion of the Gulf of Mexico and the Caribbean Sea (Fig. 20b), associated with the observed westward expansion of the NASH (Fig. 18).

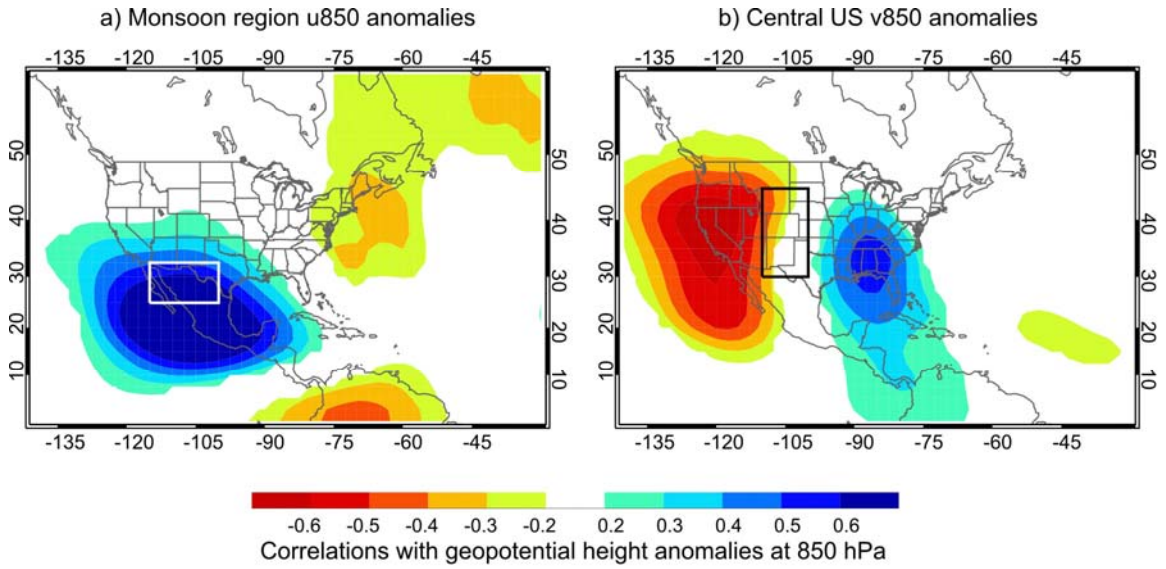

Fig. 20 a) Correlations between zonal wind anomalies averaged over the monsoon region and geopotential height anomalies at 850 hPa, five pentads before the monsoon retreat. b) Same as a) but for meridional wind at 850 hPa averaged over the central US. Correlations are statistically significant at the 5% level based on Monte Carlo test (Livezey and Chen 1993). Linear trends were removed before computing correlations. Boxes indicate the regions corresponding to wind anomalies average.

Figs. 16-20 suggest that, when the western edge of the NASH is located eastward, low-level winds over the western Gulf of Mexico and the Caribbean Sea are influenced

by the NAMS. The resultant southeasterly moisture transport is an important source of moisture for sustaining the monsoon circulation over the NAMS region, especially over NWMEX. In contrast, when the NASH expands westward, it dominates the low-level winds over the Gulf of Mexico, leading to strong southerly moisture transport to the Great Plains. Such a change cut off the moisture transport from the Gulf of Mexico to the monsoon region, consequently weakens the NAMS, and contributes to the increased frequency of early-retreat monsoons observed during the past two decades.

3.3.3.2 Variations in upper troposphere circulation

Fig. 21 shows the mean upper troposphere (200 hPa) circulation for strong and weak NAMS events. Weak monsoons were divided into those occurred during each of the two dry regimes (1948-1959 and 1990-2009, respectively). Strong monsoons correspond to those occurred during the wet regime (1960-1989). Three pentads before the strong monsoon retreats (Fig. 21a), the monsoon anticyclonic circulation is centered over NWMEX (~25˚N) and the subtropical jets over North America are located between 30°N and 45°N. During the two dry periods (Figs. 21b and 21c), the subtropical jets are wavier with a trough located over the eastern US and a ridge over the central and western US. The jets shift northward to between 40°N and 50°N over North America during the more recent dry period (Fig. 21c) relative to the earlier dry period (Fig. 21b).

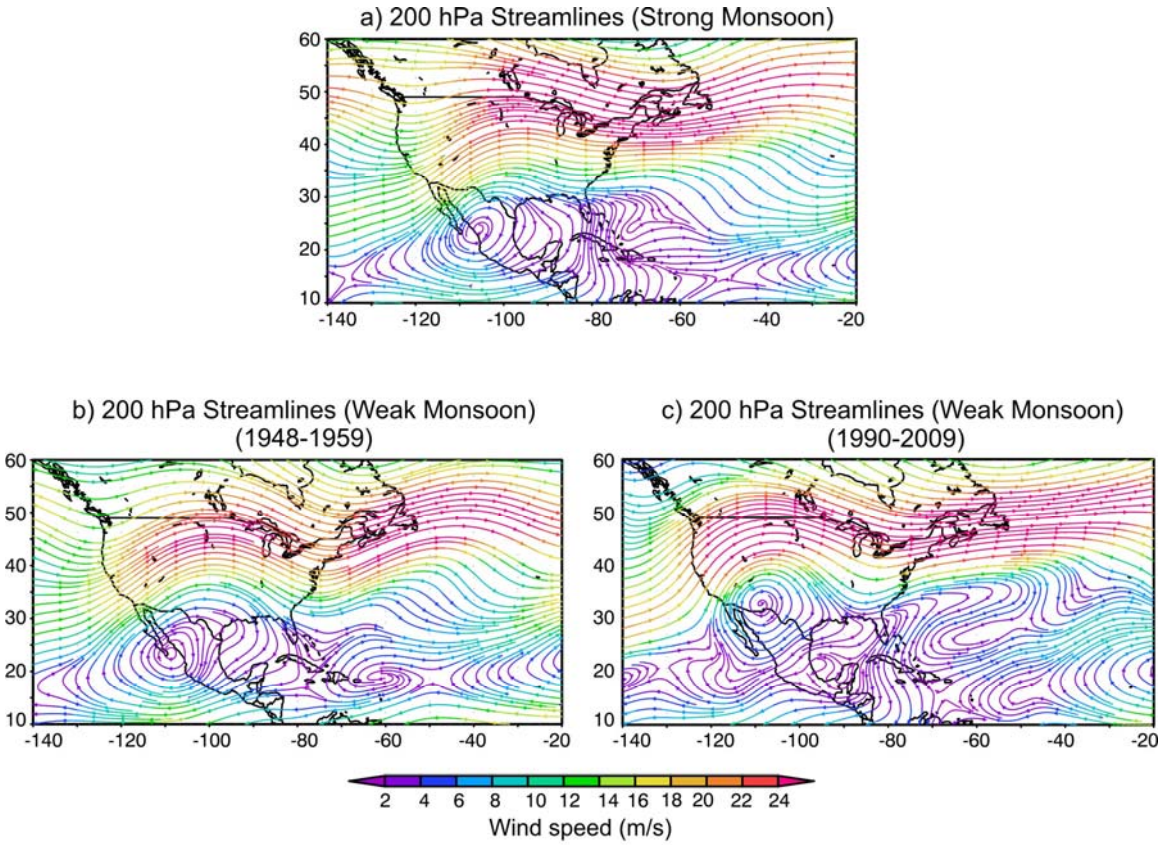

Fig. 21 200 hPa streamlines composite for strong monsoons a) and weak monsoons during b) 1948-1959 and c) 1990-2009, three pentads before the monsoon retreat. Color scale indicates wind speed in m/s.

The early-retreat monsoons occurred during the more recent dry period also show a northward shift of the subtropical jet stream over the US (Fig. 22c). This is not observed during the late-retreat events (Fig. 22a) or the early-retreat events occurred during the earlier dry period (Fig. 22b).

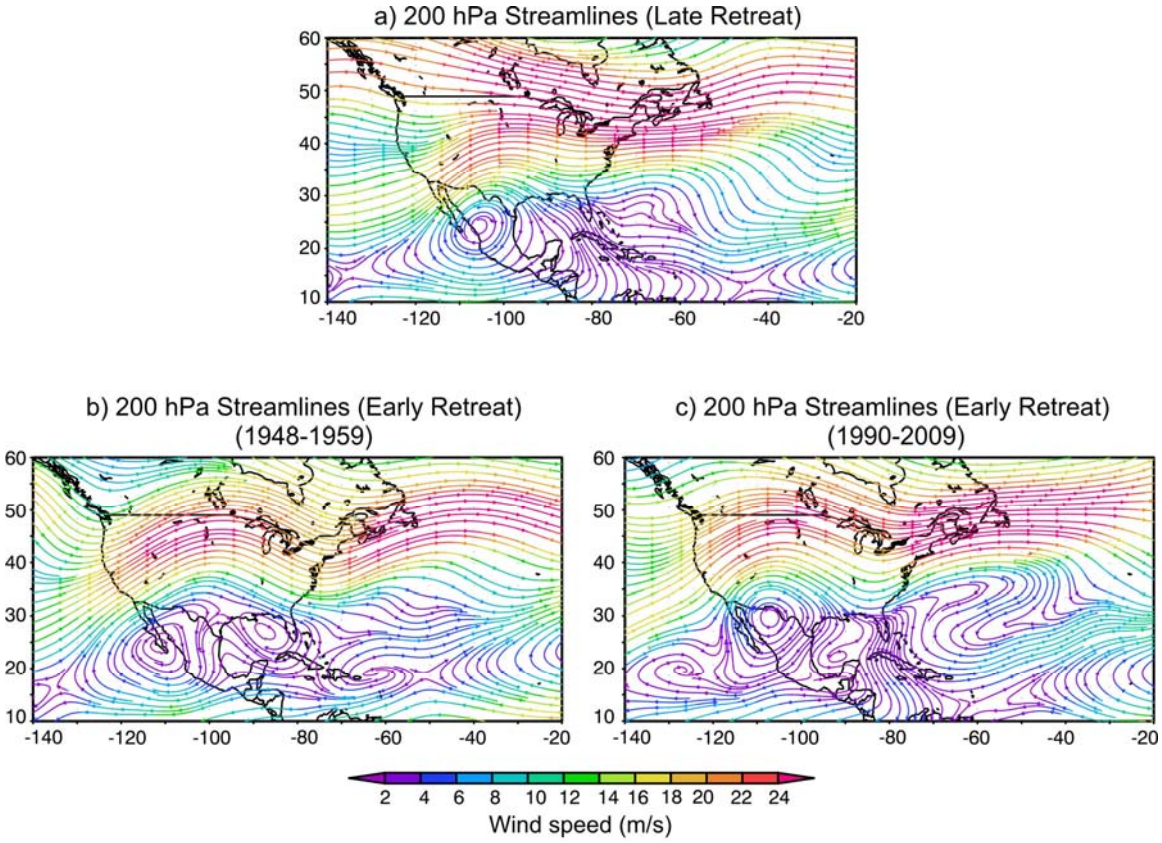

Fig. 22 Same as Fig. 21 but for early and late-retreat monsoons.

A northward displacement of the subtropical jet stream over the western US during the more recent decades would reduce the number and strength of mid-latitude synoptic disturbances that propagate to the NAMS region, which in turn would reduce monsoon convection and, consequently, weaken the monsoon and force its earlier retreat.

3.3.3.3 Connection to changes of sea surface temperatures

Previous studies have shown the influence of Pacific and Atlantic SSTs on the NAMS onset and strength. For example, Higgins et al. (1998, 1999) and Harrington et al.

(1992) show that ENSO modulates monsoon rainfall over Mexico and the SW US, affecting the monsoon strength. Changes in the thermal gradient from the Pacific Ocean to the SW US can also affect the monsoon onset (Higgins and Shi 2001; Zhu et al. 2007; Turrent and Cavazos 2009). A positive (negative) PDO phase and El Niño (La Niña) conditions favor weaker (stronger) monsoons, a southward (northward) displaced monsoon ridge, and a late (early) monsoon onset over the SW US (Castro et al. 2001). Changes in the AMO and AO phases also modulate the NAMS interannual variability (Hu and Feng 2008, 2010). A recent study by Cravatte et al. (2009) showed that the western Pacific warm pool has significantly freshened and warmed since 1955 and that the warm and fresh surface waters have extended horizontally. Since this region of the Pacific is closely related to ENSO dynamics, which in turn influences the NAMS variability, a warmer and expanded western Pacific warm pool could also affect the NAMS. Whether these changes of SSTs would influence the monsoon strength and retreat phase over Mexico is investigated.

To determine if SST changes are linked to the main known ocean-atmosphere variability modes, correlations between these modes and the NWMEX monsoon retreat dates were computed. Summer indices for (i) AO, (ii) AMO, (iii) PDO, (vi) ENSO, and (vii) WPWP expansion were considered. Niño 3, Niño 4, and Niño 3.4 indices were used to represent ENSO. Since AO and AMO are correlated, a linear regression was used to remove the AO influence from the AMO index before computing correlations. To

identify the effects of the WPWP expansion independently of ENSO, ENSO influence was removed following the same approach and using Niño3 and Niño4 indices.

Changes in the monsoon retreat are not significantly correlated with PDO, ENSO, or AO indices. Although previous studies identified the PDO as an important modulator of the monsoon rainfall over the SW US (Carleton et al. 1990; Higgins and Shi 2000; Castro et al. 2001), this analysis indicates that the PDO multi-decadal variations do not match those observed in the monsoon strength and retreat over NWMEX (not shown) during 1948-2009. The contributing factors to monsoon decadal variability may vary within the monsoon domain. The interannual influence of ENSO on the NAMS rainfall has been also previously documented (e.g. Harrington et al. 1992; Higgins et al. 1998, 1999); however, this work indicates that the observed decadal changes in the NAMS cannot be explained by an ENSO influence. Recent model experiments by Schubert et al. (2009) and Mo et al. (2009) lead to the conclusion that the AMO modulates the impact of ENSO on seasonal drought over the US. However, how the interaction between ENSO and AMO can contribute to changes of the summer NAMS, especially its retreat phase, is still not clear.

On the other hand, both the WPWP and AMO show decadal variability similar to that of the monsoon retreat and total monsoon rainfall over NWMEX (not shown). Dry regimes, characterized by weak monsoons and early retreats, coincide with an expanded WPWP and the AMO positive phase, especially after 1990. Furthermore, correlations between these SST variability indices and the NASH western boundary location are not

statistically significant, in agreement with Li et al. (2011). The underlying physical processes for the influence of the AMO and the WPWP expansion on the NAMS retreat over NWMEX are explored in the following sub-sections.

a) Influence on moisture transport to the NAMS

How would the AMO and the western Pacific warm pool influence the NAMS retreat?

To identify the possible mechanisms that influence the monsoon strength and retreat during the two dry periods, the changes that occurred during 1948-1959 and 1990-2009 were analyzed separately and compared with those during the wet period (1960-1989). Figs. 23 and 24 show changes in mean rain rate and winds at 850 hPa a few pentads before the monsoon retreat for the earlier and the more recent dry periods, respectively, relative to the wet period. Changes between a) the expansion and contraction of the WPWP and b) the positive and negative phase of the AMO were obtained. For comparison, the changes between the westward expansion and eastward withdrawal of the summer NASH (Figs. 23c and 24c) and those between early and late NAMS retreat (Figs. 23d and 24d) are also shown.

A westward expansion was identified when the NASH western edge was located westward of 90°W (mean location during weak and early-retreat NAMS events; Fig. 19a). An eastward withdrawal was selected when the NASH western boundary was located eastward of 75°W (mean location during strong and late-retreat NAMS events; Fig. 19a). A total of 123 (239) pentads with a westward location of the NASH western

ridge, out of a total of 216 (360) pentads within the monsoon season during 1948-1959 (1990-2009) were chosen. For the period 1960-1989, a total of 57 out of 540 pentads with an eastward retreat of the NASH were selected.

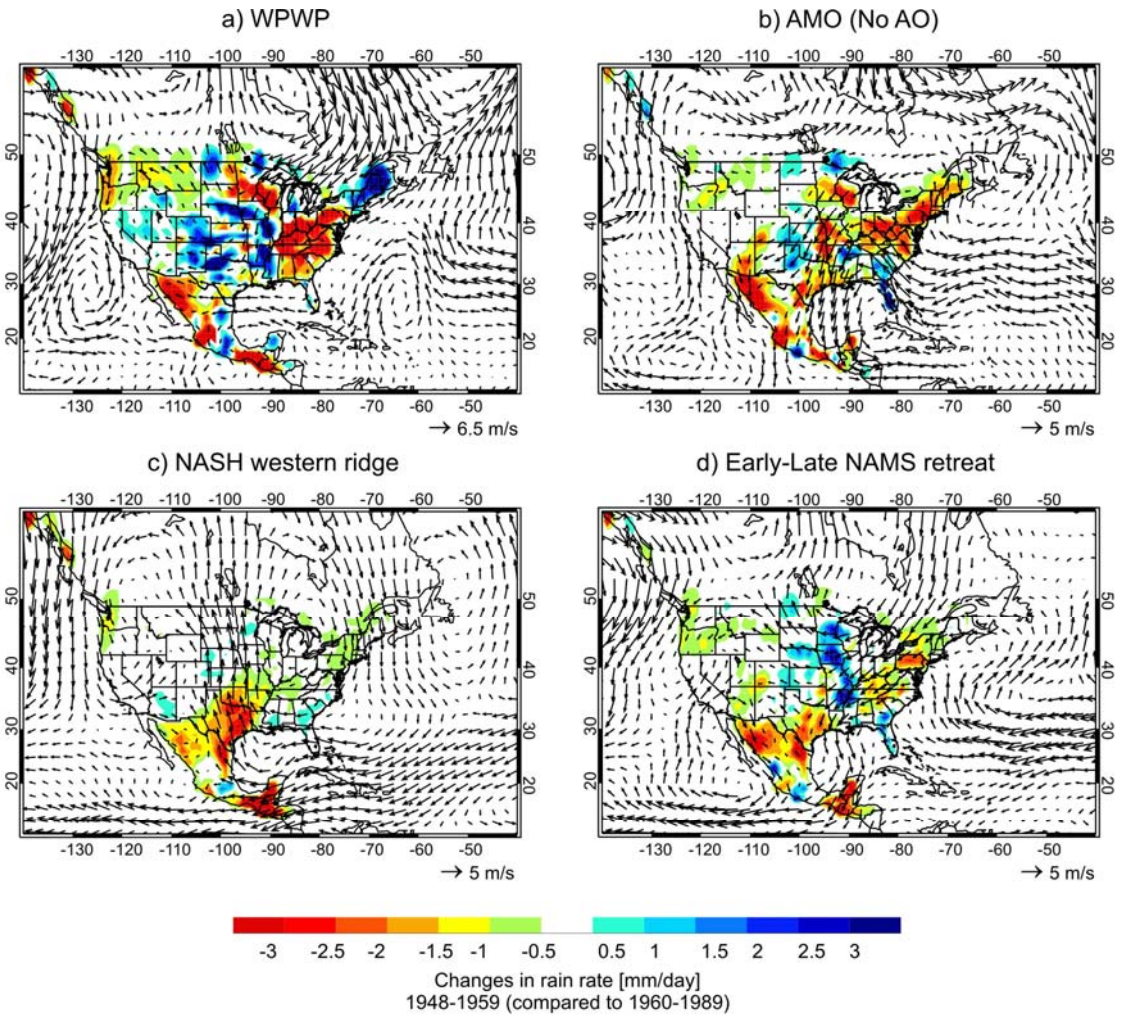

Fig. 23 Changes in SLP (shades) and wind at 850 hPa (arrows) between the positive and the negative phase of a) WPWP and b) AMO, two pentads before the NAMS retreat during 1948-1959. c) Same but for difference between westward and eastward location of the summer NASH western boundary and d) but for difference between early and late NAMS retreat events. Vector scale is shown in the right-bottom corner of each panel.

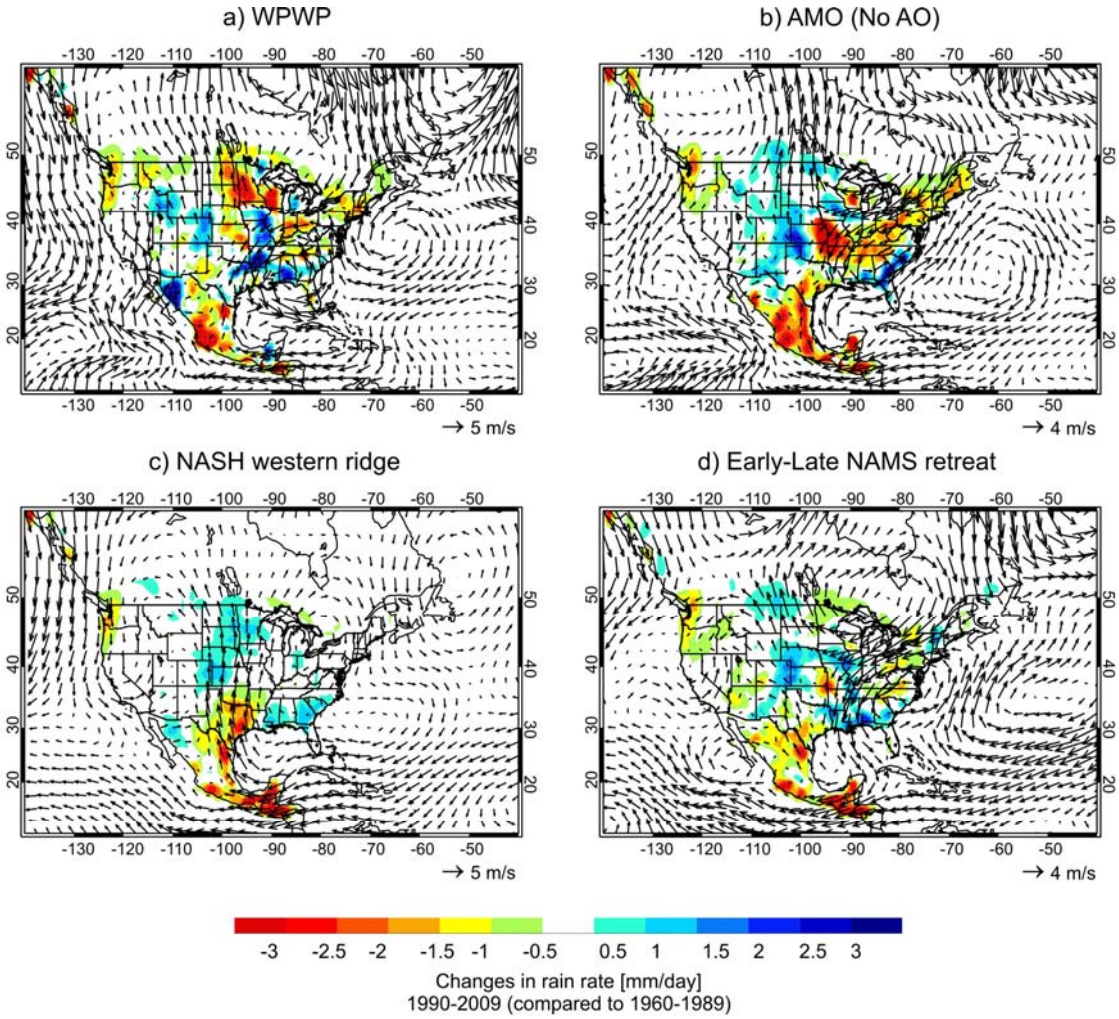

Fig. 24 Same as Fig. 23 but for 1990-2009.

Comparison of the anomalous surface circulation and rain rate patterns between early and late-retreat monsoons with those obtained during the positive phases of the AMO and the expansion of the WPWP and the NASH for the earlier dry period (1948-1960; Fig. 23) shows that the pattern associated with the positive phase of the AMO (Fig. 23b) resembles the observed changes during early-retreat monsoons (Fig. 23d). However, during the more recent dry period (Fig. 24), changes in surface circulation during early-

retreat monsoons are a combination of the pattern observed for the positive phase of the AMO and for the westward expansion of the NASH: enhanced Caribbean and Great Plains low-level jets are observed during both early retreats (Fig. 24d) and the NASH expansion (Fig. 24c) while an enhanced cyclonic center over the SE US is observed during early retreats and the positive phase of the AMO (Fig. 24b). This cyclone is also observed when the WPWP expands (Fig. 24a). These results suggest that the recent expansion of the NASH and the western Pacific warm pool also contribute to the weakening of the NAMS observed during 1990-2009, in addition to the positive phase of the AMO.

b) Influence on the subtropical jet in the upper troposphere

The effects of the decadal variability modes on the upper troposphere jet stream are investigated by Fig. 25. Since Fig. 21 suggests that the northward shift of the subtropical jets and the monsoon anticyclone is mainly observed during the weak monsoons of the more recent dry period, only composites for mean upper-troposphere circulation during 1990-2009 are shown. The change associated with the NASH expansion (Fig. 25c) mostly resembles the composite difference between early and late retreats of the NWMEX monsoon (Fig. 25d). The changes over North America associated with the WPWP expansion (Fig. 25a) also show some resemblance to those observed during the early NAMS retreats.

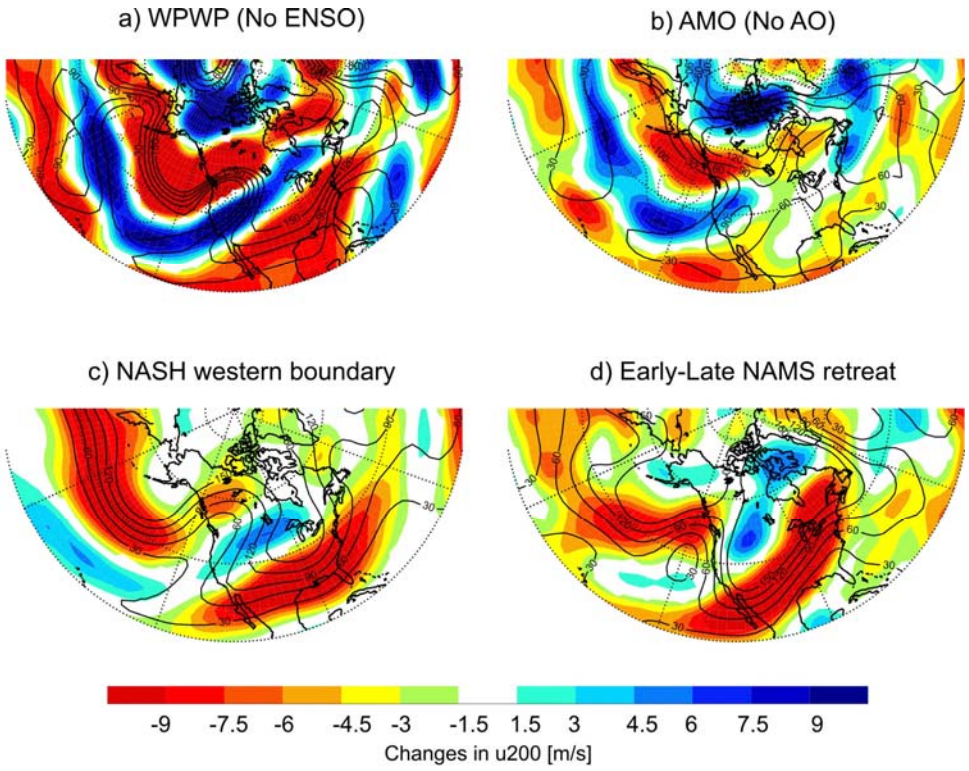

Fig. 25 Same as Fig. 24 but for zonal wind at 200 hPa (shades) and geopotential height at 200 hPa (contours) during 1990-2009.

These findings suggest that the weakening and the northward shift of the upper troposphere subtropical jets over the US and the enhanced Great Plains low-level jet associated with the westward expansion of the NASH resemble the changes observed during the early monsoon retreats after 1990 more closely than those observed during the expansion of the WPWP.

3.4. Discussion

3.4.1. Causes of the early NAMS retreat

The empirical evidence shown here suggests the occurrence of two regime types of the NAMS: two dry periods (weak monsoons, early retreats, and late onsets) during 1948-1959 and 1990-2009, and a wet period (strong monsoons, late retreats, and early onsets) during 1960-1989. Although the two weak monsoon periods are correlated with the AMO positive phase, the dominant cause for both dry periods is different. The earlier dry period is induced mainly by the positive phase of the AMO, in agreement with Hu and Feng (2008). On the other hand, the increased occurrence of weak and early-retreat events of the summer monsoon over NWMEX observed after 1990 is also associated with the westward expansion of the NASH, which weakens the low-level moisture transport from the Gulf of Mexico to the monsoon region and leads to a northward shift of the subtropical upper troposphere jet stream. The latter may be also influenced by the expansion of the WPWP.

Kushnir et al. (2010) have suggested that heating anomalies resembling those during the positive phase of the AMO would induce an anomalous subsidence in the middle troposphere over the western US and Mexico through a Gill-like response to the diabatic heating induced by warmer SSTs over the tropical Atlantic. This circulation change in turn reduces warm season rainfall over the US and northern Mexico. The

composite circulation change between the positive and negative phases of the AMO in Figs. 23b and 24b shows a low-level anticyclonic circulation anomaly over the NAMS region and a weakening of the NASH, which are consistent with those shown in Kushnir et al. (2010).

In addition to the enhanced subsidence over the western US and Mexico induced by the positive phase of AMO, the weakened NAMS rainfall and the early retreats are best correlated with the westward expansion of the NASH during the recent decades. Although the processes that link the NASH to the NAMS have not been thoroughly studied in literature, the negative correlation between rainfall anomalies over the NAMS region and that over the Great Plains have been extensively documented (Douglas et al. 1993; Douglas and Englehart 1996; Higgins et al. 1997; Mo et al. 1997; Barlow et al. 1998). The strengthening of the low-level jets over the Caribbean and the Great Plains (the latter in turn contributes to an increased rainfall over the central US) may be dominated by the westward shift of the NASH. The weakening of the NASH induced by the AMO (e.g., Hu and Feng 2008; Kushnir et al. 2010; Weaver et al. 2010) is mainly confined over the SE US (Fig. 24b). Thus, the westward expansion of the NASH allows the NASH to replace the NAMS as the main controller of the low-level flow over the western Gulf of Mexico. This change enhances northward moisture transport to the Great Plains and weakens the westward and northwestward moisture transport to the NAMS region. During 1948-1989, the western edge of the NASH oscillates interannually between 75˚W and 90˚W leading to late and early NAMS retreats, respectively. After

1990, the western edge of the NASH becomes stationary in 85˚-90˚W, leading to persistent weak and early NAMS retreats. Although the period 1948-1959 also shows an increased frequency of weak and early-retreat NAMS events compared to 1960-1989, the location of the NASH western boundary varies between east (65˚W) and west (88˚W). By contrast, the western boundary of the NASH is persistently located to the west of 80˚W after 1990 (Fig. 19a). A more westward expanded NASH during the weak early-retreat monsoons in the more recent dry period is evidenced by the increases in SLP (Figs. 16a and 17a) and the anticyclonic circulation observed over the Gulf of Mexico (Fig. 24d), which leads to a stronger moisture transport to the central US and a reduced transport to the monsoon region. This suggests that the expansion of the western ridge of the NASH is the main mechanism for the increased frequency of weak and early-retreat NAMS events observed after 1990.

The links between the northward shift of subtropical jets and the expansion of the WPWP can be explained by a planetary wave train resembling that of the Pacific-North-American (PNA) pattern (Wallace and Gutzler 1981; Lau and Peng 1992). The PNA-like wave train response to a tropical Pacific heating anomaly in summer would increase upper-level geopotential height in subtropical North America and decrease geopotential height in mid-latitude North America (Yu et al. 2007; Seager et al. 2010), which would shift the subtropical jets poleward, along with the synoptic activity over the US (Grimm and Silva Dias 1995; Seager et al. 2005).

3.4.2. Relative influence of the decadal variability versus global climate change

Previous studies have mainly attributed the decadal changes of the NAMS rainfall in the past several decades to ocean-atmosphere decadal variability modes such as the PDO, AMO, and AO (e.g., Higgins and Shi 2000, Seager et al. 2005; Castro et al. 2007; Mo 2010; Enfield et al. 2001; Schubert et al. 2004; McCabe et al. 2004; Hu and Feng 2008; Kushnir et al. 2010; Hu and Feng 2010). This analysis suggests that the change of the NAMS retreat and strength is likely caused by both decadal variability and anthropogenic forced change. In particular, while the earlier dry regime (1948-1959) is mainly caused by a positive phase of the AMO, the more recent dry regime (1990-2009) is mainly caused by the westward expansion of the NASH. This westward expansion is not correlated with any decadal variability modes known to us. Li et al. (2011) have shown the westward expansion of the NASH western edge and an intensification of the NASH's center in recent decades. They found that natural decadal modes do not appear to explain this observed change of the summer NASH and they attributed it to the increase of GHGs, based on the global climate model simulations participated in the IPCC Fourth Assessment (CMIP3).

While the observed increase in the occurrence of weak and early-retreat events of the NAMS is likely in part contributed by a human forced global climate change, it is not clear whether CMIP3 global climate models can adequately reproduce a weakening and an early retreat of the NAMS given the difficulty of simulating the NAMS by these

models, as shown in previous studies (e.g., Yang et al. 2001; Collier and Zhang 2007; Lee et al. 2007; Lin et al. 2008). The future release of IPCC AR5 model runs would be an excellent opportunity to test the impact of human forced global climate change on the weakening and early retreat of the NAMS during the past few decades.

3.5. Conclusions

The causes of the dry and wet regimes of the NAMS observed from 1948 to 2009 were analyzed: two dry periods, associated with weak monsoons and early retreats/late onsets, are observed during 1948-1959 and 1990-2009 whereas a wet regime, associated with strong monsoons and late retreats/early onsets, is observed during 1960-1989. Although the change of the NAMS regime correlates with the AMO, as found by previous studies (Hu and Feng 2008), the behavior of the monsoon retreat and the dominant cause of the dry NAMS regime for the earlier (1948-1959) and the more recent (1990-2009) periods are different.

The earlier dry regime (1948-1959) shows a strong interannual variation between weak and strong NAMS events. This dry regime is caused by circulation changes associated with the positive phase of the AMO and it ends when the AMO changes to its negative phase during 1960-1989. In contrast, the NAMS is persistently weak and its retreat is persistently early during the more recent dry regime. The main cause of these

changes is the westward expansion of the North Atlantic Surface High (NASH). As a result of this shift, the low-level winds over the western Gulf of Mexico are dominated by the anticyclonic flow of the NASH, instead of the cyclonic flow of the NAMS that occurs during strong and late-retreat NAMS events. This change leads to an enhanced Caribbean low-level jet, which in turn induces a southerly anticyclonic flow along the western edge of the NASH, transporting moisture from the Gulf of Mexico to the Great Plains, instead of the NAMS region. In addition, the warm phase of the AMO weakens the summer monsoon circulation associated with the NAMS, presumably by enhancing the mid-troposphere subsidence over the western US and northern Mexico (Kushnir et al. 2010). In the upper troposphere, the subtropical jets shift northward over the western US during the recent decades. Such a change in the jet stream location prevents synoptic disturbances from reaching the monsoon region, reducing favorable conditions for convection and, therefore, weakening the monsoon.

The expansion of the NASH and the WPWP are linked to the northward shift of the subtropical jet stream over North America during the more recent dry monsoon regime, which also contributes to the observed weakening and more frequent early retreats of the NAMS after 1990. This link is consistent with a PNA wave train induced by the expansion of the WPWP to the central Pacific (Yu et al. 2007; Seager et al. 2010). However, the causality between the westward expansion of the NASH and the northward shift of the subtropical jets over North America is not clear and needs further study.

The dry regime observed during 1948-1959 is mainly associated with a warm AMO. During 1948-1989, the western edge of the NASH oscillates interannually between 75˚W and 90˚W, leading to both late and early NAMS retreats, respectively. During 1990-2009, the western edge of the NASH becomes stationary in 85˚-90˚W, the WPWP expands (Cravatte et al. 2009), and the AMO enters to its warm phase. Anomalies linked to these phenomena reduce the moisture transport to the NAMS region and shift the subtropical jets northward over the western US and northern Mexico. These changes together are responsible for the trend toward weaker and more frequent early-retreat NAMS events observed after 1990.

Chapter 4

A connection between the North American monsoon and the southern Amazon wet season after 1978

4.1. Introduction

The results presented in Chapter 3 suggest an increased frequency of weak and early-retreat NAMS events after 1990 due to the combination of three main factors: (i) the positive phase of the AMO [as also discussed by Hu and Feng (2008)], (ii) the northward shift of the subtropical jets over North America, and (iii) the westward expansion of the North Atlantic surface high (NASH) observed after 1978 (Li et al. 2011). On the other hand, Fu et al. (2011) show evidence of a lengthening of the dry season over the Southern Amazon since 1978 due to a delayed onset of the wet season. Such a delayed wet season onset over the southern Amazon would also delay the onset of the SAMS since the intense heating released during the Amazon wet season is crucial to establish and maintain the SAMS circulation. Although the discussions presented in Chapter 3 and Fu et al. (2011) identified the main causes for these changes in the American monsoons, whether there is a common factor that induces such changes or they are the consequence of independent and unrelated causes is still not clear. Besides increased evapotranspiration and enhanced cold air incursions to the monsoon region at the end of the transition season from dry to wet conditions, increased moisture transport is the third requirement for increasing rainfall in the Amazon and diabatic heating needed

for the SAMS onset (Li and Fu 2004). Therefore, this chapter particularly focuses on the role of the NASH westward expansion on influencing the moisture transport to the southern Amazon and SAMS domain and, hence, on their wet season onset. This chapter is organized in five sections. Section 4.2 describes the data and the methodology implemented. Section 4.3 presents how the NASH westward expansion modifies the moisture transport to South America (and for instance, the SAMS onset) via changes in easterly waves (EWs) activity. Section 4.4 presents a short discussion about the possible influence of the increasing atmospheric CO_2 concentration on the changes in the American monsoons timing observed after 1978. Finally, section 4.5 presents the main conclusions.

4.2. Data and methodology

To understand the influence of the NASH westward expansion on the surface moisture transport to the southern Amazon and the SAMS domain, the evolution of surface circulation and outgoing longwave radiation (OLR) during the transition season between both monsoons and their link to the observed variations in the location of the NASH western ridge were analyzed. In addition, the possible influence of the NASH western boundary on the EWs activity over the Intra-American Sea (IAS) region and northern South America was investigated. The transition season between both monsoons

was defined as the period between the NAMS retreat date and the southern Amazon wet season onset date for each year during the period 1978-2007.

The onset/retreat dates were obtained over the spatial domains of the NAMS and the southern Amazon defined in Chapter 3 and by Fu et al. (2011), respectively. The NAMS domain corresponds to northwestern Mexico (Fig. 10a) whereas the southern Amazon domain corresponds to the region delimited by 50°W-70°W, 15°S-5°S. The onset/retreat dates were indentified using the methodology proposed by Li and Fu (2004) and described in section 3.2.

The linear trends of the resulting NAMS retreat and southern Amazon wet season onset dates and transition season length were estimated using the non-parametric Mann-Kendall test with Sen's statistics (Sen 1968). In addition, following the approach presented in Chapter 3, the NAMS retreat events were divided into early and late-retreat monsoons.

To obtain the southern Amazon wet season onset dates, two different rainfall datasets over South America were used: (i) the 1-degree grid rain gauge daily precipitation from the National Oceanic and Atmospheric Administration (NOAA) Climate Prediction Center (CPC) available during 1978-2007 (Silva et al. 2007; hereafter referred to as Silva data) and (ii) the NOAA Climate Diagnostics Center (CDC) daily precipitation gridded data version SA21 available from 1940 to 2009 at ftp://ftp.cdc.noaa.gov/Public/dallured/tran/ sa21.0907/ (Liebmann and Allured 2005;

hereafter referred to as SA21 data). Records during 1978-2007 were used to match the common period between both datasets.

The NAMS retreat dates were obtained from the NOAA CPC 1-degree grid daily precipitation over the US and Mexico described in section 3.2. To match the record period of the rainfall datasets over South America, only data during 1978-2007 was used.

Daily 2.5-degree grid data for air temperature, geopotential height, and horizontal wind at different pressure levels was obtained from the National Center for Environmental Project-National Center for Atmospheric Research (NCEP-NCAR) Reanalysis (Kalnay et al. 1996) from 1948 to present. In addition, the daily NOAA interpolated OLR described in section 2.2 (Liebmann and Smith 1996) was used as a proxy for convection.

Following Wang and Fu (2002), the area mean 925 hPa meridional wind averaged over the region 65°W-75°W, 5°S-5°N (hereafter referred to as the South American V-Index) was used to represent the variability of the cross-equatorial flow over South America, which is an important moisture source to feed the Amazon wet season and the SAMS (Wang and Fu 2002). In addition, the mean position of the 1560m of geopotential height (gpm) line was used to characterize the western ridge of the NASH during the transition season from the NAMS to the SAMS, as suggested by Li et al. (2011).

Composite and regression analyses were performed in order to understand the effects of the changes of the NASH western ridge location on moisture transport to South

America throughout the transition season between the American monsoon systems. Regression patterns were obtained considering both positive and negative fluctuations of the NASH western boundary location.

The effect of the NASH western ridge location on EWs activity over the IAS region and northern South America was analyzed using 700 hPa relative vorticity anomalies and Ertel's potential vorticity (PV). The latter was obtained by linearly interpolating daily air temperature and wind fields to isentropic surfaces each 5K and computing PV directly on each surface (Molinari et al. 1995, 1997). Ertel's PV was computed using

$$\mathrm{P}V = g\sigma^{-1}\left(\zeta_\theta + f\right) \tag{2}$$

where g is the acceleration due to gravity, θ is the potential temperature, $\sigma = -\partial p / \partial \theta$, ζ_θ represents the vertical component of the relative vorticity computed on an isentropic surface, and f corresponds to the coriolis parameter. Since EWs propagation and intensification are favored by sign reversals in the background PV field (e.g. Burpee 1972; Molinari et al. 1997, 2000), the PV fields were filtered using a low-pass Fourier filter with 20-days cutoff (Molinari et al. 1997) before composites were computed.

4.3. Results

4.3.1 A longer transition season between the American monsoon systems

The NAMS retreat and the southern Amazon wet season onset dates were identified following Li and Fu's (2004) approach using one rainfall dataset over North America (CPC US-Mex data) and two datasets over South America (Silva and SA21 data) during 1978-2007. Fig. 26 shows the corresponding time series of the NAMS retreat (gray dashed line) and the southern Amazon wet season onset (black solid line). As discussed in Chapter 3, the NAMS presented two types of regimes during 1948-2009: (i) a dry regime, associated with early retreats and late onsets, observed during 1948-1959 and 1990-2009, and (ii) a wet regime, associated with late retreats and early onsets, observed during 1960-1989. Thus, the shift from a wet monsoon regime to a dry monsoon regime occurred in 1990 explains the trend toward earlier NAMS retreats observed in Fig. 26. On the other hand, the southern Amazon wet season onset shows a trend toward late onsets using both datasets, as previously documented by Fu et al. (2011), although its statistical significance is higher when Silva data is used (Fig. 26a). Changes in the NAMS onset and the southern Amazon wet season ending dates are not statistically significant (not shown), which suggests a shortening of the American monsoon systems over the last two decades.

An earlier NAMS retreat and a delayed southern Amazon wet season onset would imply a longer transition season between both monsoon systems. Fig. 27 shows the length of the transition season between the American monsoon systems, defined as the period between the NAMS retreat pentad and the southern Amazon wet season onset pentad, corresponding to both rainfall datasets over South America. Results indicate that the transition between both monsoons shows a trend toward longer periods (about 7 pentads longer between 1978 and 2007; Fig. 27a). Furthermore, the longest transition seasons occur when the NAMS retreats earlier (asterisks in Fig. 27). These findings suggest a shortening of the American monsoon systems and a lengthening of the transition season from the NAMS to the SAMS since 1978 due to an earlier retreat of the NAMS and a delayed onset of the southern Amazon wet season onset. This result raises the question: what causes the apparent correlation between the changes in the NAMS retreat and the southern Amazon wet season onset?

The results presented in Chapter 3 and the analysis from Fu et al. (2011) attribute the shortening of the American monsoons to several causes. Chapter 3 discussed that the increased frequency of early NAMS retreats observed in the recent decades is caused by an interaction between (i) the positive phase of the AMO, (ii) the recent westward expansion of the NASH, and (iii) the northward shift of the subtropical jets over North America. On the other hand, Fu et al. (2011) explained the trend toward a delayed wet season onset over the southern Amazon and the SAMS domain by (i) an increased

atmospheric stability, (ii) a reduced moisture transport, and (iii) a southward shift of the Southern Hemisphere subtropical jets.

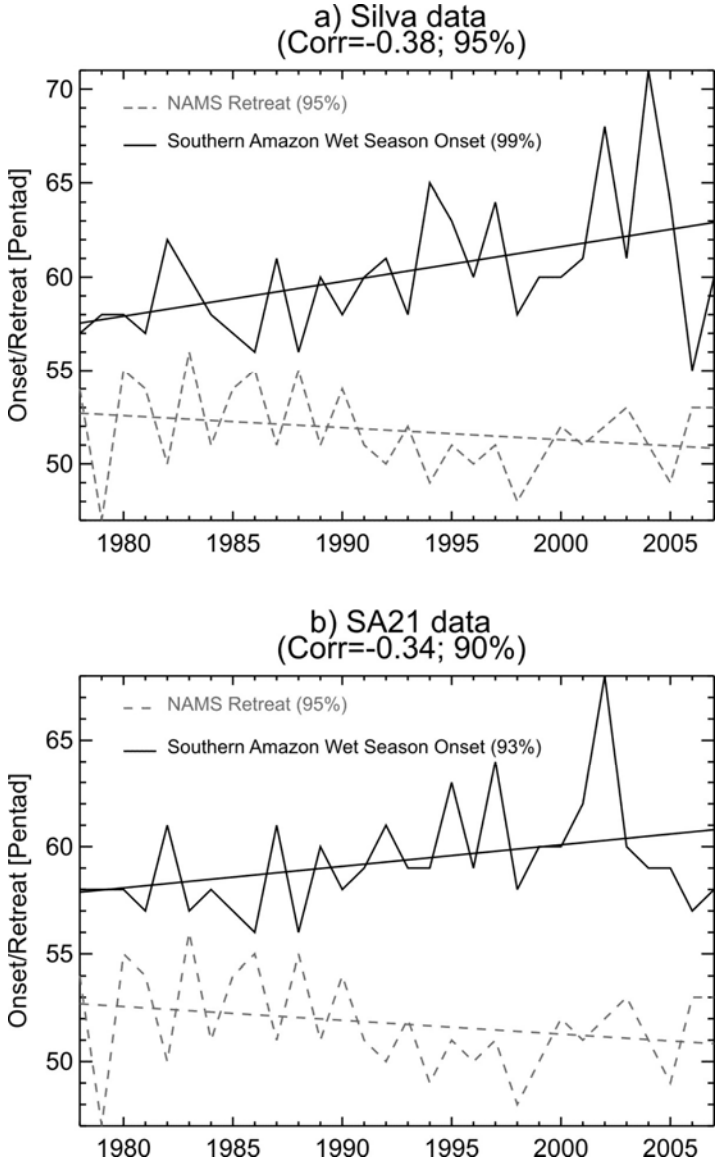

Fig. 26 NAMS retreat date obtained using CPC US-Mex data and southern Amazon wet season onset date obtained using a) Silva data and b) SA21 data. Linear trends are tested using a Mann-Kendall test with Sen's statistics (Sen 1968) and their confidence level is indicated in each panel.

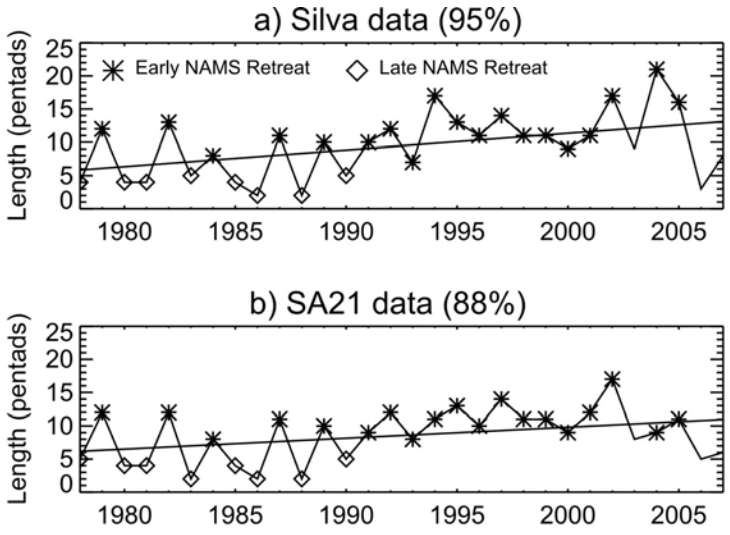

Fig. 27 Length of the transition season from the NAMS to the SAMS obtained using a) Silva data and b) SA21 data. Linear trends are tested using a Mann-Kendall test with Sen's statistics (Sen 1968) and their confidence level is indicated in each panel. Asterisks (diamonds) correspond to NAMS events with an early (late) retreat.

Furthermore, Fu et al. (2011) indicated that the delay of the wet season over the southern Amazon is not correlated with the AMO; thus, the shift toward a positive phase of the AMO cannot explain the changes observed in both monsoon systems. On the other hand, the poleward shift of the subtropical jet stream over one hemisphere may be independent of that of the other hemisphere. Therefore, the only factor that could contribute to the observed changes in both monsoon systems is the westward expansion of the NASH. Whether this expansion also influences the southern Amazon wet season onset is explored in the following subsections.

4.3.2 The role of the North Atlantic surface high expansion on delaying the wet season onset over the southern Amazon

4.3.2.1 Impact on surface circulation

The westward expansion of the NASH boundary ridge plays a relevant role in the NAMS retreat phase by inducing changes in surface moisture transport to the monsoon region, as discussed in Chapter 3. Since the summer NASH has an important control on the surface circulation over the IAS region, it could also modify the surface circulation over northern South America, which in turn could affect the moisture transport to the SAMS domain during the transition season toward the SAMS onset. To explore this possibility, 850 hPa horizontal winds, 850 hPa geopotential height, and OLR composites were obtained throughout the transition season between the American monsoons (Fig. 28). The composited 1560-gpm line is shown as an estimation of the NASH location. The boxes correspond to the South American V-Index domain, which is an important moisture source to feed the SAMS (Wang and Fu 2002). During the NAMS retreat (Fig. 28a), the NASH is expanded to the west and its corresponding anticyclone is strong, producing a dominant easterly flow over the IAS region. Surface circulation over the South American V-Index region is also dominated by easterlies; hence, the cross-equatorial flow over South America is weak, consistent with high (low) convection over northern South America (the SAMS domain). Eight pentads before the southern Amazon wet season onset (Fig. 28b), the NASH retreats eastward staying over the western

subtropical Atlantic, the NASH anticyclone weakens, and a southeasterly flow develops over the IAS region. The cross-equatorial flow over South America starts showing a stronger northerly component and convection increases over subtropical South America. By the time of the southern Amazon wet season onset (Fig. 28c), the NASH retreats to the central Atlantic and becomes much weaker. The cross-equatorial flow over South America reverses, showing a clear northerly component. Convection is fully developed over South America, consistent with an enhanced moisture transport due to a stronger V-Index.

The evolution depicted by Fig. 28 suggests that an anomalous westward expansion of the NASH would inhibit the reversal of the cross-equatorial flow necessary to trigger the onsets of the southern Amazon wet season and the SAMS. Such an anomalous expansion has been occurring since 1978, as reported by Li et al. (2011). Furthermore, such westward expansion of the NASH contributes to the trend toward earlier retreats of the NAMS during the past two decades. Therefore, to determine if the South American V-Index changes when the NAMS retreats early relative to when the NAMS retreats late, Fig. 29 shows an evolution of this index throughout the transition season toward the SAMS for the early and the late-retreat events of the NAMS. A total of 19 (8) early-retreat (late-retreat) events of the NAMS were observed during the period of analysis considered here (1978-2007).

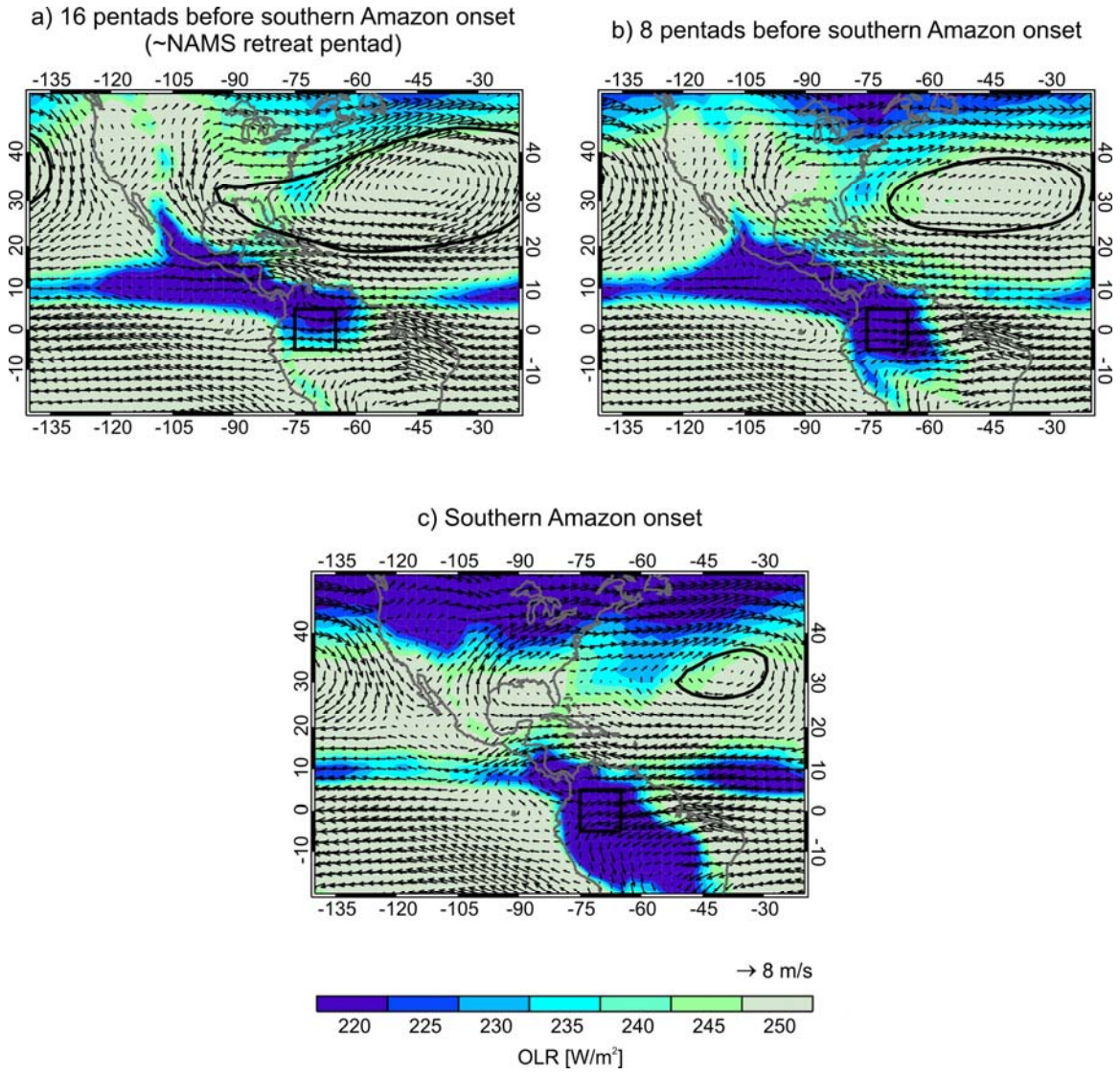

Fig. 28 OLR (shades), 850 hPa horizontal winds (arrows), and 1560-gpm line (contour) composited throughout the transition season from the NAMS to the SAMS. Composites correspond to a) 16 pentads before the southern Amazon wet season onset (~NAMS retreat pentad), b) 8 pentads before the southern Amazon wet season onset, and c) the southern Amazon wet season onset pentad. Southern Amazon wet season onset dates were obtained using Silva data. Boxes indicate the South American V-Index domain.

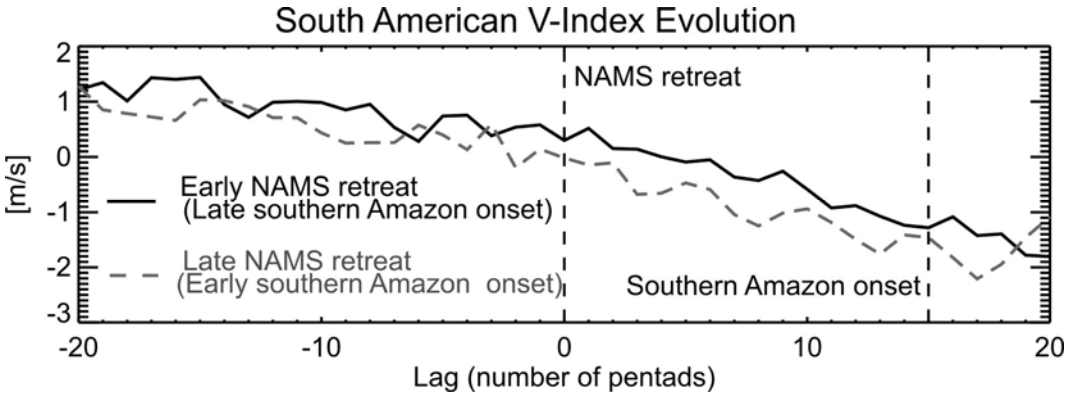

Fig. 29 South American V-Index evolution from the NAMS to the SAMS season for early NAMS retreat events (black solid line) and late NAMS retreat events (gray dashed line).

Fig. 29 indicates that the northerly flow over South America is weaker during the entire transition season corresponding to the early-retreat events of the NAMS. Since such early retreats of the NAMS have been shown to be caused by an anomalous westward expansion of the NASH, this expansion may be also associated with a weaker northerly cross-equatorial flow over South America. This is supported by correlations between the V-Index and the longitude of the NASH western ridge (not shown). A weaker northerly flow after these events would be associated with a weaker moisture transport to the southern Amazon and SAMS domains and, in turn, would delay the onset of the wet season over these regions.

To quantify the changes in surface circulation and convection associated with the westward expansion or the eastward retreat of the NASH, composites based on the linear regression between 850 hPa horizontal winds (OLR) and the location of the NASH western boundary were computed. These composites were obtained considering

fluctuations of -30 and +30 degrees of longitude in the location of the NASH, in order to represent when the NASH expands westward to the North American continent and when it retreats eastward to the central Atlantic, respectively. Fig. 30a shows the regression pattern associated with a westward expansion of the NASH. The stronger Caribbean and Great Plains low-level jets are consistent with the stronger and westward expanded NASH anticyclone. Convection is observed over Central America and northern South America whereas the cross-equatorial flow over South America is mainly easterly. When the NASH retreats eastward to the central Atlantic (Fig. 30b), the regression patterns show weaker low-level jets over Central and North America and convection shifts southward over tropical and subtropical South America. In order to identify better the differences between these regression patterns, Fig. 30c shows the difference pattern between those associated with the NASH westward expansion and its eastward retreat (i.e., Fig. 30a minus Fig. 30b) zoomed over northern South America. Increases in OLR are observed over the SAMS domain (>8 W/m^2) consistent with a suppressed northerly flow over the region.

In summary, the westward expansion of the NASH is associated with a weaker northerly cross-equatorial flow over South America, which in turn would reduce the moisture transport necessary to support the development of the wet season monsoon circulation (Wang and Fu 2002). This is consistent with the reductions in moisture reported by Fu et al. (2011) who suggest that such reductions contribute to the onset delay observed over the southern Amazon.

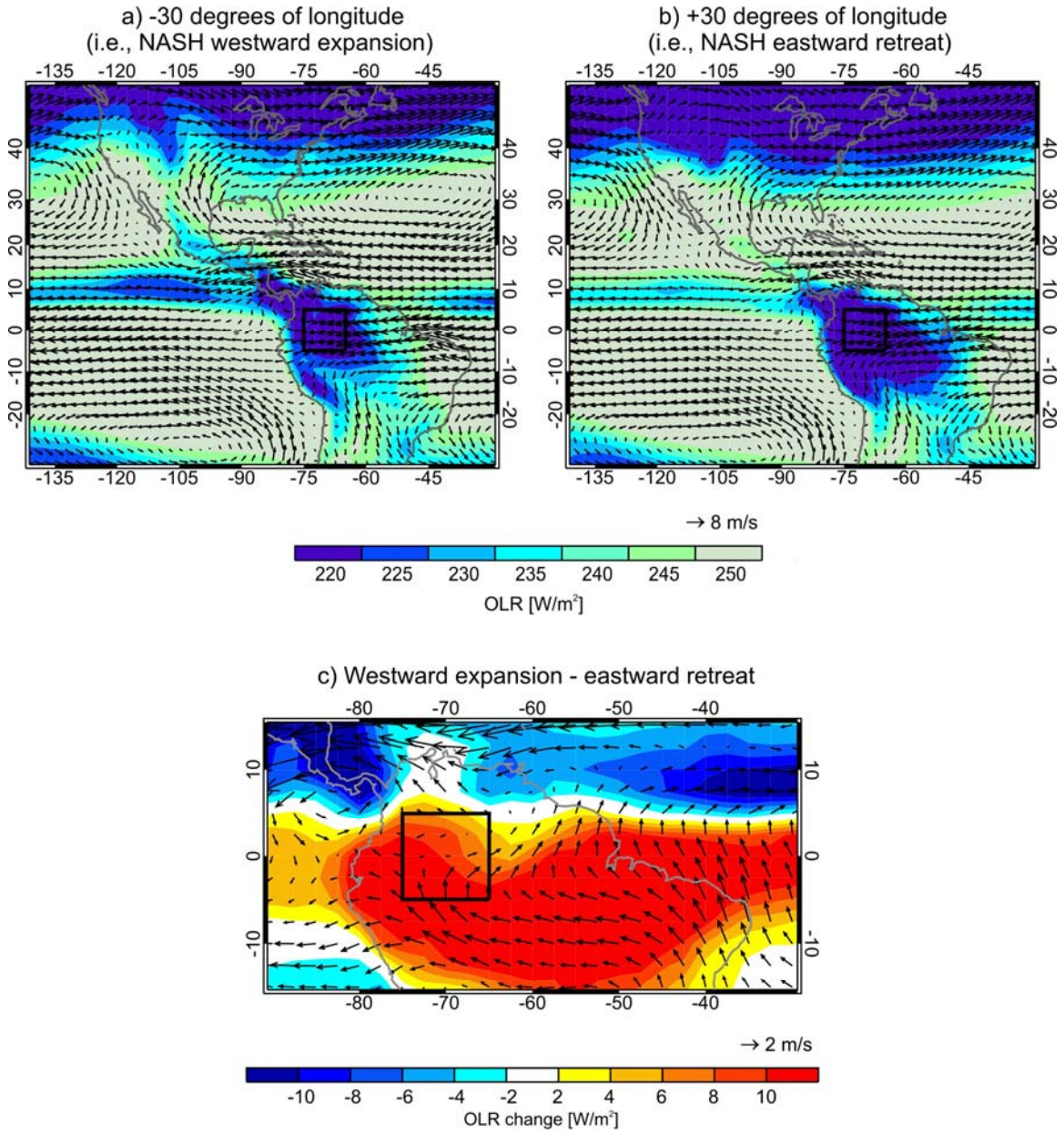

Fig. 30 Regression patterns of 850 hPa horizontal winds (arrows) and OLR (shades) associated with a) -30 longitude degrees (westward expansion) and b) +30 longitude degrees (eastward retreat) fluctuations of the NASH western ridge during SON. c) Pattern difference a)-b) zoomed over northern South America. Boxes indicate the South American V-Index domain.

4.3.2.2 Impact on easterly waves activity

How could the westward expansion of the NASH affect the moisture transport to South America?

A stronger and westward expanded NASH would generate a stronger easterly flow over the southern Caribbean Sea and northern South America and enhance the EWs activity in those regions. Such an anomalous easterly flow over the South American V-Index region would inhibit the reversal of the cross-equatorial flow that brings moisture to the southern Amazon and SAMS domains, which would contribute to the wet season onset delay observed over the region. To test this hypothesis and since EWs show more clearly in the relative vorticity anomalies field (Agudelo et al. 2010), composites based on the linear regression between the 700 hPa relative vorticity anomalies and the location of the NASH western boundary were obtained. Figs. 6a and 6b show the regression pattern associated with -30 and +30 longitude degrees fluctuations in location of the NASH western ridge, respectively. Results suggest that an anomalous westward expansion of the NASH is linked to cyclonic relative vorticity anomalies over the southern Caribbean Sea and northern South America (Fig. 31a) whereas an eastward retreat is linked to anticyclonic relative vorticity anomalies over the region (Fig. 31b). Such a positive change in relative vorticity anomalies during the westward expansion of the NASH is shown more clearly in Fig. 31c, which presents the difference between both regression patterns, zoomed over northern South America. The increases of positive relative vorticity anomalies over the Caribbean Sea and northern South America suggest

that the EWs activity over the region is enhanced when the NASH expands westward over the North American continent.

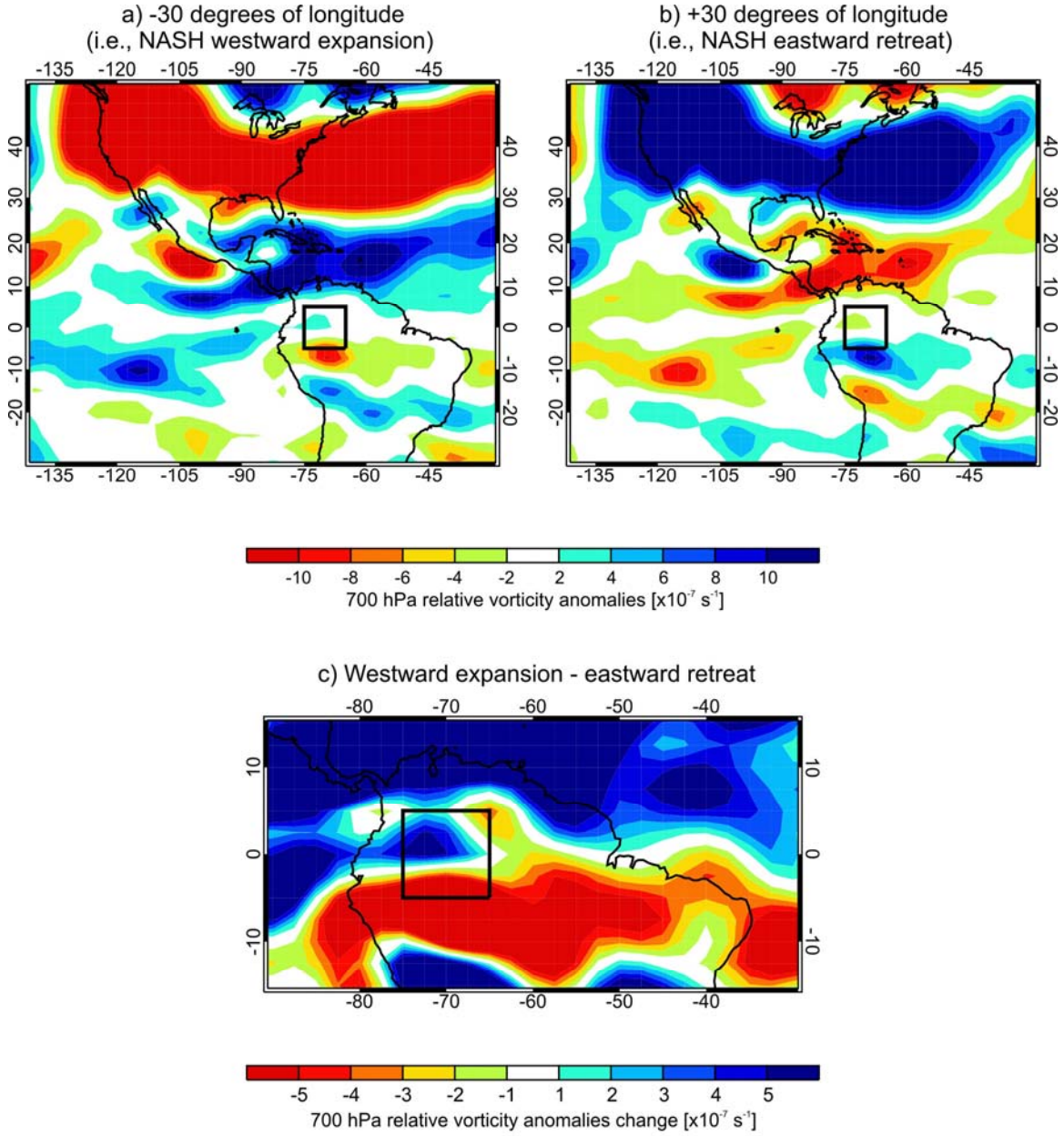

Fig. 31 Same as Fig. 30 but for 700 hPa relative vorticity anomalies.

Several studies (e.g. Burpee 1972; Molinari et al. 1997, 2000) have shown that the EWs propagation and intensification are favored by meridional sign reversals in the background PV field. Furthermore, the additional Fjortoff condition for instability (Fjortoff 1950; Eliassen 1983) requires the mean zonal flow to be positively correlated with the PV meridional gradient. Hence, a stronger meridional sign reversal in the PV field (positively correlated with the mean zonal flow) over the southern Caribbean Sea and northern South America would favor a stronger EWs activity. Since PV changes are generally small, the linear regression approach applied in this study would filter the PV variations necessary for a sign reversal. Thus, the wind and low-filtered PV fields at different isentropic levels (see section 4.2) were composited considering the events with a westward expansion (or an eastward retreat) of the NASH during the transition season from the NAMS to the SAMS. Following the approach presented in Chapter 3, a westward expansion was identified when the NASH western edge was located westward of 90°W (southeastern United States) whereas an eastward retreat was selected when the NASH western boundary was located eastward of 70°W (central Atlantic). A total of 356 (139) pentads with a westward expansion (eastward retreat) out of a total of 696 pentads during SON were chosen. Fig. 32a (Fig. 32b) shows the composites at 310K associated with the westward expansion (eastward retreat) of the NASH. Results indicate a stronger meridional sign reversal in the background PV field over the southern Caribbean Sea during the westward expansion events, as suggested by the folding in the 0.2-PVU line over the domain 80°W-85°W, 10°N-17.5°N (Fig. 32a). This sign reversal is also observed at 315K (not shown). Such a negative meridional PV gradient is associated with

easterly isentropic winds, meeting the additional Fjortoff condition necessary for instability. The isentropic flow at 310K indicates a weak northerly cross-equatorial flow over South America during the NASH westward expansion events (Fig. 32a) whereas a flow reversal is clear when the NASH retreats eastward (Fig. 32b).

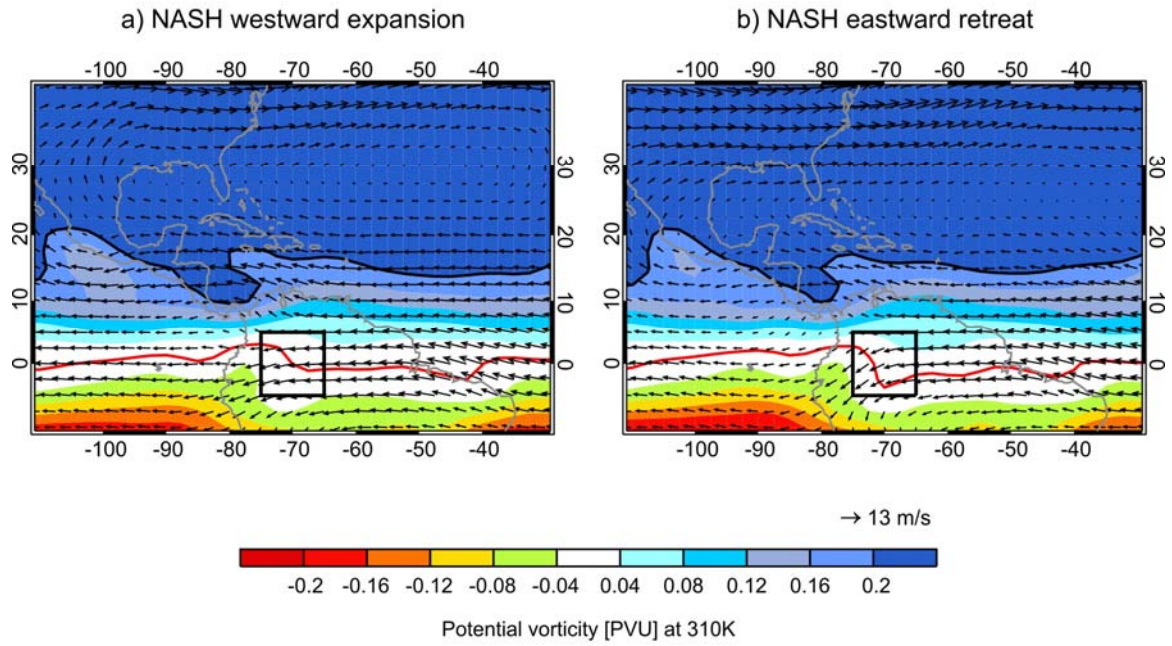

Fig. 32 Isentropic winds (arrows) and low-pass filtered potential vorticity (shades) at 310K composited for events with a) a NASH westward expansion and b) a NASH eastward retreat during SON. Contours for 0 and 0.2 PVU correspond to the red and black lines, respectively. Boxes indicate the South American V-Index domain.

These results suggest a reversal in the background PV meridional gradient in association with an anomalous westward expansion of the NASH, which favors an enhancement of the EWs activity over the southern Caribbean Sea and northern South America. Such an increased EWs activity produces a dominant easterly flow over the region, which prevents the reversal of the cross-equatorial flow in the South American V-

Index region. Since this northerly cross-equatorial flow transports important amounts of moisture to the southern Amazon and the SAMS domain, its weakening observed during the NASH westward expansion would contribute to the delayed wet season onset observed over this region. Therefore, the westward expansion of the NASH observed since 1978 has weaken the moisture transport not only to the NAMS region, but also to the SAMS domain. Such a weaker moisture transport has contributed to the increased frequency of early retreats of the NAMS and the delayed onset of the southern Amazon wet season (and hence of the SAMS) observed during the recent two decades.

4.4 Discussion

The analysis presented here suggests a longer transition season between the NAMS and the SAMS during the period 1978-2007. This lengthening is the result of the trend toward earlier retreats of the NAMS and delayed onsets of the southern Amazon wet season onset observed after 1978. Although the causes of such changes in the American monsoons have been previously identified, whether there is a common factor influencing the timing of the American monsoons or the observed changes are the consequence of independent and unrelated causes was not clear until now. Furthermore, the analysis discussed here indicates that the observed changes in the NAMS retreat and the southern Amazon wet season onset are partially a consequence of the same large-scale change: the westward expansion of the NASH since 1978.

A recent study by Li et al. (2011) shows that the westward expansion of the NASH is not caused by natural variability but by the increasing concentration of atmospheric greenhouse gases (GHGs). However, the mechanism behind the causality between this westward expansion and the increasing GHGs needs further study. In addition, the poleward shift of the subtropical jets over both hemispheres is associated with the broadening of the Hadley cell, which could be also forced by the increasing CO_2 concentrations in the atmosphere (e.g., Lu et al. 2007). Moreover, Fu et al. (2011) reported that the IPCC AR4 models that better reproduce the wet season onset over the southern Amazon are able to project the observed delayed onset only when increasing GHGs and biomass burning aerosols are prescribed. This suggests that the shortening of the American monsoons and the lengthening of the transition season between them may be associated with anthropogenic forcing. The near-future release of the IPCC AR5 model runs would give an excellent opportunity to test the impact of the anthropogenic activity on the length and the strength of the American monsoon systems.

4.5 Conclusions

The results discussed here suggest a longer transition season between the American monsoon systems during the period 1978-2007 due to a trend toward earlier retreats of the NAMS and delayed onsets of the southern Amazon wet season. In

particular, the longest transition seasons are observed after the earlier retreats of the NAMS. In addition, the northerly flow over northern South America, an important moisture source to initiate the SAMS, is weakened when the NAMS has an earlier retreat.

Although the causes of such changes were identified in Chapter 3 and in a previous study by Fu et al. (2011), whether these changes in the American monsoons are the consequence of independent and unrelated causes or there exists a common factor behind such changes was not clear until now. The analyses presented here indicate that the observed changes in the NAMS retreat and the southern Amazon wet season onset are partially a consequence of the westward expansion of the NASH observed since 1978, which is associated with a weakening of the moisture transport not only to the NAMS region (as discussed in Chapter 3) but also to the SAMS domain.

To understand the mechanism behind the weakening of the surface moisture transport to South America during this anomalous westward expansion of the NASH, composite and regression analyses were performed using surface horizontal winds, OLR, relative vorticity, and potential vorticity. These results suggest that an anomalous westward expansion of the NASH produces a dominant easterly flow over northern South America, due to an enhanced EWs activity, preventing the reversal of the cross-equatorial flow necessary to transport moisture to the SAMS domain. This weakening of the northerly flow over South America is consistent with the increases in OLR and the delayed wet season onset observed over the southern Amazon and the SAMS domain.

The discussion presented in this chapter suggests that the changes observed in both American monsoon systems are partially caused by the same large-scale change: the westward expansion of the NASH since 1978, which may be a consequence of the increasing GHGs concentration in the atmosphere.

Chapter 5

General conclusions and future work

This dissertation focused on the climate variability observed over the American monsoon regions during the last decades. In particular, the main objective of this work was to determine whether these monsoon systems have changed during the recent decades and whether there exists an interaction between those changes. To address this, several observational and reanalysis datasets were used. The results obtained from this study were derived from satellite records from ISCCP, products from the NCEP/NCAR reanalysis, surface data for temperature and humidity, NOAA interpolated OLR, reconstructed SST, and rain-gauge rainfall data over both continents.

This manuscript was divided in three main chapters. Chapter 2 focused on the study of the recent changes of cloudiness over the Amazon forests (which are deeply related to those in rainfall), identified their possible causes, and discussed their impact on forest activity. The analyses presented in Chapter 2 showed evidence of a change toward decreasing cloudiness over the Amazon forests during 1984-2007 based on the ISCCP cloud and radiation data. The change in total cloudiness is mainly the consequence of the decreased high clouds and is not caused by changes in the satellite viewing angle of the ISCCP geostationary satellites or by deforestation and land use. Furthermore, such a change is consistent with changes in the large-scale circulation determined independently from the cloud observations.

Although high clouds decrease during all seasons except the dry season, the spatial patterns of these changes and their links to the decadal oceanic variability modes vary seasonally. The analysis suggests that these changes are linked to the expansion of the western Pacific warm pool during DJF, to the Atlantic Multidecadal Oscillation and the eastern Pacific SST anomalies during MAM, and to the tropical Atlantic SST gradient and the western Pacific warm pool expansion during SON.

The results discussed in Chapter 2 indicate that changes in the direct thermal circulation, which could reduce moisture transport and stabilize the upper troposphere, are probably responsible for the decreasing high clouds in the northern Amazon. By contrast, the changes in moisture transport and low-level anomalous winds in the southern Amazon are not well correlated to the tropical SSTAs. Further analyses suggest that anomalous Pacific-South American planetary wave trains may reduce high clouds over the southern Amazon. Such a decreased cloudiness over the Amazon and the resultant increase of solar surface radiation since 1984 support the hypothesis that increasing surface solar radiation have contributed to the increasing forest growth rate observed during the recent decades over the Amazon forests.

Chapter 3 investigated the main changes observed in the NAMS regime during the last decades with emphasis on its retreat phase. Particularly, this chapter reported the existence of two monsoon regimes over the North American monsoon domain during 1948-2009 associated with both natural and anthropogenic variability. The analyses performed in this chapter suggest the occurrence of two NAMS regimes during 1948-

2009: two dry periods, associated with weak monsoons and early retreats/late onsets, are observed during 1948-1959 and 1990-2009 whereas a wet regime, associated with strong monsoons and late retreats/early onsets, is observed during 1960-1989. Although the change of the NAMS regime correlates with the AMO, as found by previous studies, the behavior of the monsoon retreat and the dominant cause of the dry NAMS regime for the earlier (1948-1959) and the more recent (1990-2009) periods are different. The earlier dry regime shows a strong interannual variation between weak and strong NAMS events. This dry period is caused by circulation changes associated with the positive phase of the AMO and it ends when the AMO changes to its negative phase during 1960-1989. In contrast, the NAMS is persistently weak and its retreat is persistently early during the more recent dry regime. The main cause of these changes is the westward expansion of the North Atlantic Surface High. Such a shift leads to an enhanced Caribbean low-level jet, which in turn induces a southerly anticyclonic flow along the western edge of the NASH, transporting moisture from the Gulf of Mexico to the Great Plains, instead of the NAMS region. In addition to the circulation anomalies induced by the positive phase of the AMO, the northward shift of the subtropical jets over the western US also contributes to the dry NAMS regime observed after 1990. Such a change in the jet stream location prevents synoptic disturbances from reaching the monsoon region, reducing favorable conditions for convection and, therefore, weakening the monsoon.

Finally, Chapter 4 combined the findings obtained in Chapter 3 with those reported by Fu et al. (2011). The latter reported a delayed onset of the wet season over

the southern Amazon due to reductions in moisture transport and atmospheric instability, and to the poleward shift of the southern hemispheric jet stream. The discussion presented in this chapter suggest a longer transition season between the American monsoon systems during the period 1978-2007 due to a trend toward earlier retreats of the NAMS and delayed onsets of the southern Amazon wet season (as suggested by Fu et al. 2011), and hence of the SAMS. In particular, the longest transition seasons are observed after the earlier retreats of the NAMS. In addition, the northerly flow over northern South America, an important moisture source to initiate the SAMS, is weakened when the NAMS has an earlier retreat.

Although the causes of such changes were identified in Chapter 3 and Fu et al. (2011), whether these changes in the American monsoons are the consequence of independent and unrelated causes or there exists a common factor behind such changes was not clear until now. The analyses presented here indicate that the observed changes in the NAMS retreat and the SAMS onset are partially a consequence of the westward expansion of the NASH observed since 1978, which is associated with a weakening of the moisture transport not only to the NAMS region (as discussed in Chapter 3) but also to the SAMS domain.

The results from the composite and regression analyses show that an anomalous westward expansion of the NASH is associated with a dominant easterly flow over northern South America, due to an enhanced EWs activity, and prevents the reversal of the cross-equatorial flow necessary to transport moisture to the SAMS domain. Such a

weakening of the northerly flow over South America is consistent with the increases in OLR and the delayed wet season onset observed over the SAMS domain.

Thus, the findings obtained from this investigation indicate that the changes observed in both American monsoon systems are partially caused by the same large-scale forcing: the westward expansion of the NASH since 1978. Such an expansion is found to be explained by the increasing concentration of greenhouse gases in the atmosphere instead of by natural variability. This suggests that the shortening and weakening of the American monsoons and the lengthening of the transition season between them may be associated with anthropogenic forcing.

There are still many aspects of the American monsoons and their interaction that need to be understood. In particular, the mechanism for the retreat of the North American monsoon is still an open question. Although Chapter 3 focused on the changes of the NAMS regime, especially its retreat phase, during the last decades, it did not discuss the climatological features of the retreat and the main factors involved. As a near-future goal, I will lead a fourth paper addressing this question.

The development of the WCRP/CLIVAR/VAMOS program and the availability of better quality data, especially over South America, will be crucial to advance toward a better understanding of the American monsoons. Also, the eventual improvement of the different models involved in the IPCC AR5 to adequately reproduce the monsoon circulation over the Americas would give us different tools to address this issue.

Furthermore, the near-future release of the IPCC AR5 model runs would be an excellent opportunity to test the impact of the anthropogenic activity on the American monsoon systems. The collaborative research between the pan-American countries will also increase the opportunities to acquire a better knowledge and understanding of the region's climate. My current position as an assistant professor in the Universidad de Antioquia in Colombia, my deep interest to keep working on the South American climate, and the contacts I made during my PhD experience would hopefully allow me to contribute to such goal.

References

Adams, D.K., and A.C. Comrie, 1997: The North American monsoon. *Bull. Amer. Meteor. Soc.*, **78**, 2197-2213.

Agudelo, P.A., C.D. Hoyos**,** J.A. Curry, P.J. Webster, 2010: Probabilistic discrimination between large-scale environments of intensifying and decaying African Easterly Waves. *Clim. Dyn.*, doi: 10.1007/s00382-010-0851-x.

Anderson, B.T., H. Kanamaru, and J.O. Roads, 2004: The summertime atmospheric hydrologic cycle over the southwestern United States. *J. Climate*, **5**, 679– 692.

Arias, P.A., R. Fu, C.D. Hoyos, W. Li, and L. Zhou, 2010: Decadal changes in cloudiness over the Amazon forests: Observations and potential causes. *Clim. Dyn.*, doi: 10.1007/s00382-010-0903-2.

Arias, P.A., and R. Fu, 2011: A connection between the earlier retreats of the North American monsoon and the delayed onsets of the southern Amazon wet season observed since 1978. In preparation for *J. Climate*.

Arias, P.A., R. Fu, and K.C. Mo, 2011: Changes in monsoon regime over northwestern Mexico in recent decades and its potential causes. *J. Clim.*, in review.

Artaxo, P., J.V. Martins, M.A. Yamasoe, A.S. Procópio, T.M. Pauliquevis, M.O. Andreae, P. Guyon, L.V. Gatti, and A.M.C. Leal, 2002: Physical and chemical properties of aerosols in the wet and dry seasons in Rondônia, Amazonia. *J Geophys Res*, **107**(D20): 8081. doi:10.1029/2001JD000666.

Barlow, M., S. Nigam, and E.H. Berbery, 1998: Evolution of the North American Monsoon System. *J. Climate*, **11**, 2238-2257.

Berbery, E.H., and V.R. Barros, 2002: The hydrologic cycle of the La Plata basin in South America. *J. Hydrometeor*., **3**, 630–645.

Burpee, R. W., 1972: The origin and structure of easterly waves in the lower troposphere of North Africa. *J. Atmos. Sci*., **29**, 77– 90.

Campbell, G.G., 2004: View angle dependence of cloudiness and the trend in ISCCP cloudiness. http://ams.confex.com/ams/pdfpapers/79041.pdf.

Carleton, A. M., D. A. Carpenter, and P. J. Weser, 1990: Mechanisms of interannual variability of the southwest United States summer rainfall maximum. *J. Climate*, **3**, 999–1015.

Carvalho, L.M.V., C. Jones, and B. Liebmann, 2004: The South Atlantic convergence zone: Intensity, form, persistence, and relationships with intraseasonal to interannual activity and extreme rainfall. *J. Climate*, **17**, 88–108.

Castro, C.L., T.B. McKee, and R.A. Pielke, 2001: The relationship of the North American monsoon to tropical and North Pacific Sea surface temperatures as revealed by observational analyses. *J. Climate*, **14**, 4449–4473.

Castro, C.L., R.A. Pielke, J.O. Adegoke, S.D. Schubert, and P.J. Pegion, 2007: Investigation of the summer climate of the contiguous United States and Mexico using the Regional Atmospheric Modeling System, RAMS). Part II: Model climate variability. *J. Climate*, **20**, 3866–3887.

Chan, S.C., S.K. Behera, and T. Yamagata, 2008: Indian Ocean Dipole influence on South American rainfall. *Geophys. Res. Lett*., **35,** L14S12. doi:10.1029/2008GL034204.

Chang, P., Y. Fang, R. Saravanan, L. Ji, and H. Seidel, 2006: The cause of the fragile relationship between the Pacific El Niño and the Atlantic Niño. *Nature*, **443**, 324-328.

Chen, J., B.W. Carlson, and A.D Del Genio, 2002: Evidence for Strengthening of the Tropical General Circulation in the 1990s. *Science,* **295**, 838-841.

Chen, T.C., J.H. Yoon, K.J. St. Croix, and E.S. Takle, 2001: Suppressing impacts of the Amazonia deforestation by the global circulation change. *Bull. Amer. Meteor. Soc*., **82**, 2209-2216.

Chiang, J.C.H., Y. Kushnir, and S.E. Zebiak, 2000: Interdecadal changes in eastern Pacific ITCZ variability and its influence on the Atlantic ITCZ. *Geophys. Res. Lett.,* **27**, 3687–3690.

Chiang, J., and A. Sobel, 2002: Tropical tropospheric temperature variations caused by ENSO and their influence on the remote tropical climate. *J. Climate.*, **15**, 2616-2631.

Chu, P.S., Z.P. Yu, and S. Hastenrath, 1994: Detecting climate change concurrent with deforestation in the Amazon Basin: Which way has it gone? *Bull. Amer. Meteor. Soc.,* **75**, 579-583.

Coe, M.T., M.H. Costa, and B.S Soares-Filho, 2009: The influence of historical and potential future deforestation on the stream flow of the Amazon River – Land surface processes and atmospheric feedbacks. *J. Hydrol*., **369**, 165–174.

Collier, J. C., and G. J. Zhang, 2006: Simulation of the North American monsoon by the NCAR CCM3 and its sensitivity to convection parameterization. *J. Climate,* **19,** 2851–2866.

Cravatte, S., T. Delcroix, D. Zhang, M. McPhaden, and J. Leloup, 2009: Observed freshening and warming of the western Pacific Warm Pool. *Clim. Dyn*., **33**, 565-589.

Dai, A., 2006: Recent climatology, variability, and trends in global surface humidity. *J. Climate*., **19**, 3589-3606.

Douglas, A.V., and P.J. Englehart, 1996: An analysis of the starting date for the summer monsoon in Western Mexico and Southeast Arizona. *Proc. Twentieth Ann. Climate Diagnostics Workshop*, U.S. Department of Commerce, NOAA 207-211.

Douglas, A.V., and P. Englehart, 2007: A climatological perspective of transient synoptic features during NAME 2004. *J. Climate*, **20**, 1947–1954.

Douglas, M.W., R.A. Maddox, K. Howard, and S. Reyes, 1993: The Mexican monsoon. *J. Climate*, **6**, 1665-1677.

Drigo, R., and A. Marcoux, 1999: Population dynamics and the assessment of land use changes and deforestation, Part 1. http://www.fao.org/sd/wpdirect/WPan0030.htm.

Efron B., 1979: Bootstrap methods: Another look at the jackknife. *Ann. Stat*., ***7***, 1-26.

Eliassen, A., 1983: The Charney–Stern theorem on barotropic–baroclinic instability. *Pure Appl. Geophys.*, **121**, 563–573.

Enfield, D.B., A.M. Mestas-Nuñez, and P.J. Trimble, 2001: The Atlantic Multidecadal Oscillation and its relationship to rainfall and river flows in the continental U.S. *Geophys. Res. Lett.*, **28**, 2077-2080.

Evan, A.T., A.K. Heidinger, and D.J. Vimont, 2007: Arguments against a physical long-term trend in global ISCCP cloud amounts. *Geophys. Res. Lett.*, **34**, L04701. doi:10.1029/2006GL028083.

Figueroa, S. N., and C. Nobre, 1990: Precipitation distribution over central and western tropical South America. *Climanalise*, **5**, 36–44.

Fjortoff, R., 1950: Application of integral theorems in deriving criteria of stability for laminar flows and for the baroclinic circular vortex. *Geofis. Publ.*, **17**(6), 1–52.

Fu, R., R.E. Dickinson, M. Chen, and H. Wang, 2001: How do tropical sea surface temperatures influence the seasonal distribution of precipitation in the equatorial Amazon? *J. Climate.*, **14**, 4003–4026.

Fu, R., W. Li, P.A. Arias, K. Fernandes, L. Yin, and R.E. Dickinson, 2011: An increase of the dry season length over the Southern Amazonia in recent decades-Is it caused by natural variability or by human forced climate change? *Nature*, submitted.

Gedney, N., P.M. Cox, R.A. Betts, O. Boucher, C. Huntingford, and P.A. Stott, 2006: Detection of a direct carbon dioxide effect in continental river runoff records. *Nature*, **439**, 835–838.

Giannini, A., J.C. H. Chiang, M. Cane, Y. Kushnir, and R. Seager, 2001: The ENSO teleconnection to the tropical Atlantic Ocean: Contributions of the remote and local SSTs to rainfall variability in the tropical Americas. *J. Clim.*, **14**, 4530–4544.

Giannini, A., R. Saravanan, and P. Chang, 2004: The preconditioning role of Tropical Atlantic Variability in the development of the ENSO teleconnection: implications for the prediction of Nordeste rainfall. *Clim. Dyn.*, **22**, 839–855.

Grantz, K, B. Rajagopalan, M. Clark, and E. Zagona, 2007: Seasonal Shifts in the North American Monsoon. *J. Climate*, **20**, 1923–1935.

Grimm, A.M, and P.L.D. Silva Dias, 1995: Analysis of tropical extratropical interactions with influence functions of a barotropic model. *J. Atmos. Sci.*, **52**, 3538–3555.

Grimm, A.M., S. Ferraz, and J. Gomez, 1998: Precipitation anomalies in southern Brazil associated with El Niño and La Niña events. *J. Clim.*, **11**, 2863–2880.

Grimm, A.M., V. R. Barros, and M. E. Doyle, 2000: Climate variability in southern South America associated with El Niño and La Niña events. *J. Clim.*, **13**, 35–58.

Gonzalez, M., C. Vera, B. Liebmann, J. Marengo, V. Kousky, and D. Allured, 2007: The nature of the rainfall onset over central South America. *Atmósfera*, **20**(4), 379–396.

Gu, L., D.D. Baldocchi, S.C. Wofsy, J.W. Munger, J.J. Michalsky, S.P. Urbanski, and T.A. Boden, 2003: Response of a Deciduous Forest to the Mount Pinatubo Eruption: Enhanced Photosynthesis. *Science*, **299**, 2035–2038.

Gutzler, D.S., 2004: An index of interannual precipitation variability in the core of the North American monsoon region. *J. Climate*, **17**, 4473–4480.

Harrington, J. A., R. S. Cerveny, and R. C. Balling, 1992: Impact of the Southern Oscillation on the North American monsoon. *Phys. Geogr*., **13**, 318–330.

Higgins, R.W., J.E. Janowiak, and X. Wang, 1997: Influence of the North American Monsoon System on the United States summer precipitation regime. *J. Climate*, **10**, 2600–2622.

Higgins, R.W., K.C. Mo, and Y. Yao, 1998: Interannual variability of the U.S. summer precipitation regime with emphasis on the southwestern monsoon. *J. Climate*, **11**, 2582–2606.

Higgins, R.W., Y. Chen, and A.V. Douglas, 1999: Interannual variability of the North American warm season precipitation regime. *J. Climate,* **12**, 653–680.

Higgins, R.W., and W. Shi, 2000: Dominant factors responsible for interannual variability of the summer monsoon in the southwestern United States. *J. Climate*, **13**, 759–776.

Higgins, R.W., W. Shi, E. Yarosh, and R. Joyce, 2000a: Improved United States precipitation quality control system and analysis *NCEP/Climate Prediction Center ATLAS No7*, NCEP/NWS/NOAA, 40 pp.

Higgins, R.W., A. Leetmaa, Y. Xue, and A. Barnston, 2000b: Dominant factors influencing the seasonal predictability of U.S. precipitation and surface air temperature. *J. Clim.*, **13**, 3994–4017.

Higgins, R.W., and W. Shi, 2001: Intercomparison of the principal modes of interannual and intraseasonal variability of the North American Monsoon System. *J. Climate*, **14**, 403–417.

Higgins, R.W., W. Shi, and C. Hain, 2004: Relationships between Gulf of California moisture surges and precipitation in the southwestern United States. *J. Climate*, **17**, 2983–2997.

Hu, Q., and S. Feng, 2008: Variation of the North American Summer Monsoon Regimes and the Atlantic Multidecadal Oscillation. *J. Climate*, **21**(11), 2371-2383.

Hu, Q., and S. Feng, 2010: Influence of the Arctic oscillation on central United States summer rainfall. *J. Geophys. Res*., **115**, D01102, doi:10.1029/2009JD011805.

Ichii, K., H. Hashimoto, R. Nemani, and M. White, 2005: Modeling the interannual variability and trends in gross and net primary productivity of tropical forests from 1982 to 1999. *Glob. Planet. Change*., **48**, 274–286.

Kalnay, E., M. Kanamitsu, R. Kistler , W. Collins, D. Deaven, L. Gandin, M. Iredell, S. Saha, G. White, J. Woollen, Y. Zhu, M. Chelliah, W. Ebisuzaki, W. Higgins, J. Janowiak, K. Mo, C. Ropelewski, J. Wang, A. Leetma, R. Reynolds, R. Jenne, and D.

Joseph, 1996: The NCEP-NCAR 40-Year Reanalysis Project. *Bull. Amer. Meteor. Soc*., **77**, 437–471.

Kalnay, E., K.C. Mo, and J. Paegle, 1986: Large-amplitude, shortscale stationary Rossby waves in the Southern Hemisphere: Observations and mechanistic experiments to determine their origin. *J. Atmos. Sci*., **43**, 252–275.

Katz, R.W., M.B. Parlange, and C. Tebaldi, 2003: Stochastic modeling of the effects of large-scale circulation on daily weather in the southeastern US. *Climatic Change*, **60**, 189-216.

Kayano, M.T., and R.V. Andreoli, 2007: Relations of South American summer rainfall interannual variations with the Pacific Decadal Oscillation. *Int. J. Climatol*., **27**, 531–540.

Kerr, R.A., 2000: A North Atlantic climate pacemaker for the centuries. *Science*, **288**(5473), 1984-1986.

Knight, J.R. and coauthors, 2006: Climate impacts of the Atlantic Multidecadal Oscillation. *Geophys. Res. Lett*., L17706, doi:10.1029/2006GL026242.

Kushnir, Y., R. Seager, M. Ting, N. Naik, and J. Nakamura, 2010: Mechanisms of Tropical Atlantic SST Influence on North American Hydroclimate Variability. *J. Climate*, in press.

Lau, K.M, and P.H. Chan, 1983: Short-term climate variability and atmospheric teleconnections from satellite-observed outgoing longwave radiation. I: Simultaneous relationships. *J. Atmos. Sci*., **40**, 2735-2750.

Lau, K.M., and L. Peng, 1992: Dynamics of atmospheric teleconnections during the northern summer. *J. Climate*, **5**, 146–158.

Laurance, W.F., A.A. Oliveira, S.G. Laurance, R. Condit, H.E.M Nascimento, A.C. Sanchez-Thorin, T.E. Lovejoy, A. Andrade, S. D'Angelo, J.E. Ribeiro, and C.W. Dick, 2004: Pervasive alteration of tree communities in undisturbed Amazonian forests. *Nature*, **428**(6979), 171-175.

Lee, M.-I., and Coauthors, 2007: Sensitivity to horizontal resolution in the AGCM simulations of warm season diurnal cycle of precipitation over the United States and northern Mexico. *J. Climate*, 20, 1862–1881.

Lenters, J.D., and K.H. Cook, 1995: Simulation and diagnosis of the regional summertime precipitation climatology of South America. *J. Climate*., **8**, 2988–3005.

Lewis, S.L., and coauthors, 2004a: Concerted changes in tropical forest structure and dynamics: evidence from 50 South American long-term plots. *Phil. Trans. Roy. Soc. Lond. B.*, **359**(1443), 421-436.

Lewis, S.L., Y. Malhi, and O.L. Phillips, 2004b: Fingerprinting the impacts of global change on tropical forests. *Phil. Trans. Roy. Soc. Lond. B.*, **359**(1443), 437-462.

Li, W., and R. Fu, 2004: Transition of the large-scale atmospheric and land surface conditions from the dry to the wet season over Amazonia as diagnosed by the ECMWF Reanalysis. *J. Climate*, **17**, 2637-2651.

Li, W., and coauthors, 2011: Changes of the North Atlantic Subtropical High and Its Role in the Intensification of Summer Rainfall Variability in the Southeastern United States. *J. Climate*, in press.

Liebmann, B. and C.A. Smith CA, 1996: Description of a Complete (Interpolated) Outgoing Longwave Radiation Dataset. *Bull. Amer. Meteor. Soc.*, **77**, 1275-1277.

Liebmann, B. and D. Allured, 2005: Daily Precipitation Grids for South America. *Bull. Amer. Meteor. Soc.*, **86**, 1567-1570.

Liebmann, B., G.N. Kiladis, C.S. Vera, and A.C. Saulo, 2004: Subseasonal variations of rainfall in South America in the vicinity of the lowlevel jet east of the Andes and comparison to those in the South Atlantic convergence zone. *J. Climate*., **17**, 3829–3842.

Liebmann, B., G.N. Kiladis, L.M.V. Carvalho, C. Jones, C.S. Vera, I. Bladé, and D. Allured, 2009: Origin of Convectively Coupled Kelvin Waves over South America. *J. Climate*., **22**, 300-315.

Liebmann, B., and C.A. Smith, 1996: Description of a Complete (Interpolated) Outgoing Longwave Radiation Dataset. *Bull. Amer. Meteor. Soc*., **77**, 1275-1277.

Lin, J.L., B.E. Mapes, K.M. Weickmann, G.N. Kiladis, S.D. Schubert, M.J. Suarez, J.T. Bacmeister, and M.I. Lee, 2008: North American monsoon and convectively coupled equatorial waves simulated by IPCC AR4 coupled GCMs. *J. Climate*, **21**, 2919-2937.

Livezey, R.E., and W.Y. Chen, 1983: Statistical field significance and its determination by Monte Carlo Techniques. *Mon. Wea. Rev*., **111**, 46-59.

Lu, J., G.A. Vecchi, and T. Reichler, 2007: Expansion of the Hadley cell under global warming. *Geophys. Res. Lett*., **34**, L06805, doi:10.1029/2006GL028443.

Madden, R. A., and P. R. Julian, 1994: Observations of the 40-50 day tropical oscillation: a review. *Mon. Wea. Rev.*, **122**, 814-837.

Malhi, Y., and J. Wright, 2004: Spatial patterns and recent trends in the climate of tropical rainforest regions. *Phil. Trans. Roy. Soc. Lond.*, **359**, 311-329.

Mantua, N.J., S.R. Hare, Y. Zhang, J.M. Wallace, and R.C. Francis, 1997: A Pacific interdecadal climate oscillation with impacts on salmon production. *Bull. Amer. Meteor. Soc.*, **78**, 1069-1079.

Marengo, J.A., 1992: Interannual variability of surface climate in the Amazon basin. *Int. J. Climatol.*, **12**, 853–863.

Marengo, J.A., 2004: Interdecadal variability and trends of rainfall across the Amazon basin. *Theor. Appl. Climatol.*, **78**, 79–96.

Marengo, J.A., W. Soares, W. Saulo, and M. Nicolini, 2004: Climatology of the LLJ east of the Andes as derived from the NCEP reanalyses. *J. Clim.*, **17**, 2261–2280.

Marengo, J.A., 2005: Characteristics and spatio-temporal variability of the Amazon River basin water budget. *Clim. Dyn.*, **24**, 11-22.

Marengo, J.A., B. Liebmann, A.M. Grimm, V. Misra, P.L. Silva Dias, I.F.A. Cavalcanti, L.M.V. Carvalho, E.H. Berbery, T. Ambrizzi, C.S. Vera, A.C. Saulo, J. Nogués-Paegle, E. Zipser, A. Seth, and L. M. Alves, 2010: Recent developments on the South American monsoon system. *Int. J. Climatol*., doi: 10.1002/joc2254.

McCabe, G.J., M.A. Palecki, and J.L. Betancourt, 2004: Pacific and Atlantic Ocean influences on multidecadal drought frequency in the United States. *Proceed. Natl. Acad. Sci*., **101**, 4136-4141.

Mechoso, C. R., S. Lyons, and J. Spahr, 1990: The impact of sea surface temperature anomalies on the rainfall in northeast Brazil. *J. Clim*., **3**, 812–826.

Mo, K.C., J.N. Paegle, and R.W. Higgins, 1997: Atmospheric processes associated with summer floods and droughts in the central United States. *J. Climate*, **10**, 3028–3046.

Mo, K.C., J.E. Schemm, and S.H. Yoo, 2009: ENSO and the Atlantic multi decadal oscillation on drought over the United States. *J. Climate*, **22**, 5962-5982.

Mo, K.C., 2010: Interdecadal Modulation of the Impact of ENSO on Precipitation and Temperature over the United States. *J. Climate*, submitted.

Molinari, J., S. Skubis, and D. Vollaro, 1995: External influences on hurricane intensity. Part III: Potential vorticity evolution. *J. Atmos. Sci*., **52**, 3593–3606.

Molinari, J., D. Knight, M. Dickinson, D. Vollaro, and S. Skubis, 1997: Potential vorticity, easterly waves, and tropical cyclogenesis. *Mon. Wea. Rev.,* **125,** 2699-2708.

Molinari, J., D. Vollaro, S. Skubis, and M. Dickinson, 2000: Origins and mechanisms of eastern Pacific tropical cyclogenesis: A case study. *Mon. Wea. Rev.*, **128**, 125-139.

Moura, A.D., and J. Shukla, 1981: On the dynamics of droughts in northeast Brazil: Observations, theory and numerical experiments with a general circulation model. *J. Atmos. Sci*., **38**, 2653– 2675.

Murakami, T., 1980: Empirical Orthogonal Function analysis of satellite-observed outgoing longwave radiation during summer. *Mon. Wea. Rev*., **108**, 205-222.

Myneni B, and coauthors, 2007: Large Seasonal Swings in Leaf Area of Amazon rainforests. *PNAS*, **104**(12), 4280-4283.

Neelin, J.D., C. Chou, and H. Su, 2003: Tropical drought regions in global warming and El Niño teleconnections. *Geophys. Res. Lett*., **30**(24), 2275. doi:10.1029/2003GL018625.

Nemani, R., C.D. Keeling, H. Hashimoto, W. Jolly, S. Piper, C. Tucker, R. Myneni, and S. Running, 2003: Climate-driven increases in Global Terrestrial Net Primary Production from 1982 to 1999. *Science*, **300**, 1560-1563.

Nobre, P., and J. Shukla, 1996: Variations of sea surface temperature, wind stress, and rainfall over the tropical Atlantic and South America. *J. Climate*., **9**, 2464-2479.

Nogues-Paegle, J., and K.C. Mo, 1997: Alternating wet and dry conditions over South America during summer. *Mon. Wea. Rev*., **125**, 279–291.

Norris, J.R., 2005: Multidecadal changes in near-global cloud cover and estimated cloud cover radiative forcing. *J. Geophys. Res*., **110**, D08206, doi:10.1029/2004JD005600.

Phillips, O.L., Y. Malhi, N. Higuchi, W.F. Laurance, V.P. Nuñez, R.M. Vásquez, S.G. Laurance, L.V. Ferreira, M. Stern, S. Brown, and J. Grace, 1998: Changes in the carbon balance of tropical forest: evidence from long-term plots. *Science*, **282**, 439-442.

Pisciottano, G., A. Diaz, G. Cazes, and C. R. Mechoso, 1994: El Niño–Southern Oscillation impact on rainfall in Uruguay. *J. Clim.*, **7**, 1286–1302.

Raia, A., and I.F.A. Cavalcanti, 2008: The Life Cycle of the South American Monsoon System. *J. Clim*., **21**, 6227–6246.

Ramage, C., 1971: *Monsoon Meteorology*. International Geophysics Series, vol. 15. San Diego, CA. Academic Press.

Reynolds, R.W., 1988: A real-time global sea surface temperature analysis. *J. Climate*, **1**, 75-86.

Rickenbach, T.M., 2004: Nocturnal cloud systems and the diurnal variation of clouds and rainfall in southwestern Amazonia. *Mon. Wea. Rev*., **132,** 1201–1219.

Rickenbach, T.M., R.N. Ferreira, J. Halverson, and M.A.F. Silva Dias, 2002: Modulation of convection in the southwestern Amazon basin by extratropical stationary fronts. *J. Geophys. Res*, **107**, 8040, doi:10.1029/2000JD000263.

Rossow, W.B., and R.A. Schiffer, 1999: Advances in understanding clouds from ISCCP. *Bull. Amer. Meteor. Soc*., **80**, 2261-2288.

Rossow, W.B., A.W. Walker, D.E. Beuschel, and M.D. Roiter, 1996: International Satellite Cloud Climatology Project (ISCCP), Documentation of New Cloud Datasets.

Saji, N.H., B.N. Goswami, P.N. Vinayachandran, and T. Yamagata, 1999: A dipole mode in the tropical Indian Ocean. *Nature*, **401**, 360-363.

Saji, N.H., and T. Yamagata, 2003: Possible impacts of Indian Ocean Dipole mode events on global climate. *Clim. Res*., **25**, 151–169.

Schubert, S.D., M.J. Suarez, P.J. Pegion, R.D. Koster, and J.T. Bacmeister, 2004: On the cause of the 1930s dust bowl. *Science*, **303**, 1855-1859.

Schubert S.D., and coauthors, 2009: A USCLIVAR project to assess and compare the responses of global climate models to drought related SST forcing patterns: Overview and Results. *J. Climate*, **22**, 5251-5272.

Seager R., N. Harnik, W.A. Robinson, Y. Kushnir, M. Ting, H.P. Huang, and J. Velez, 2005: Mechanisms of ENSO-forcing of hemispherically symmetric precipitation variability. *Q. J. R. Meteorol. Soc*., **131**, 1501–1527.

Seager R., N. Naik, M. Ting, M.A. Cane, N. Harnik, and Y. Kushnir, 2010: Adjustment of the atmospheric circulation to tropical Pacific SST anomalies: Variability of transient eddy propagation in the Pacific–North America sector. *Q. J. R. Meteorol. Soc*., **136**, 277–296.

Sen, P.K., 1968: Estimates of the regression coefficient based on Kendall's Tau. *Amer. Stat. Assoc. J*., **63**, 1379-1389.

Shuttleworth, W.J., 1989: Micrometeorology of temperate and tropical forest. *Phil. Trans. Roy. Soc. Lond. B.*, **324**, 299-334.

Silva, V.B., Kousky, S.V.E., Shi, W., and Higgins, R.W, 2007: An improved gridded historical daily precipitation analysis for Brazil. *J. Hydrometeorol*., **8**, 847–861.

Silvestri, G. E., and C. S. Vera, 2003: Antarctic Oscillation signal on precipitation anomalies over southeastern South America. *Geophys. Res. Lett*., **30**, 2115, doi:10.1029/2003GL018277.

Slingo, J.M., 2002: *Monsoon Overview*, Contribution to 'Encyclopedia of Atmospheric Sciences'. Academic Press, 1365 - 1370.

Stensrud, D.J., R.L. Gall, S.L. Mullen, and K.W. Howard, 1995: Model climatology of the Mexican monsoon. *J. Climate*, **8**, 1775–1794.

Thompson, D.W.J., and J. M. Wallace, 1998: The Arctic Oscillation signature in the wintertime geopotential height and temperature fields. *Geophys. Res. Lett*., **25**(9), 1297-1300.

Turrent, C., and T. Cavazos, 2009: Role of the land-sea thermal contrast in the interannual modulation of the North American Monsoon. *Geophys. Res. Lett.*, **36**(L02808), doi:10.1029/2008GL036299.

Vera, C., and Coauthors, 2006: Toward a unified view of the American monsoon systems. *J. Climate*, **19**, 4977–5000.

Wallace, J.M., and D.S. Gutzler, 1981: Teleconnections in the geopotential height field during the Northern Hemisphere Winter. *Mon. Wea. Rev*., **109**, 784-812.

Wang, C., 2002: Atlantic climate variability and its associated atmospheric circulation cells. *J. Climate*., **15**, 1516-1536.

Wang, H., and R. Fu, 2002: Cross-equatorial flow and seasonal cycle of precipitation over South America. *J. Climate.*, **15**, 1591-1608.

Warren, S.G., R.M. Eastman, and C.J. Hahn, 2007: A survey of changes in cloud cover and cloud types over land from surface observations, 1971-96. *J. Climate*., **20**, 717-738.

Weaver, S.J., S. Schubert, and H. Wang, 2010: Warm Season Variations in the Low-Level Circulation and Precipitation over the Central United States in Observations, AMIP Simulations, and Idealized SST Experiments. *J. Climate*, **22**, 5401-5420.

Wielicki, B.A., and coauthors, 2002: Evidence for Large Decadal Variability in the Tropical Mean Radiative Energy Budget. *Science*, **295**(5556), 841-844.

Wright, S.J., and C. van Schaik, 1994: Light and the phenology of tropical trees. *Amer. Nat.*, **143**, 192-199.

Yang, Z.-L., D. Gochis, and W. J. Shuttleworth, 2001: Evaluation of the simulations of the North American monsoon in the NCAR CCM3. *Geophys. Res. Lett.*, **28**, 1211–1214.

Yoon, J.H., and N. Zeng, 2010: An Atlantic influence on Amazon rainfall. *Clim. Dyn.*, **34**, 249-264.

Yu, B., A. Shabbar, and F.W. Zwiers, 2007: The enhanced PNA-like climate response to Pacific interannual and decadal variability. *J. Climate*, **20**, 5285 - 5300.

Zeng, X., and E. Lu, 2004: Globally unified monsoon onset and retreat indexes. *J. Climate*, **17**, 2241–2248.

Zhang, Y., W.B. Rossow, and A.A. Lacis, 1995: Calculation of surface and top of atmosphere radiative fluxes from physical quantities based on ISCCP datasets 1. Method and sensitivity to input data uncertainties. *J. Geophys. Res.*, **100**, 1149-1165.

Zhang, Y., W.B. Rossow, A.A. Lacis, V. Oinas, and M.I. Mishchenko, 2004: Calculation of radiative fluxes from the surface to top of atmosphere based on ISCCP and other global data sets: Refinements of the radiative transfer model and the input data. *J. Geophys. Res.*, **109**, D19105, doi:10.1029/2003JD004457.

Zhou, J., and K.-M. Lau, 1998: Does a monsoon climate exist over South America? *J. Climate*, **11**, 1020–1040.

Zhu, C., T. Cavazos, and D.P. Lettenmaier, 2007: Role of antecedent land surface conditions in warm season precipitation over northwestern Mexico. *J. Climate*, **20**, 1774–1791.

Vita

I was born in Medellin, Colombia. I attended high school at Liceo Salazar y Herrera and graduated in 1995. I then enrolled in the Universidad Nacional de Colombia, where I obtained a bachelor degree in Civil Engineering in 2001. After taking several courses in hydroclimatology during my senior year and writing a thesis on the diurnal cycle of precipitation in the tropical Andes, I decided to study atmospheric sciences in graduate school. I completed a Master's degree in water resources management at the Universidad Nacional de Colombia. My goal was to understand the intraseasonal variability of Colombian hydroclimatology under the supervision of Dr. German Poveda. In the course of my scientist research, I made contact with Dr. Rong Fu, a scientist who has made significant advances in climate research in South America, especially the Amazonia. After I finished my masters in Colombia, I moved to Atlanta, Georgia, and enrolled in the Earth and Atmospheric Sciences program at the Georgia Institute of Technology (Georgia Tech), where Dr. Fu was a professor. In 2006, I became a PhD student and began my research on changes in cloudiness over the Amazon forests. I received a second Master's degree from Georgia Tech in 2008. In 2009, after my advisor accepted a position at the Jackson School of Geosciences at the University of Texas at Austin (UT), I transferred from Georgia Tech to UT, where I continued my PhD studies. My research interests broadened and I studied climate variability of the American monsoon regions over the past half century. After my graduation from UT, I plan to go back to my native country, where a faculty position in one of the most recognized universities in the country, Universidad de Antioquia, awaits me.

Contact email: paola.arias@mail.utexas.edu

This dissertation was typed by Paola A. Arias